

# Bayesian Weighted Mendelian Randomization for Causal Inference based on Summary Statistics

Jia Zhao

School of Mathematical Sciences, Beijing Normal University  
Department of Mathematics,  
The Hong Kong University of Science and Technology

Jingsi Ming

Department of Mathematics,  
The Hong Kong University of Science and Technology

Xianghong Hu

Department of Mathematics, Hong Kong Baptist University  
Department of Mathematics,  
Southern University of Science and Technology

Gang Chen

The WeGene Company

Jin Liu

Centre for Quantitative Medicine, Duke-NUS Medical School  
Can Yang

Department of Mathematics,  
The Hong Kong University of Science and Technology

April 30, 2019

## Abstract

The results from Genome-Wide Association Studies (GWAS) on thousands of phenotypes provide an unprecedented opportunity to infer the causal effect of one phenotype (exposure) on another (outcome). Mendelian randomization (MR), an instrumental variable (IV) method, has been introduced for causal inference using GWAS data. Due to the polygenic architecture of complex traits/diseases and the ubiquity of pleiotropy, however, MR has many unique challenges compared to conventional IV methods. We propose a Bayesian weighted Mendelian randomization (BWMR) for causal inference to address these challenges. In our BWMR model, the

uncertainty of weak effects owing to polygenicity has been taken into account and the violation of IV assumption due to pleiotropy has been addressed through outlier detection by Bayesian weighting. To make the causal inference based on BWMR computationally stable and efficient, we developed a variational expectation-maximization (VEM) algorithm. Moreover, we have also derived an exact closed-form formula to correct the posterior covariance which is often underestimated in variational inference. Through comprehensive simulation studies, we evaluated the performance of BWMR, demonstrating the advantage of BWMR over its competitors. Then we applied BWMR to make causal inference between 130 metabolites and 93 complex human traits, uncovering novel causal relationship between exposure and outcome traits. The BWMR software is available at <https://github.com/jiazhao97/BWMR>

*Keywords:* Mendelian randomization; Causal inference; GWAS; Summary Statistics

# 1 Introduction

Determination of the causal effect of a risk factor (exposure) on a complex trait or disease (outcome) is critical for health management and medical intervention. Random controlled trial (RCT) is often considered as the golden standard for causal inference. When the evidence from RCT is lacking, Mendelian Randomization (MR) (Katan, 1986; Evans and Davey Smith, 2015) was proposed to mimic RCT using natural genetic variations for causal inference. The idea is that the genotypes are randomly assigned from one generation to next generation according to Mendelian Laws of Inheritance. Therefore, genotypes which should be unrelated to confounding factors can serve as instrumental variables (IVs) (Lawlor et al., 2008; Baiocchi et al., 2014), helping to eliminate the possibility of reverse causality.

In recent years, MR becomes more and more popular because Genome-Wide Association Studies (GWAS) have been performed on thousands of phenotypes. In particular, summary statistics from GWAS are available through public gateways (e.g., <https://www.ebi.ac.uk/gwas/downloads/summary-statistics>). These data sets contain very rich information, such as reference allele frequency of single nucleotide polymorphisms (SNPs), the effect size of a SNP on the phenotype and its standard error, such that MR can be performed without accessing individual-level GWAS data.

From the statistical point of view, MR can be viewed as an instrumental variable method. However, due to the complexity of human genetics (e.g., polygenicity (Visscher et al., 2017), pleiotropy (Solovieff et al., 2013; Yang et al., 2015) and linkage disequilibrium (LD) in human genome (The 1000 Genomes Project Consortium et al., 2012) and complicated data processing and sharing (e.g., sample overlap in multiple GWAS), MR has several unique challenges compared with conventional IV methods. First, in the presence of polygenic architecture, there exist many weak SNP-exposure effects rather than strong effects only. The uncertainty of estimated weak effects needs to be taken into account. Second, based on current GWAS results, it is often observed that a SNP can affect both exposure and outcome traits. This phenomenon is referred as “pleiotropy” or “horizontal pleiotropy”. The ubiquity of horizontal pleiotropy easily makes the assumption in classical IV methods invalid, resulting in many false positives if horizontal pleiotropy is not taken into account. Third, a number of potential risks may be involved in summary statistics-

based MR, such as, different LD patterns in exposure and outcome traits, selection bias of SNP-exposure effects and other bias due to overlapped samples.

To address these challenges, much efforts have been devoted in MR recently. To name a few, PRESSO has been proposed to handle horizontal pleiotropy (Verbanck et al., 2018). A sampling strategy is used in PRESSO to detect outliers due to horizontal pleiotropy and then inverse variance weighted (IVW) regression (Burgess et al., 2013) is applied to estimate causal effects. However, estimation uncertainty of SNP-exposure effects is ignored in the PRESSO model. It is also not computationally efficient owing to the sampling strategy. By assuming that horizontal pleiotropic effects are unknown constant, Egger (Bowden et al., 2015) extends the IVW method by introducing an additional intercept term. Despite this improvement over IVW, Egger suffers from high estimation error in presence of many weak horizontal pleiotropic effects as its assumption fails in this situation. Moreover, Egger would be biased when there exist a few large pleiotropic effects (i.e., outliers). GSMR (Zhu et al., 2018) improves existing methods by introducing outlier detection to remove the influence of large pleiotropic effects and take the linkage disequilibrium between IVs into account. However, GSMR adopts an ad-hoc outlier detection procedure and it does not take weak pleiotropic effects into consideration. Therefore, its type I error rate can be inflated in real data analysis. RAPS is a newly developed method (Zhao et al., 2018), aiming to improve statistical power for causal inference by including weak effects in GWAS and removing outliers due to horizontal pleiotropy. Although the theoretical property of RAPS has been established, its accompanying algorithm is numerically unstable, resulting in unreliable estimated causal effects (see our experimental results in supplementary Figs. 43-45).

In this paper, we propose a method named ‘Bayesian Weighted Mendelian Randomization (BMWR)’ for causal inference using summary statistics from GWAS. In BWMR, uncertainty of estimated weak effects in GWAS and influence of horizontal pleiotropy have been addressed in a unified statistical framework. To make BWMR computationally efficient and stable, we developed a variational expectation-maximization algorithm to infer the posterior mean of the causal effects. Importantly, we further derived an exact closed-form formula to correct the posterior covariance which was often underestimated in varia-

tional inference. Through comprehensive simulation studies, we showed that BMWR was computationally stable and statistically efficient, compared to existing related methods. Then we applied BWMR to real data analysis, further demonstrating the statistical properties of BWMR and revealing novel causal relationships between exposure and outcome traits.

## 2 Methods

### 2.1 Model

We primarily focus on estimating the causal effect of an exposure  $X$  on an outcome  $Y$  with unknown confounding factors  $U$  in the framework of MR. To perform the standard MR, an instrumental variable method for causal inference, the following three criteria ensuring the validity of IVs should be satisfied:

- Relevance criterion: IVs are associated with the exposure  $X$ .
- Effective random assignment criterion: IVs are independent of confounders  $U$ .
- Exclusion restriction criterion: IVs only affect the outcome  $Y$  through the exposure  $X$ .

Assuming the validity of IVs, we begin with the following linear model for MR:

$$X = \sum_{j=1}^N \gamma_j G_j + \eta_X U + \epsilon_X, Y = \beta X + \eta_Y U + \epsilon_Y, \quad (1)$$

where  $G_j$  ( $j = 1, 2, \dots, N$ ) are independent SNPs serving as IVs,  $\gamma_j$  ( $j = 1, 2, \dots, N$ ) are SNP-exposure effects,  $\eta_X$  and  $\eta_Y$  are effects of confounders  $U$  on exposure  $X$  and outcome  $Y$ ,  $\epsilon_X$  and  $\epsilon_Y$  are independent error terms, i.e.,  $(\epsilon_X, \epsilon_Y) \perp\!\!\!\perp (G_1, G_2, \dots, G_N, U)$ ,  $\epsilon_X \perp\!\!\!\perp \epsilon_Y$ , and  $\beta$  denotes the causal effect of interest. Eq. (1) implies

$$Y = \sum_{j=1}^N \beta \gamma_j G_j + (\beta \eta_x + \eta_y) U + \beta \epsilon_x + \epsilon_y. \quad (2)$$

Let  $\Gamma_j$  be the effect of  $G_j$  on outcome  $Y$ . From Eq. (2), we have

$$\Gamma_j = \beta \gamma_j, j = 1, 2, \dots, N. \quad (3)$$

This equation implies that we can estimate  $\beta$  based on  $\Gamma_j$  and  $\gamma_j$ .

In practice, we do not know  $\Gamma_j$  and  $\gamma_j$ , but have their estimates from summary statistics of GWAS. Let  $\{\hat{\gamma}_j, \sigma_{X_j}, p_{X_j}\}$  and  $\{\hat{\Gamma}_j, \sigma_{Y_j}, p_{Y_j}\}$  be estimated effect sizes of  $G_j$ , standard errors and  $p$ -values for both exposure  $X$  and outcome  $Y$ , respectively. Because of the large sample size of GWAS, we ignore the uncertainty in estimating  $\sigma_{X_j}, \sigma_{Y_j}$ . To ensure the relevance criterion, we first select SNPs which are significantly associated with exposure  $X$  (e.g.,  $p_{X_j} \leq 5 \times 10^{-8}$ ). We further apply LD clumping to those selected SNPs to ensure the independence of IVs (Purcell et al., 2007). The remaining summary statistics are denoted as  $D = \{\hat{\gamma}, \hat{\Gamma}, \sigma_X, \sigma_Y\}$  serving as the input data of our model, where  $\hat{\gamma} = (\hat{\gamma}_1, \dots, \hat{\gamma}_N)$ ,  $\hat{\Gamma} = (\hat{\Gamma}_1, \dots, \hat{\Gamma}_N)$ ,  $\sigma_X = (\sigma_{X_1}, \dots, \sigma_{X_N})$ ,  $\sigma_Y = (\sigma_{Y_1}, \dots, \sigma_{Y_N})$ . Note that the relationship between estimated effect sizes and the corresponding true effect sizes is given in the following probabilistic model:

$$\hat{\gamma}_j | \gamma_j \sim \mathcal{N}(\gamma_j, \sigma_{X_j}^2), \hat{\Gamma}_j | \Gamma_j \sim \mathcal{N}(\Gamma_j, \sigma_{Y_j}^2), j = 1, 2, \dots, N. \quad (4)$$

According to Mendel's Law, it is also reasonable to assume that effective random assignment criterion is satisfied in real-data application. However, the exclusion restriction criterion does not often hold because of the ubiquity of horizontal pleiotropy (i.e., IVs may have direct effects on outcome  $Y$ ).

To address this challenge, we notice that Eq. (3) can be relaxed as

$$\Gamma_j = \beta \gamma_j + \alpha_j, j = 1, 2, \dots, N, \quad (5)$$

by assuming that

$$\alpha_j \stackrel{\text{i.i.d.}}{\sim} \mathcal{N}(0, \tau^2), (\alpha_1, \alpha_2, \dots, \alpha_N) \perp\!\!\!\perp (\gamma_1, \gamma_2, \dots, \gamma_N), \quad (6)$$

where  $\tau^2$  is an unknown parameter to be estimated from data. In such a way, estimating  $\beta$  from Eq. (5) can be viewed as a noisy version of estimation from Eq. (3), where  $\alpha_1, \dots, \alpha_N$  are viewed with independent random noise. In fact, the linear model corresponding to Eq. (5) is

$$X = \sum_{j=1}^N \gamma_j G_j + \eta_X U + \epsilon_X, Y = \beta X + \sum_{j=1}^N \alpha_j G_j + \eta_Y U + \epsilon_Y. \quad (7)$$

The presence of term  $\alpha_j G_j$  indicates that the exclusion restriction criterion can be relaxed as long as the direct effect  $\alpha_j$  satisfies (6). The nonzero variance  $\tau^2$  naturally accounts for the influence of weak pleiotropic effects  $\alpha_j$ ,  $j = 1, \dots, N$ .

Combining Eqs. (4,5,6), we have

$$\hat{\gamma}_j | \gamma_j \sim \mathcal{N}(\gamma_j, \sigma_{X_j}^2), \hat{\Gamma}_j | \beta, \gamma_j \sim \mathcal{N}(\beta \gamma_j, \sigma_{Y_j}^2 + \tau^2). \quad (8)$$

If we treat  $\gamma_j$  ( $j = 1, \dots, N$ ) as model parameters, then the number of model parameters is going to increase as the number of samples  $\{\hat{\gamma}_j, \hat{\Gamma}_j\}$  increases. Therefore, we assign a prior distribution on  $\gamma_j$ ,

$$\gamma_j \stackrel{\text{i.i.d.}}{\sim} \mathcal{N}(0, \sigma^2), \quad (9)$$

with an unknown parameter  $\sigma^2$  to be estimated from data. To facilitate statistical inference in Bayesian framework, we also assign a non-informative prior on  $\beta$

$$\beta \sim \mathcal{N}(0, \sigma_0^2). \quad (10)$$

When  $\sigma_0 \rightarrow \infty$ , the result from Bayesian inference on  $\beta$  will naturally converge to the inference result based on maximum likelihood estimation. Let  $\boldsymbol{\gamma}$  be the collection of  $\{\gamma_1, \dots, \gamma_N\}$ . Combining Eq. (8) with Eq. (9) and Eq. (10), our probabilistic model becomes

$$\begin{aligned} & p(\hat{\boldsymbol{\gamma}}, \hat{\boldsymbol{\Gamma}}, \beta, \boldsymbol{\gamma} | \boldsymbol{\sigma}_X^2, \boldsymbol{\sigma}_Y^2, \tau^2, \sigma^2, \sigma_0^2) \\ &= \mathcal{N}(\beta | 0, \sigma_0^2) \prod_{j=1}^N \mathcal{N}(\gamma_j | 0, \sigma^2) \\ & \quad \prod_{j=1}^N \mathcal{N}(\hat{\gamma}_j | \gamma_j, \sigma_{X_j}^2) \prod_{j=1}^N \mathcal{N}(\hat{\Gamma}_j | \beta \gamma_j, \sigma_{Y_j}^2 + \tau^2). \end{aligned} \quad (11)$$

In the presence of strong horizontal pleiotropy, the direct effect  $\alpha_j$  in Eq. (7) may become extremely large and thus it does not satisfy Eq. (6). To ensure that our model works well in this case, we cast those  $\alpha_j$  as outliers. As inspired by reweighed probabilistic models (Wang et al., 2016), here we propose a strategy to guarantee the robustness of the above model. Let  $\boldsymbol{w} = [w_1, \dots, w_N]$ , where  $w_j \in \{0, 1\}$  is the weight corresponding to the  $j$ -th observation. We would like to assign  $w_j = 0$  if  $\alpha_j$  deviates from model (11), and  $w_j = 1$  otherwise. With this consideration, we assume

$$w_j | \pi_1 \stackrel{\text{i.i.d.}}{\sim} \text{Bernoulli}(\pi_1), \pi_1 \sim \text{Beta}(a_0, 1),$$

where  $a_0$  is specified as 100 throughout this paper, preferring there is a small proportion of outliers. Then we reformulate model (11) as

$$\begin{aligned}
& p(\hat{\boldsymbol{\gamma}}, \hat{\boldsymbol{\Gamma}}, \beta, \pi_1, \boldsymbol{\gamma}, \mathbf{w} | \boldsymbol{\sigma}_X^2, \boldsymbol{\sigma}_Y^2, \tau^2, \sigma^2, \sigma_0^2, a_0) \\
&= \frac{1}{A} \mathcal{N}(\beta | 0, \sigma_0^2) \Pr(\pi_1 | a_0) \prod_{j=1}^N \mathcal{N}(\gamma_j | 0, \sigma^2) \prod_{j=1}^N \Pr(w_j | \pi_1) \\
& \quad \prod_{j=1}^N \mathcal{N}(\hat{\gamma}_j | \gamma_j, \sigma_{X_j}^2) \prod_{j=1}^N \mathcal{N}(\hat{\Gamma}_j | \beta \gamma_j, \sigma_{Y_j}^2 + \tau^2)^{w_j}.
\end{aligned} \tag{12}$$

where  $A$  is the normalization constant to ensure (12) is a valid probability model.

To sum up, we refer to our model (12) as Bayesian Weighted Mendelian Randomization (BWMR). BWMR takes summary statistics  $D = \{\hat{\boldsymbol{\gamma}}, \hat{\boldsymbol{\Gamma}}, \boldsymbol{\sigma}_X, \boldsymbol{\sigma}_Y\}$  as its input, aiming to provide the posterior mean and variance on causal effect  $\beta$ , in which  $\mathbf{z} = \{\beta, \pi_1, \mathbf{w}, \boldsymbol{\gamma}\}$  is the collection of latent variables,  $\boldsymbol{\theta} = \{\tau^2, \sigma^2\}$  is the set of the model parameters to be optimized, and  $\mathbf{h}_0 = \{\sigma_0 = 1 \times 10^6, a_0 = 100\}$  is the collection of fixed hyper-parameters.

## 2.2 Algorithm

To provide accurate statistical inference, we are interested in posterior distribution of the latent variables:

$$p(\mathbf{z} | D, \boldsymbol{\theta}, \mathbf{h}_0) = \frac{p(\hat{\boldsymbol{\gamma}}, \hat{\boldsymbol{\Gamma}}, \mathbf{z} | \boldsymbol{\sigma}_X^2, \boldsymbol{\sigma}_Y^2, \boldsymbol{\theta}, \mathbf{h}_0)}{p(\hat{\boldsymbol{\gamma}}, \hat{\boldsymbol{\Gamma}} | \boldsymbol{\sigma}_X^2, \boldsymbol{\sigma}_Y^2, \boldsymbol{\theta}, \mathbf{h}_0)},$$

where

$$p(\hat{\boldsymbol{\gamma}}, \hat{\boldsymbol{\Gamma}} | \boldsymbol{\sigma}_X^2, \boldsymbol{\sigma}_Y^2, \boldsymbol{\theta}, \mathbf{h}_0) = \int_{\mathbf{z}} p(\hat{\boldsymbol{\gamma}}, \hat{\boldsymbol{\Gamma}}, \mathbf{z} | \boldsymbol{\sigma}_X^2, \boldsymbol{\sigma}_Y^2, \boldsymbol{\theta}, \mathbf{h}_0) d\mathbf{z}.$$

However, exact evaluation of the posterior distribution is very challenging because the integration is intractable.

Instead, we propose a variational expectation-maximization (VEM) algorithm to approximate the posterior. Let  $q(\mathbf{z})$  be a variational distribution. The logarithm of the

marginal likelihood can be written as

$$\begin{aligned}
& \log p(\hat{\boldsymbol{\gamma}}, \hat{\boldsymbol{\Gamma}} | \boldsymbol{\sigma}_X^2, \boldsymbol{\sigma}_Y^2, \boldsymbol{\theta}, \mathbf{h}_0) \\
&= \mathbb{E}_{q(\mathbf{z})} [\log p(\hat{\boldsymbol{\gamma}}, \hat{\boldsymbol{\Gamma}} | \boldsymbol{\sigma}_X^2, \boldsymbol{\sigma}_Y^2, \boldsymbol{\theta}, \mathbf{h}_0)] \\
&= \mathbb{E}_{q(\mathbf{z})} \left[ \log \frac{p(\hat{\boldsymbol{\gamma}}, \hat{\boldsymbol{\Gamma}}, \mathbf{z} | \boldsymbol{\sigma}_X^2, \boldsymbol{\sigma}_Y^2, \boldsymbol{\theta}, \mathbf{h}_0)}{q(\mathbf{z})} + \log \frac{q(\mathbf{z})}{p(\mathbf{z} | D, \boldsymbol{\theta}, \mathbf{h}_0)} \right] \\
&= \mathcal{L}(q, \boldsymbol{\theta}) + KL(q(\mathbf{z}) \| p(\mathbf{z} | D, \boldsymbol{\theta}, \mathbf{h}_0)),
\end{aligned}$$

where

$$\begin{aligned}
\mathcal{L}(q; \boldsymbol{\theta}) &:= \mathbb{E}_{q(\mathbf{z})} \left[ \log \frac{p(\hat{\boldsymbol{\gamma}}, \hat{\boldsymbol{\Gamma}}, \mathbf{z} | \boldsymbol{\sigma}_X^2, \boldsymbol{\sigma}_Y^2, \boldsymbol{\theta}, \mathbf{h}_0)}{q(\mathbf{z})} \right], \\
KL(q(\mathbf{z}) \| p(\mathbf{z} | D, \boldsymbol{\theta}, \mathbf{h}_0)) &= \mathbb{E}_{q(\mathbf{z})} \left[ \log \frac{q(\mathbf{z})}{p(\mathbf{z} | D, \boldsymbol{\theta}, \mathbf{h}_0)} \right].
\end{aligned}$$

Given that the Kullback-Leibler (KL) divergence  $KL(\cdot \| \cdot)$  is non-negative,  $\mathcal{L}(q; \boldsymbol{\theta})$  is an evidence lower bound (ELBO) of marginal likelihood. Thus, maximization of ELBO  $\mathcal{L}(q; \boldsymbol{\theta})$  w.r.t. variational distribution  $q$  and parameters  $\boldsymbol{\theta}$  is commonly referred to as E-step and M-step: In the E-step, variational distribution  $q$  is updated to approximate the true posterior distribution. In the M-step, the set of model parameters  $\boldsymbol{\theta}$  is optimized to increase EBLO and thus increase the marginal likelihood.

We adopt mean-field variational Bayes (MFVB) and assume that  $q(\mathbf{z}; \boldsymbol{\eta})$  can be factorized as

$$q(\mathbf{z}; \boldsymbol{\eta}) = q(\beta; \boldsymbol{\eta}) q(\pi_1; \boldsymbol{\eta}) \prod_{j=1}^N q(\gamma_j; \boldsymbol{\eta}) \prod_{j=1}^N q(w_j; \boldsymbol{\eta}).$$

where  $\boldsymbol{\eta}$  collects all the variational parameters. Without further assuming any specific forms of the variational distributions, the optimal variational distributions in the E-step can be obtained naturally as

$$\begin{aligned}
q(\beta | \mu_\beta, \sigma_\beta^2) &= \mathcal{N}(\beta | \mu_\beta, \sigma_\beta^2), \quad q(\boldsymbol{\gamma} | \{\mu_{\gamma_j}, \sigma_{\gamma_j}^2\}) = \prod_{j=1}^N \mathcal{N}(\gamma_j | \mu_{\gamma_j}, \sigma_{\gamma_j}^2), \\
q(\mathbf{w} | \pi_{w_j}) &= \text{Bernoulli}(w_j | \{\pi_{w_j}\}), \quad q(\pi_1 | a, b) = \text{Beta}(\pi_1 | a, b),
\end{aligned}$$

with the updating equations

$$\begin{aligned}
\sigma_\beta^2 &= \left[ \frac{1}{\sigma_0^2} + \sum_{j=1}^N \frac{\pi_{w_j} (\mu_{\gamma_j}^2 + \sigma_{\gamma_j}^2)}{\sigma_{Y_j}^2 + \tau^2} \right]^{-1} \\
\mu_\beta &= \left( \sum_{j=1}^N \frac{\pi_{w_j} \mu_{\gamma_j} \hat{\Gamma}_j}{\sigma_{Y_j}^2 + \tau^2} \right) \sigma_\beta^2, \\
\sigma_{\gamma_j}^2 &= \left[ \frac{1}{\sigma_{X_j}^2} + \frac{\pi_{w_j} (\mu_\beta^2 + \sigma_\beta^2)}{\sigma_{Y_j}^2 + \tau^2} + \frac{1}{\sigma^2} \right]^{-1}, \\
\mu_{\gamma_j} &= \left( \frac{\hat{\gamma}_j}{\sigma_{X_j}^2} + \frac{\pi_{w_j} \mu_\beta \hat{\Gamma}_j}{\sigma_{Y_j}^2 + \tau^2} \right) \sigma_{\gamma_j}^2, \\
a &= a_0 + \sum_{j=1}^N \pi_{w_j}, \quad b = N + 1 - \sum_{j=1}^N \pi_{w_j}, \quad \pi_{w_j} = \frac{q_{j1}}{q_{j0} + q_{j1}}, \\
q_{j0} &= \exp[\psi(b) - \psi(a + b)], \\
q_{j1} &= \exp \left[ -\frac{\log(2\pi)}{2} - \frac{\log(\sigma_{Y_j}^2 + \tau^2)}{2} + \psi(a) - \psi(a + b) \right] \\
&\quad + \exp \left[ -\frac{(\mu_\beta^2 + \sigma_\beta^2)(\mu_{\gamma_j}^2 + \sigma_{\gamma_j}^2) - 2\mu_\beta \mu_{\gamma_j} \hat{\Gamma}_j + \hat{\Gamma}_j^2}{2(\sigma_{Y_j}^2 + \tau^2)} \right],
\end{aligned}$$

where variational parameters are collected in

$$\boldsymbol{\eta} = \{ \mu_\beta, \sigma_\beta^2; a, b; \{ \mu_{\gamma_j}, \sigma_{\gamma_j}^2 \}_{j=1}^N; \{ \pi_{w_j} \}_{j=1}^N \},$$

and  $\psi(\cdot)$  represents the digamma function. In the M-step, by setting the derivative of ELBO w.r.t.  $\sigma^2$  to zero, the updating equation for  $\sigma^2$  can be easily obtained as

$$\sigma^2 = \sum_{j=1}^N (\mu_{\gamma_j}^2 + \sigma_{\gamma_j}^2) / N.$$

Derivation of the updating equation for  $\tau^2$  is much more technical. We have made use of a number of tricks in convex optimization and obtain a closed-form updating equation for  $\tau^2$  as

$$\tau^2 = \sqrt{\frac{\sum_{j=1}^N \frac{\pi_{w_j} [(\mu_\beta^2 + \sigma_\beta^2)(\mu_{\gamma_j}^2 + \sigma_{\gamma_j}^2) - 2\mu_\beta \mu_{\gamma_j} \hat{\Gamma}_j + \hat{\Gamma}_j^2] (\tau^{(\text{old})})^4}{[\sigma_{Y_j}^2 + (\tau^{(\text{old})})^2]^2}}{\sum_{j=1}^N \frac{\pi_{w_j}}{\sigma_{Y_j}^2 + (\tau^{(\text{old})})^2}}},$$

where  $(\tau^{(\text{old})})^2$  is the estimate of  $\tau^2$  at previous iteration. Importantly, all updating approaches in VEM algorithm have closed-forms, ensuring the efficiency and stability of

our proposed algorithm. The details of the above derivation are given in the supplementary document. After convergence of the VEM algorithm, we can obtain the set of optimized variational parameters  $\boldsymbol{\eta}^*$  and the set of estimated model parameters  $\hat{\boldsymbol{\theta}}$ . The posterior mean of  $\beta$  has been naturally given by  $\mu_\beta^*$ , which is very accurate as shown later. However, the posterior variance of  $\beta$  given by MFVB, i.e.,  $(\sigma_\beta^2)^*$ , often underestimates the true posterior variance. We address this issue in next section.

## 2.3 Inference

As inspired by the linear response methods (Giordano et al., 2015, 2018), we propose a closed-form formula to correct the underestimated posterior variance, yielding an accurate inference for  $\beta$ .

For notation convenience, we denote  $p_0(\mathbf{z})$  as the true posterior of interest. We define a perturbation of the true posterior as

$$p_t(\mathbf{z}) := p_0(\mathbf{z}) \exp(t\beta - C(t)),$$

where  $t$  is a scalar and  $C(t)$  normalizes  $p_t(\mathbf{z})$ . When  $t = 0$ ,  $p_t(\mathbf{z})$  becomes the unperturbed posterior  $p_0(\mathbf{z})$ . Clearly,  $p_t(\mathbf{z})$  forms an exponential family parameterized by  $t$ . By the property of the cumulant generating function of exponential families, we have

$$\mathbb{E}_{p_t}[\beta] = \frac{dC(t)}{dt}, \quad \text{Var}_{p_t}[\beta] = \frac{d^2C(t)}{dt^2},$$

implying that the posterior variance of  $\beta$  can be written as

$$\text{Var}_{p_0}[\beta] = \left. \frac{d\mathbb{E}_{p_t}[\beta]}{dt} \right|_{t=0}. \quad (13)$$

This implies that the sensitivity of posterior mean at  $t = 0$  can provide information about the true posterior variance.

Now we introduce the key idea to approximate the posterior variance in Eq. (13) from MFVB. Let  $q_t(\mathbf{z})$  be the mean-field approximation to  $p_t(\mathbf{z})$ , i.e.,  $q_t(\mathbf{z}) := q(\mathbf{z}; \boldsymbol{\eta}_t^*) = \arg \min_q KL(q(\mathbf{z}; \boldsymbol{\eta}) || p_t(\mathbf{z}))$ . Since MFVB often provides accurate inference on posterior mean (Blei et al., 2017), we assume the following conditions hold:

$$\begin{aligned} \text{Condition 1: } & \mathbb{E}_{q_t}[\beta] \approx \mathbb{E}_{p_t}[\beta] \text{ for all } t, \text{ and} \\ \text{Condition 2: } & \left. \frac{d\mathbb{E}_{q_t}[\beta]}{dt} \right|_{t=0} \approx \left. \frac{d\mathbb{E}_{p_t}[\beta]}{dt} \right|_{t=0}. \end{aligned} \quad (14)$$

Condition 1 says that MFVB can provide good approximations to posterior means of all the perturbations. Condition 2 further requires the accuracy of the first order approximation at  $t = 0$ . As we shall show in the supplementary document, the following equation holds:

$$\left. \frac{d\mathbb{E}_{q_t}[\beta]}{dt} \right|_{t=0} = -\mathbf{g}^T \mathbf{H}^{-1} \mathbf{g}, \quad (15)$$

where

$$\mathbf{g} = \left. \frac{d\mathbb{E}_{q(\mathbf{z};\boldsymbol{\eta})}[\beta]}{d\boldsymbol{\eta}^T} \right|_{\boldsymbol{\eta}=\boldsymbol{\eta}_0^*}, \quad \mathbf{H} = \left. \frac{\partial \mathcal{L}(q, \boldsymbol{\theta})}{\partial \boldsymbol{\eta} \partial \boldsymbol{\eta}^T} \right|_{\boldsymbol{\eta}=\boldsymbol{\eta}_0^*}$$

with  $\boldsymbol{\eta}_0^*$  being the set of optimal variational parameters obtained at  $t = 0$ . Note that  $\boldsymbol{\eta}_0^*$  is exactly the parameter set  $\boldsymbol{\eta}^*$  obtained by the MFVB algorithm in Section 2.2. Consequently, combining Eqs. (13,14,15), the posterior variance of  $\beta$  can be approximated by

$$\text{Var}_{p_0}[\beta] = \left. \frac{d\mathbb{E}_{p_t}[\beta]}{dt} \right|_{t=0} \approx \left. \frac{d\mathbb{E}_{q_t}[\beta]}{dt} \right|_{t=0} = -\mathbf{g}^T \mathbf{H}^{-1} \mathbf{g}.$$

To provide statistical inference on  $\beta$  as what many MR methods offered, we specify  $\sigma_0$  in Eq. (10) as  $1 \times 10^6$  throughout this paper. In such a way, BWMR can provide the estimate of  $\beta$  using  $\mu_\beta^*$ , its standard error using  $\sqrt{\text{Var}_{p_0}[\beta]}$  and corresponding  $p$ -value. We shall use simulation study to evaluate whether the above proposed method indeed provides an accurate inference.

## 3 Results

### 3.1 Simulation study

To closely mimic real data analysis, we simulated individual-level data, and then obtained  $(\hat{\gamma}_j, \sigma_{X_j}, p_{X_j})$  and  $(\hat{\Gamma}_j, \sigma_{Y_j}, p_{Y_j})$  by simple linear regression. We also included the IVs selection procedure in the simulation study to investigate the potential effect of selection bias. Let  $\mathbf{G}_1 \in \mathbb{R}^{n_1 \times N_0}$  and  $\mathbf{G}_2 \in \mathbb{R}^{n_2 \times N_0}$  be the individual-level genotype data for exposure  $X$  and outcome  $Y$ , where  $N_0$  was the number of genotyped SNPs,  $n_1$  and  $n_2$  were sample sizes of exposure data and outcome data, respectively. The columns of  $\mathbf{G}_1$  and  $\mathbf{G}_2$  were generated independently such that these independent SNPs could serve as IVs. The minor allele frequencies of the SNPs were drawn from the uniform distribution  $U[0.05, 0.5]$ . The

vectors of effect sizes  $\boldsymbol{\gamma}$  and  $\boldsymbol{\Gamma} = \beta\boldsymbol{\gamma} + \boldsymbol{\alpha}$  were simulated based on a four-group model (Chung et al., 2014) to investigate the influence of horizontal pleiotropy. Let  $\mathcal{G}_{00}, \mathcal{G}_{10}, \mathcal{G}_{01}$ , and  $\mathcal{G}_{11}$  denote these four groups of SNPs, and  $\pi_{00}, \pi_{10}, \pi_{01}$  and  $\pi_{11}$  denote the proportions of SNPs in these four groups, respectively. The four groups of SNPs were given as follows.

- In  $\mathcal{G}_{00}$ , the SNPs affected neither exposure  $X$  nor outcome  $Y$ , i.e.,  $\gamma_j = 0, \alpha_j = 0$ . The SNPs in this group were irrelevant, serving as noise IVs.
- In  $\mathcal{G}_{10}$ , the SNPs affected exposure  $X$  only, i.e.,  $\gamma_j \neq 0$  and  $\alpha_j = 0$ . The SNPs included in this group served as valid IVs in the framework of MR.
- In  $\mathcal{G}_{01}$ , the SNPs affected outcome  $Y$  only, i.e.,  $\gamma_j = 0$  and  $\alpha_j \neq 0$ . The SNPs in this group are noise IVs.
- In  $\mathcal{G}_{11}$ , the SNPs directly affected both exposure  $X$  and outcome  $Y$ , i.e.,  $\gamma_j, \alpha_j \neq 0$ . This group was used to mimic the phenomenon of horizontal pleiotropy. The SNPs in this group could be selected as IVs, but they were actually invalid.

For nonzero  $\gamma_j$  and  $\alpha_j$ , they were simulated from  $\mathcal{N}(0, \sigma_\gamma^2)$  and  $\mathcal{N}(0, \sigma_\alpha^2)$ . Given the vectors of effect sizes, we generated the vectors of phenotypes as  $\mathbf{x} = \mathbf{G}_1\boldsymbol{\gamma} + \boldsymbol{\varepsilon}_1$  and  $\mathbf{y} = \mathbf{G}_2\boldsymbol{\Gamma} + \boldsymbol{\varepsilon}_2$ , where  $\boldsymbol{\varepsilon}_1$  and  $\boldsymbol{\varepsilon}_2$  were independent noises from  $\mathcal{N}(0, \sigma_{\varepsilon_1}^2)$  and  $\mathcal{N}(0, \sigma_{\varepsilon_2}^2)$ , respectively. To evaluate the type I error and statistical power of different methods, we varied  $\beta \in \{0.0, 0.1, 0.2, 0.3, 0.4, 0.5\}$  and group proportions  $\{\pi_{00}, \pi_{10}, \pi_{01}, \pi_{11}\}$  while controlled the two signal-noise-ratios ( $SNR_1 := \sqrt{\text{Var}(\mathbf{G}_1\boldsymbol{\gamma})/\text{Var}(\boldsymbol{\varepsilon}_1)}$  and  $SNR_2 := \sqrt{\text{Var}(\mathbf{G}_2\boldsymbol{\Gamma})/\text{Var}(\boldsymbol{\varepsilon}_2)}$ ) at 1:1 by specifying the variance parameters  $\{\sigma_\gamma^2, \sigma_\alpha^2, \sigma_{\varepsilon_1}^2, \sigma_{\varepsilon_2}^2\}$ . Throughout the simulation study, we set sample sizes for exposure and outcome data as  $n_1 = n_2 = 5,000$  and the number of total SNPs as  $N_0 = 10,000$ .

With individual-level data  $\{\mathbf{G}_1, \mathbf{G}_2, \mathbf{x}, \mathbf{y}\}$ , we obtained the summary-level statistics  $\hat{\gamma}_j, \hat{\Gamma}_j$ , with their standard errors  $\sigma_{X_j}, \sigma_{Y_j}$  and  $p$ -values  $p_{X_j}, p_{Y_j}$ ,  $j = 1, 2, \dots, N_0$ , by regressing  $\mathbf{x}$  on each column of  $\mathbf{G}_1$  and  $\mathbf{y}$  on each column of  $\mathbf{G}_2$ , respectively. Then we selected SNPs as IVs if their  $p$ -values were smaller than a given threshold at  $1 \times 10^{-5}$ . As a result, the input data set for four MR methods (i.e., BWMR, Egger, GSMR, and RAPS) was given as  $D = \{\hat{\gamma}_j, \sigma_{X_j}^2, \hat{\Gamma}_j, \sigma_{Y_j} | p_{X_j} \leq 1 \times 10^{-5}\}$ . In our simulation study, we observed that all the MR methods gave biased estimates of  $\beta$  (see results in Fig. 24 of the supplementary

document). In fact, this phenomenon should be attributed to winner’s curse in the context of GWAS (Zhong and Prentice, 2008) or selection bias in statistical literature (Efron, 2011). Briefly speaking,  $\hat{\gamma}_j$  in the input data set  $D$  is selected based on  $p_{X_j} \leq 1 \times 10^{-5}$ , and thus  $\mathbb{E}[\hat{\gamma}_j | \gamma_j; p_{X_j} \leq 1 \times 10^{-5}] \neq \mathbb{E}[\hat{\gamma}_j | \gamma_j] = \gamma_j$ , i.e., the extracted effect size  $\hat{\gamma}_j$  would be a biased estimate of  $\gamma_j$  due to the selection process ( $p_{X_j} < 1 \times 10^{-5}$ ). To avoid selection bias, we simulated two independent datasets for the exposure (i.e.,  $\mathbf{x} = \mathbf{G}_1\boldsymbol{\gamma} + \boldsymbol{\varepsilon}_1$  and  $\tilde{\mathbf{x}} = \tilde{\mathbf{G}}_1\boldsymbol{\gamma} + \tilde{\boldsymbol{\varepsilon}}_1$  with equal sample sizes  $n_1 = \tilde{n}_1$ ). We used one data set (i.e.,  $\{\mathbf{G}_1, \mathbf{x}\}$ ) to compute  $p$ -values for SNP selection and used another data set (i.e.,  $\{\tilde{\mathbf{G}}_1, \tilde{\mathbf{x}}\}$ ) to extract the corresponding estimated SNP-exposure effects and its standard error  $\{\hat{\gamma}_j, \sigma_{X_j}\}$ . In such a way, the issue of selection bias was avoided in our simulation study.

To investigate the performance of BWMR and three other related MR methods on the influence of horizontal pleiotropy, we varied the proportion  $\frac{\pi_{11}}{\pi_{10} + \pi_{11}} \in \{0.2, 0.5, 0.8\}$ , approximately controlling the proportion of IVs affected by horizontal pleiotropy among all IVs at 20%, 50%, 80% respectively. We observed that BWMR showed satisfactory performance in terms of estimation accuracy, type I error control and statistical power, as shown in Fig. 1. The satisfactory performance of BWMR can be attributed to its following properties: 1. adaptive use of variance component  $\tau^2$  to account for weak pleiotropic effects; 2. robustness to strong horizontal pleiotropy guaranteed by the Bayesian weighting scheme; 3. stable and efficient algorithm for parameter estimation and inference. From the simulation study, we also observed that GSMR seemed to have the highest statistical power among all the MR methods. However, the  $p$ -value of GSMR was also observed to be inflated in the qq-plot when a higher proportion of IVs (e.g., 50%, 80%) affected by horizontal pleiotropy (see supplementary Fig. S20). Thus, the type I error rate of GSMR was unable to be controlled at the nominal level. This is because GSMR ignored the weak pleiotropic effects and underestimated the standard error of the casual effect. Egger was found to be the most conservative one among the four MR methods. Its estimation was observed to have the largest variance because the intercept term introduced in Egger was unable to model the weak pleiotropic effects which should not be simply treated as a constant. Among the four MR methods, BWMR and RAPS had similar performance in this simulation study, but RAPS was found to be numerically not stable in the next real

data analysis part. To have a better understanding of the four MR methods, we provided a detailed discussion about their relationship in the supplementary document (see our supplementary note). To make the simulation results easily reproducible, we have made the code of our simulation study available at <https://github.com/jiazha097/sim-BWMR>.

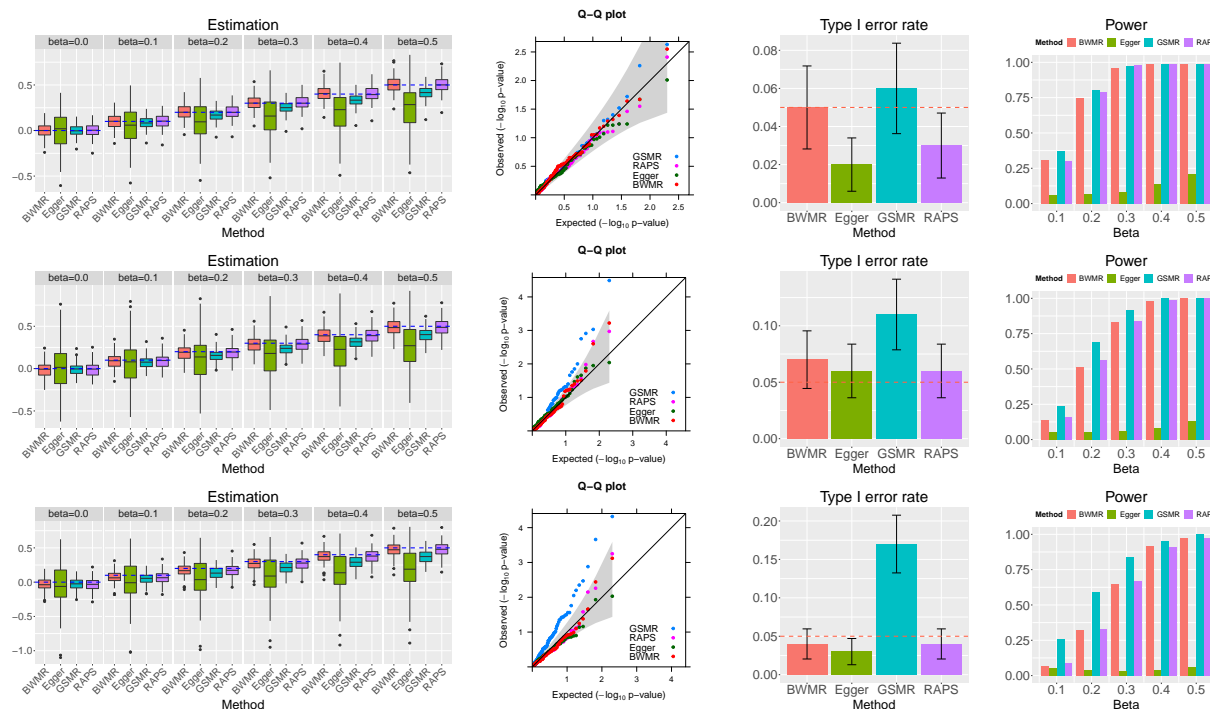


Figure 1: Comparison of MR methods affected by horizontal pleiotropy (the proportions of horizontal pleiotropic IVs were specified as  $\frac{\pi_{11}}{\pi_{10} + \pi_{11}} = 20\%$ ,  $50\%$ , and  $80\%$ , in the top, middle and bottom panel, respectively). The parameters were chosen to be  $N_0 = 10,000$ ,  $n_1 = n_2 = 5,000$ ,  $\beta \in \{0.0, 0.1, 0.2, 0.3, 0.4, 0.5\}$ ,  $SNR_1 = SNR_2 = 1 : 1$ , and  $p$ -value threshold  $= 1 \times 10^{-5}$ . We evaluated the empirical type I error rate and power by controlling type I error rates at the nominal level 0.05. The results were summarized from 100 replications.

## 3.2 Real Data Analysis

### 3.2.1 Materials

To investigate the influence of selection bias on real data analysis and the reliability of the four MR methods, we collected three different GWASs of four global lipids, i.e., high-density

lipoprotein (HDL) cholesterol (HDL-C), low-density lipoprotein (LDL) cholesterol (LDL-C), triglycerides (TG) and total cholesterol (TC). For narrative convenience, we shall refer them as Data-A (Willer et al., 2013), Data-B (Kettunen et al., 2016) and Data-C (Klarin et al., 2018) (the details of the three GWASs are given in the supplementary document). It is worthwhile to note that Data-C only includes SNPs significantly associated with global lipids.

Besides the four global lipids in Data-A, Data-B, and Data-C, we further collected GWAS summary statistics, covering 126 metabolites (Kettunen et al., 2016) and 93 human complex traits. These metabolites include lipoprotein (e.g. very-low-density lipoprotein (VLDL) and LDL), fasting glucose, Vitamin D levels and serum urate. The 93 human complex traits include anthropometric traits (e.g. body mass index (BMI)), cardiovascular measures (e.g. coronary artery disease (CAD)), immune system disorders (e.g. atopic dermatitis), metabolic traits (e.g. dyslipidemia), neurodegenerative diseases (e.g. Alzheimers disease (AD)), psychiatric disorders (e.g. bipolar disorder), social traits (e.g. intelligence) and other complex traits (e.g. breast cancer). The details of summary statistics are given in the supplementary document.

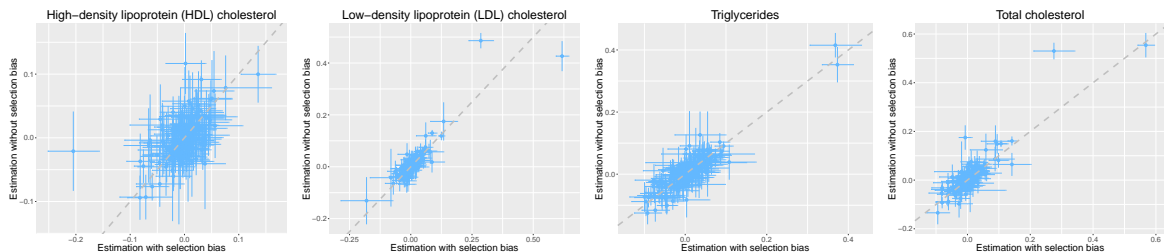


Figure 2: Comparisons of analysis results provided by BWMR with selection bias ( $x$ -axis) and without selection bias ( $y$ -axis). The dots represent estimated causal effect sizes  $\hat{\beta}$  and the bars represent their standard errors  $se(\hat{\beta})$ . The diagonal is indicated by the dashed line.

### 3.2.2 Examination of selection bias

In this subsection, we consider estimating the causal effect  $\beta$  of each of four global lipids (i.e., HDL-C, LDL-C, TG and TC) on 93 complex traits. Given Data-A and Data-B,

to avoid potential selection bias, we used one exposure data set (e.g., Data-A) to select IVs and extracted the corresponding estimated effect sizes and their standard errors in another exposure data set (e.g., Data-B), i.e.,  $\{\hat{\gamma}_j, \sigma_{X_j}\}$ . Based on the selected IVs, we also obtained effect sizes and their standard errors from the outcome data sets, i.e.,  $\{\hat{\Gamma}_j, \sigma_{Y_j}\}$ . The analysis based on this type of input data was expected to provide unbiased estimation results. To investigate selection bias, we selected IVs and extracted the estimated effect sizes and standard errors using the same data set (e.g., Data-A). Therefore, this type of input data was expected to suffer from selection bias. We applied BWMR to both unbiased and biased input data sets, and compared the analysis results to evaluate the influence of selection bias. The results from BWMR are shown in Fig. 2, and the results from other three methods are shown in the supplementary Figs. 26, 27 and 28. Although the analysis results were expected to be different, no systematic discrepancies between biased results and unbiased results were observed. As we illustrated in simulation study, the influence of selection bias decreases as the sample size increases (see supplementary Fig. 25). Note that the sample sizes of Data-A and Data-B are very large ( $n_A = 188,577$  and  $n_B = 24,925$ , respectively). The sample sizes are large enough such that the influence of selection bias would be ignorable. As a result, we concluded that selection bias might not introduce much bias when we were analyze the causal effects between those metabolites and complex traits in this paper.

### 3.2.3 Consistency of BWMR’s analysis results

Before applying BWMR to infer the causal effects between hundreds of metabolites and complex traits, we first checked the reliability of BWMR’s analysis results on the four global lipids. To do so, we explored the third data set, i.e., Data-C, to select IVs, and then used Data-A and Data-B to extract exposure effect sizes and their standard errors, denoted as  $\{\hat{\gamma}_j^{(A)}, \sigma_{X_j}^{(A)}\}$  and  $\{\hat{\gamma}_j^{(B)}, \sigma_{X_j}^{(B)}\}$ , and then extracted the outcome effect sizes and their standard errors  $\{\hat{\Gamma}_j, \sigma_{Y_j}\}$ . After that, we applied BWMR to  $\{\hat{\gamma}_j^{(A)}, \sigma_{X_j}^{(A)}, \hat{\Gamma}_j, \sigma_{Y_j}\}$  and  $\{\hat{\gamma}_j^{(B)}, \sigma_{X_j}^{(B)}, \hat{\Gamma}_j, \sigma_{Y_j}\}$ . The analysis results are shown in Fig. 3. The results of other three MR methods are shown in supplementary Figs. 29, 30 and 31. We can see clearly that the results based on Data-A and Data-B agree well with each other, indicating that estimating

the causal relationship between metabolites and complex traits by BWMR can be quite reliable.

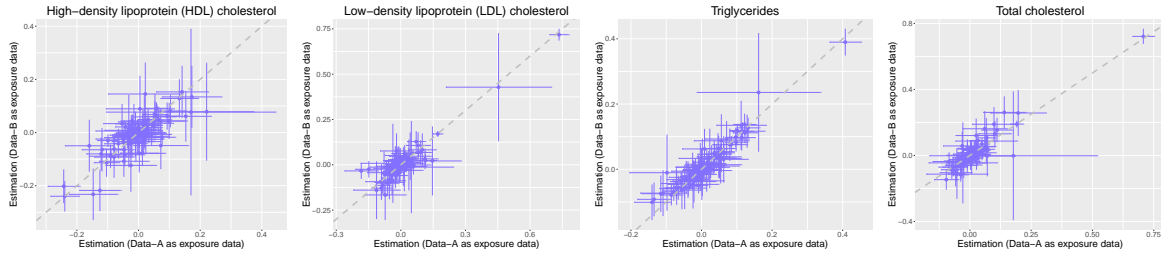


Figure 3: Comparisons of analysis results provided by BWMR using Data-A as exposure data ( $x$ -axis) and using Data-B as exposure data ( $y$ -axis). The dots represent estimated causal effect sizes  $\hat{\beta}$  and the bars represent their standard errors  $se(\hat{\beta})$ . The diagonal is indicated by the dashed line.

### 3.2.4 MR-based causal inference between metabolites and complex traits

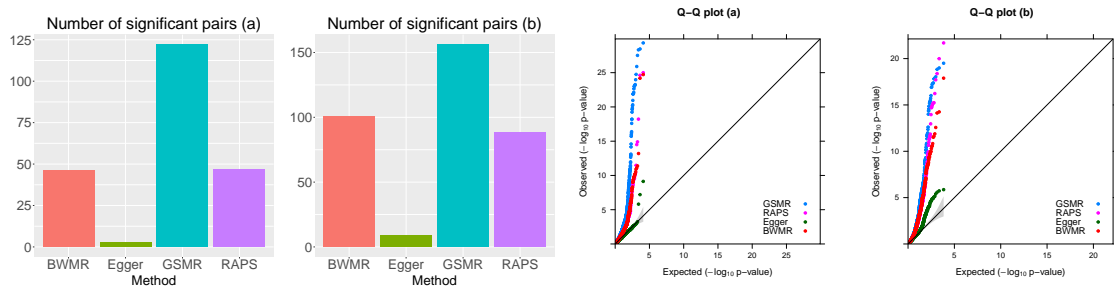


Figure 4: Left: numbers of significant causal effects of metabolites on complex traits; Middle Left: numbers of significant causal effects of complex traits on metabolites; Middle Right: QQ plot of  $p$ -values based on estimates of causal effects of metabolites on complex traits; Right: QQ plot of  $p$ -values based on estimates of causal effects of complex traits on metabolites.

After carefully examining the selection bias issue and consistency of four MR methods, it is ready for us to apply BWMR and the other three MR methods to estimate: (a) the causal effects of metabolites on complex human traits, and (b) the causal effects of complex traits on metabolites. The analysis results are summarized in supplementary Figs. 37-49.

We observed a protective effect of HDL-C against the trait dyslipidemia ( $\hat{\beta} = -0.20$ ,  $p$ -value =  $1.36 \times 10^{-5}$ ), and positive effects of LDL-C ( $\hat{\beta} = 0.62$ ,  $p$ -value =  $2.64 \times 10^{-128}$ ) and TG ( $\hat{\beta} = 0.37$ ,  $p$ -value =  $1.26 \times 10^{-22}$ ) on dyslipidemia. Note that the diagnostic criterion for dyslipidemia includes abnormally low level of HDL-C and abnormally high levels of LDL-C and / or TG (Teramoto et al., 2007). Our observations are consistent with the diagnostic criterion, indicating the reliability of our real data analysis results.

Besides those identified significant causal effects between metabolites and dyslipidemia, we identified 46, 101 significant associations based on Bonferroni correction at level 0.05 in (a), (b) respectively. Among these significant findings, some previous research outcomes are successfully replicated in our analysis. For example, we observed LDL-C had a significant risk effect on CAD ( $\hat{\beta} = 0.13$ ,  $p$ -value =  $1.90 \times 10^{-25}$ ) as confirmed by RCTs (FERENCE et al., 2017). Similarly, positive causal effects of metabolites included in the class of HDL on CAD were also observed. Serum urate was found to have a positive causal effect on gout ( $\hat{\beta} = 0.27$ ,  $p$ -value =  $1.49 \times 10^{-36}$ ), supporting the result of a previous individual participant data analysis (Dalbeth et al., 2018). Importantly, our results also provided several new insights. For example, we found AD positively affected 47 metabolites (e.g., apoB, metabolites included in LDL and VLDL). As expected, the effect of AD on HDL-C was opposite to its corresponding effect on LDL-C, i.e., a negative effect of AD on HDL-C ( $\hat{\beta} = -0.13$ ,  $p$ -value =  $9.34 \times 10^{-6}$ ) was identified. We also observed significant causal effects of BMI on 37 metabolites, including 30 positive effects (e.g., effects on TG, serum urate, and metabolites included in VLDL) and seven negative effects on metabolites included in HDL. Interestingly, although AD and BMI were found to significantly affect many metabolites, no metabolites were observed to have causal effects on AD or BMI. Additionally, we found that glycated hemoglobin levels had positive effects on TC ( $\hat{\beta} = 0.22$ ,  $p$ -value =  $4.93 \times 10^{-6}$ ) and LDL-C ( $\hat{\beta} = 0.19$ ,  $p$ -value =  $1.01 \times 10^{-5}$ ). On the contrary, height was found to have negative effects on TC ( $\hat{\beta} = -0.07$ ,  $p$ -value =  $2.16 \times 10^{-10}$ ) and LDL-C ( $\hat{\beta} = -0.05$ ,  $p$ -value =  $2.29 \times 10^{-7}$ ).

To have a better understanding of the statistical properties of four MR methods, we compared the numbers of causal associations identified by four MR methods after Bonferroni correction, and conducted qq-plots for  $p$ -value from the four methods, displayed in Fig.

4. Consistent with our simulation study, the power of GSMR seems to be the highest among the four MR methods. As we explained in simulation, the high power of GSMR comes along with an expensive price, that is, its type I error rate can not be controlled at the nominal level. To be more specific, we offered real data illustrative examples in supplementary Figs. 32, 30. As we can see more clearly, the inflated type I error of GSMR can be attributed to the ignored weak pleiotropic effects and the ad-hoc procedure for outlier detection. Egger was observed to have the lowest statistical power among the four methods. Although the intercept term may help to correct for the bias caused by horizontal pleiotropic effects, the presence of weak pleiotropic effects leads to a large variance of Egger’s estimation. In addition, we found that Egger was not robust to large pleiotropic effects (i.e., outliers), and would suffer from improper outlier detection as shown in supplementary Figs. 34 and 35. It seems that the results of BWMR and RAPS are quite similar to each other. However, we found RAPS was numerically unstable in real data analysis (see supplementary Figs. 43-45), while BWMR provided stable estimates.

## 4 Conclusion

We have introduced a statistical approach, BWMR, for causal inference based on summary statistics from GWAS. BWMR can not only accounts for the uncertainty of estimated weak effects and weak horizontal pleiotropic effects, but also adaptively detect outliers due to a few large horizontal pleiotropic effects. Through comprehensive simulations and real data analysis, BWMR is shown to be statistically efficient and computationally stable. As more summary data will become publicly available, BWMR is believed to be of widely use in the future.

## SUPPLEMENTARY MATERIAL

**Supplementary Document.pdf** The document includes the detailed derivation of the algorithm for BWMR, comparison of MR methods, more simulation results, sources of GWAS summary statistics datasets used in the this paper, and more real data analysis results. (PDF)

**R-package for BWMR** R-package 'BWMR'. The package containing the functions used in BWMR and an example of applying BWMR to real data is available at <https://github.com/jiazhao97/BWMR>.

# Supplementary Document

## A The variational EM algorithm

Let  $D = \{\hat{\gamma}, \hat{\Gamma}, \boldsymbol{\sigma}_X, \boldsymbol{\sigma}_Y\}$  denote the summary statistics serving as the input data,  $\mathbf{z} = \{\beta, \pi_1, \mathbf{w}, \boldsymbol{\gamma}\}$  be the collection of latent variables,  $\boldsymbol{\theta} = \{\tau^2, \sigma^2\}$  be the set of the model parameters to be optimized and  $\mathbf{h}_0 = \{\sigma_0 = 1 \times 10^6, a_0 = 100\}$  be the collection of fixed hyperparameters. Then according to BWMR, the logarithm of complete-data likelihood is given as

$$\begin{aligned}
 & \log \Pr(\hat{\gamma}, \hat{\Gamma}, \mathbf{z} | \boldsymbol{\sigma}_X^2, \boldsymbol{\sigma}_Y^2, \boldsymbol{\theta}, \mathbf{h}_0) \\
 &= \sum_{j=1}^N \left[ -\frac{\log(\sigma_{X_j}^2)}{2} - \frac{(\hat{\gamma}_j - \gamma_j)^2}{2\sigma_{X_j}^2} \right] \\
 & \quad + \sum_{j=1}^N w_j \left[ -\frac{\log(2\pi)}{2} - \frac{\log(\sigma_{Y_j}^2 + \tau^2)}{2} - \frac{(\hat{\Gamma}_j - \beta\gamma_j)^2}{2(\sigma_{Y_j}^2 + \tau^2)} \right] \\
 & \quad - \frac{\beta^2}{2\sigma_0^2} + \sum_{j=1}^N \left[ -\frac{\log(\sigma^2)}{2} - \frac{\gamma_j^2}{2\sigma^2} \right] \\
 & \quad + \sum_{j=1}^N [w_j \log(\pi_1) + (1 - w_j) \log(1 - \pi_1)] \\
 & \quad + (a_0 - 1) \log(\pi_1) + \text{constant}.
 \end{aligned}$$

To provide accurate statistical inference, we are interested in posterior distribution of the latent variables:

$$\Pr(\mathbf{z} | D, \boldsymbol{\theta}, \mathbf{h}_0) = \frac{\Pr(\hat{\gamma}, \hat{\Gamma}, \mathbf{z} | \boldsymbol{\sigma}_X^2, \boldsymbol{\sigma}_Y^2, \boldsymbol{\theta}, \mathbf{h}_0)}{\Pr(\hat{\gamma}, \hat{\Gamma} | \boldsymbol{\sigma}_X^2, \boldsymbol{\sigma}_Y^2, \boldsymbol{\theta}, \mathbf{h}_0)},$$

where

$$\Pr(\hat{\gamma}, \hat{\Gamma} | \boldsymbol{\sigma}_X^2, \boldsymbol{\sigma}_Y^2, \boldsymbol{\theta}, \mathbf{h}_0) = \int_{\mathbf{z}} \Pr(\hat{\gamma}, \hat{\Gamma}, \mathbf{z} | \boldsymbol{\sigma}_X^2, \boldsymbol{\sigma}_Y^2, \boldsymbol{\theta}, \mathbf{h}_0) d\mathbf{z}.$$

However, exact evaluation of the posterior distribution is very challenging because the integration is intractable.

Instead, we propose a variational expectation-maximization (VEM) algorithm to approximate the posterior. Let  $q(\mathbf{z})$  be a variational distribution. The logarithm of the

marginal likelihood can be written as

$$\begin{aligned}
& \log \Pr(\hat{\boldsymbol{\gamma}}, \hat{\boldsymbol{\Gamma}} | \boldsymbol{\sigma}_X^2, \boldsymbol{\sigma}_Y^2, \boldsymbol{\theta}, \mathbf{h}_0) \\
&= \mathbb{E}_{q(\mathbf{z})} [\log \Pr(\hat{\boldsymbol{\gamma}}, \hat{\boldsymbol{\Gamma}} | \boldsymbol{\sigma}_X^2, \boldsymbol{\sigma}_Y^2, \boldsymbol{\theta}, \mathbf{h}_0)] \\
&= \mathbb{E}_{q(\mathbf{z})} \left[ \log \frac{\Pr(\hat{\boldsymbol{\gamma}}, \hat{\boldsymbol{\Gamma}}, \mathbf{z} | \boldsymbol{\sigma}_X^2, \boldsymbol{\sigma}_Y^2, \boldsymbol{\theta}, \mathbf{h}_0)}{q(\mathbf{z})} + \log \frac{q(\mathbf{z})}{\Pr(\mathbf{z} | D, \boldsymbol{\theta}, \mathbf{h}_0)} \right] \\
&= \mathcal{L}(q, \boldsymbol{\theta}) + D_{KL}(q(\mathbf{z}) \| \Pr(\mathbf{z} | D, \boldsymbol{\theta}, \mathbf{h}_0)),
\end{aligned}$$

where

$$\begin{aligned}
\mathcal{L}(q, \boldsymbol{\theta}) &:= \mathbb{E}_{q(\mathbf{z})} \left[ \log \frac{\Pr(\hat{\boldsymbol{\gamma}}, \hat{\boldsymbol{\Gamma}}, \mathbf{z} | \boldsymbol{\sigma}_X^2, \boldsymbol{\sigma}_Y^2, \boldsymbol{\theta}, \mathbf{h}_0)}{q(\mathbf{z})} \right], \\
D_{KL}(q(\mathbf{z}) \| \Pr(\mathbf{z} | D, \boldsymbol{\theta}, \mathbf{h}_0)) &= \mathbb{E}_{q(\mathbf{z})} \left[ \log \frac{q(\mathbf{z})}{\Pr(\mathbf{z} | D, \boldsymbol{\theta}, \mathbf{h}_0)} \right].
\end{aligned}$$

Given that the Kullback-Leibler (KL) divergence  $D_{KL}(\cdot \| \cdot)$  is non-negative,  $\mathcal{L}(q; \boldsymbol{\theta})$  is an evidence lower bound (ELBO) of marginal likelihood. Thus, maximization of ELBO  $\mathcal{L}(q; \boldsymbol{\theta})$  w.r.t. variational distribution  $q$  and parameters  $\boldsymbol{\theta}$  is commonly referred to as E-step and M-step: In the E-step, variational distribution  $q$  is updated to approximate the true posterior distribution. In the M-step, the set of model parameters  $\boldsymbol{\theta}$  is optimized to increase EBLO and thus increase the marginal likelihood.

## A.1 E-step

We adopt mean-field variational Bayes (MFVB) and assume that  $q(\mathbf{z})$  can be factorized as

$$q(\mathbf{z}) = q(\beta)q(\pi_1) \prod_{j=1}^N q(\gamma_j) \prod_{j=1}^N q(w_j).$$

Then to optimize ELBO  $\mathcal{L}(q, \boldsymbol{\theta})$  w.r.t.  $q(\beta)$ , we re-arrange it into the terms with and without  $q(\beta)$ :

$$\begin{aligned}
& \mathcal{L}(q, \boldsymbol{\theta}) \\
&= \mathbb{E}_{q(\mathbf{z})} \left[ \log \frac{\Pr(\hat{\boldsymbol{\gamma}}, \hat{\boldsymbol{\Gamma}}, \mathbf{z} | \boldsymbol{\sigma}_X^2, \boldsymbol{\sigma}_Y^2, \boldsymbol{\theta}, \mathbf{h}_0)}{q(\mathbf{z})} \right] \\
&= \int q(\beta) q(\pi_1) \prod_{j=1}^N q(\gamma_j) \prod_{j=1}^N q(w_j) [\log \Pr(\hat{\boldsymbol{\gamma}}, \hat{\boldsymbol{\Gamma}}, \mathbf{z} | \boldsymbol{\sigma}_X^2, \boldsymbol{\sigma}_Y^2, \boldsymbol{\theta}, \mathbf{h}_0) - \log q(\beta)] d\mathbf{z} \\
&\quad - \int q(\beta) q(\pi_1) \prod_{j=1}^N q(\gamma_j) \prod_{j=1}^N q(w_j) [\log(\pi_1) + \sum_{j=1}^N (\log q(\gamma_j) + \log q(w_j))] d\mathbf{z} \\
&= \int q(\beta) \left[ \mathbb{E}_{q_{-\beta}} (\log \Pr(\hat{\boldsymbol{\gamma}}, \hat{\boldsymbol{\Gamma}}, \mathbf{z} | \boldsymbol{\sigma}_X^2, \boldsymbol{\sigma}_Y^2, \boldsymbol{\theta}, \mathbf{h}_0)) - \log q(\beta) \right] d\beta + \text{constant},
\end{aligned} \tag{16}$$

where  $q_{-\beta}$  denotes  $q(\pi_1) \prod_{j=1}^N q(\gamma_j) \prod_{j=1}^N q(w_j)$  and the constant does not relate to  $q(\beta)$ . By defining a new distribution

$$\tilde{p}(\beta) \propto \mathbb{E}_{q_{-\beta}} (\log \Pr(\hat{\boldsymbol{\gamma}}, \hat{\boldsymbol{\Gamma}}, \mathbf{z} | \boldsymbol{\sigma}_X^2, \boldsymbol{\sigma}_Y^2, \boldsymbol{\theta}, \mathbf{h}_0)),$$

we can further summarize Eq. (16) as

$$\mathcal{L}(q, \boldsymbol{\theta}) = -D_{KL}(q(\beta) \| \tilde{p}(\beta)) + \text{constant}. \tag{17}$$

From Eq. (17) we can see that the optimal  $q(\beta)$  is given as

$$q(\beta) = \tilde{p}(\beta) \propto \mathbb{E}_{q_{-\beta}} [\log \Pr(\hat{\boldsymbol{\gamma}}, \hat{\boldsymbol{\Gamma}}, \mathbf{z} | \boldsymbol{\sigma}_X^2, \boldsymbol{\sigma}_Y^2, \boldsymbol{\theta}, \mathbf{h}_0)].$$

Thus,

$$\begin{aligned}
\log q(\beta) &= \mathbb{E}_{q_{-\beta}} [\log \Pr(\hat{\boldsymbol{\gamma}}, \hat{\boldsymbol{\Gamma}}, \mathbf{z} | \boldsymbol{\sigma}_X^2, \boldsymbol{\sigma}_Y^2, \boldsymbol{\theta}, \mathbf{h}_0)] + \text{constant} \\
&= \mathbb{E}_{q_{-\beta}} \left[ -\frac{\beta^2}{2\sigma_0^2} - \sum_{j=1}^N \frac{w_j}{2(\sigma_{Y_j}^2 + \tau^2)} (\hat{\Gamma}_j - \beta \gamma_j)^2 \right] + \text{constant} \\
&= \left[ -\frac{1}{2\sigma_0^2} - \sum_{j=1}^N \frac{\mathbb{E}_q(w_j \gamma_j^2)}{2(\sigma_{Y_j}^2 + \tau^2)} \right] \beta^2 + \left( \sum_{j=1}^N \frac{\mathbb{E}_q(w_j \gamma_j) \hat{\Gamma}_j}{\sigma_{Y_j}^2 + \tau^2} \right) \beta + \text{constant},
\end{aligned}$$

Because  $\log q(\beta)$  is a quadratic form, we know  $q(\beta)$  is the density function of an Gaussian distribution  $q(\beta) = \mathcal{N}(\mu_\beta, \sigma_\beta^2)$ :

$$\sigma_\beta^2 = \left[ \frac{1}{\sigma_0^2} + \sum_{j=1}^N \frac{\mathbb{E}(w_j \gamma_j^2)}{\sigma_{Y_j}^2 + \tau^2} \right]^{-1}, \quad \mu_\beta = \left[ \sum_{j=1}^N \frac{\mathbb{E}(w_j \gamma_j) \hat{\Gamma}_j}{\sigma_{Y_j}^2 + \tau^2} \right] \sigma_\beta^2.$$

Similarly, the optimal solution of  $q(\gamma_j)$  is given by

$$\begin{aligned}
\log q(\gamma_j) &= \mathbb{E}_{q-\gamma_j} [\log \Pr(\hat{\boldsymbol{\gamma}}, \hat{\boldsymbol{\Gamma}}, \mathbf{z} | \boldsymbol{\sigma}_X^2, \boldsymbol{\sigma}_Y^2, \boldsymbol{\theta}, \mathbf{h}_0)] + \text{constant} \\
&= \mathbb{E}_{q-\gamma_j} \left[ -\frac{1}{2\sigma_{X_j}^2} (\hat{\gamma}_j - \gamma_j)^2 - \frac{w_j}{2(\sigma_{Y_j}^2 + \tau^2)} (\hat{\Gamma}_j - \beta\gamma_j)^2 - \frac{1}{2\sigma^2} \gamma_j^2 \right] + \text{constant} \\
&= -\frac{\gamma_j^2 - 2\hat{\gamma}_j\gamma_j + \hat{\gamma}_j^2}{2\sigma_{X_j}^2} - \frac{\mathbb{E}(w_j\beta^2)\gamma_j^2 - 2\hat{\Gamma}_j\mathbb{E}(w_j\beta)\gamma_j}{2(\sigma_{Y_j}^2 + \tau^2)} - \frac{\gamma_j^2}{2\sigma^2} + \text{constant} \\
&= \left[ -\frac{1}{2\sigma_{X_j}^2} - \frac{\mathbb{E}_q(w_j\beta^2)}{2(\sigma_{Y_j}^2 + \tau^2)} - \frac{1}{2\sigma^2} \right] \gamma_j^2 + \left[ \frac{\hat{\gamma}_j}{\sigma_{X_j}^2} + \frac{\mathbb{E}_q(w_j\beta)\hat{\Gamma}_j}{\sigma_{Y_j}^2 + \tau^2} \right] \gamma_j + \text{constant}.
\end{aligned}$$

The quadratic form of  $\log q(\gamma_j)$  indicates that  $q(\gamma_j)$  is the density of a Gaussian distribution, i.e.,  $q(\gamma_j) = \mathcal{N}(\mu_{\gamma_j}, \sigma_{\gamma_j}^2)$  with

$$\sigma_{\gamma_j}^2 = \left[ \frac{1}{\sigma_{X_j}^2} + \frac{\mathbb{E}(w_j\beta^2)}{\sigma_{Y_j}^2 + \tau^2} + \frac{1}{\sigma^2} \right]^{-1}, \quad \mu_{\gamma_j} = \left[ \frac{\hat{\gamma}_j}{\sigma_{X_j}^2} + \frac{\mathbb{E}(w_j\beta)\hat{\Gamma}_j}{\sigma_{Y_j}^2 + \tau^2} \right] \sigma_{\gamma_j}^2.$$

For latent variable  $\pi_1$ , accordingly, we have

$$\begin{aligned}
q(\pi_1) &= \mathbb{E}_{q-\pi_1} [\log \Pr(\hat{\boldsymbol{\gamma}}, \hat{\boldsymbol{\Gamma}}, \mathbf{z} | \boldsymbol{\sigma}_X^2, \boldsymbol{\sigma}_Y^2, \boldsymbol{\theta}, \mathbf{h}_0)] + \text{constant} \\
&= \mathbb{E}_{q-\pi_1} \left\{ \sum_{j=1}^N [w_j \log \pi_1 + (1 - w_j) \log(1 - \pi_1)] + (a_0 - 1) \log \pi_1 \right\} + \text{constant} \\
&= \left[ a_0 - 1 + \sum_{j=1}^N \mathbb{E}_q(w_j) \right] \log(\pi_1) + \left[ N - \sum_{j=1}^N \mathbb{E}_q(w_j) \right] \log(1 - \pi_1) + \text{constant}.
\end{aligned}$$

The form of  $\log q(\pi_1)$  suggests that  $q(\pi_1)$  is the density of a Beta distribution, i.e.,  $\text{Beta}(\pi_1 | a, b)$ :

$$a = a_0 + \sum_{j=1}^N \mathbb{E}_q(w_j), \quad b = N + 1 - \sum_{j=1}^N \mathbb{E}_q(w_j).$$

Eventually, for latent variable  $w_j$ , according to coordinate ascent MFVB,

$$\begin{aligned}
q(w_j) &= \mathbb{E}_{q-w_j} [\log \Pr(\hat{\boldsymbol{\gamma}}, \hat{\boldsymbol{\Gamma}}, \mathbf{z} | \boldsymbol{\sigma}_X^2, \boldsymbol{\sigma}_Y^2, \boldsymbol{\theta}, \mathbf{h}_0)] + \text{constant} \\
&= \mathbb{E}_{q-w_j} \left\{ w_j \left[ -\frac{1}{2} \log(2\pi) - \frac{1}{2} \log(\sigma_{Y_j}^2 + \tau^2) - \frac{1}{2(\sigma_{Y_j}^2 + \tau^2)} (\hat{\Gamma}_j - \beta\gamma_j)^2 \right] \right\} \\
&\quad + \mathbb{E}_{q-w_j} [w_j \log \pi_1 + (1 - w_j) \log(1 - \pi_1)] + \text{constant} \\
&= w_j \left[ -\frac{1}{2} \log(2\pi) - \frac{1}{2} \log(\sigma_{Y_j}^2 + \tau^2) - \frac{\mathbb{E}_q(\hat{\Gamma}_j - \beta\gamma_j)^2}{2(\sigma_{Y_j}^2 + \tau^2)} \right] \\
&\quad + w_j \mathbb{E}_q[\log \pi_1] + (1 - w_j) \mathbb{E}[\log(1 - \pi_1)] + \text{constant}.
\end{aligned}$$

Notice that  $w_j$  is binary and the constant has no connection with  $w_j$ , here we derive

$$\frac{q(w_j = 0)}{q(w_j = 1)} = \frac{\exp\{\mathbb{E}[\log(1 - \pi_1)]\}}{\exp\left\{-\frac{1}{2}\log(2\pi) - \frac{1}{2}\log(\sigma_{Y_j}^2 + \tau^2) - \frac{\mathbb{E}_q(\hat{\Gamma}_j - \beta\gamma_j)^2}{2(\sigma_{Y_j}^2 + \tau^2)} + \mathbb{E}_q[\log \pi_1]\right\}}.$$

Thus,  $q(w_j)$  is the density of the following Bernoulli distribution:  $q(w_j) = \text{Bernoulli}(\pi_{w_j})$  with

$$\pi_{w_j} = q(w_j = 1) = \mathbb{E}_q(w_j) = \frac{q(w_j = 1)}{q(w_j = 0) + q(w_j = 1)}.$$

Considering the form of the optimal variational distribution, the expectations of latent variables are written as

$$\begin{aligned}\mathbb{E}_q(\beta) &= \mu_\beta, \mathbb{E}_q(\beta^2) = \mu_\beta^2 + \sigma_\beta^2, \\ \mathbb{E}_q(\gamma_j) &= \mu_{\gamma_j}, \mathbb{E}_q(\gamma_j^2) = \mu_{\gamma_j}^2 + \sigma_{\gamma_j}^2, \\ \mathbb{E}_q[\log(\pi_1)] &= \psi(a) - \psi(a + b), \mathbb{E}_q[\log(1 - \pi_1)] = \psi(b) - \psi(a + b), \\ \mathbb{E}_q(w_j) &= \pi_{w_j},\end{aligned}$$

where  $\psi(\cdot)$  represents the digamma function. Noticing the independence between latent variables under the variational posterior distribution, finally we derive the updating equations for the variational E-step:

$$\begin{aligned}\sigma_\beta^2 &= \left[ \frac{1}{\sigma_0^2} + \sum_{j=1}^N \frac{\pi_{w_j}(\mu_{\gamma_j}^2 + \sigma_{\gamma_j}^2)}{\sigma_{Y_j}^2 + \tau^2} \right]^{-1}, \mu_\beta = \left( \sum_{j=1}^N \frac{\pi_{w_j} \mu_{\gamma_j} \hat{\Gamma}_j}{\sigma_{Y_j}^2 + \tau^2} \right) \sigma_\beta^2, \\ \sigma_{\gamma_j}^2 &= \left[ \frac{1}{\sigma_{X_j}^2} + \frac{\pi_{w_j}(\mu_\beta^2 + \sigma_\beta^2)}{\sigma_{Y_j}^2 + \tau^2} + \frac{1}{\sigma^2} \right]^{-1}, \mu_{\gamma_j} = \left( \frac{\hat{\gamma}_j}{\sigma_{X_j}^2} + \frac{\pi_{w_j} \mu_\beta \hat{\Gamma}_j}{\sigma_{Y_j}^2 + \tau^2} \right) \sigma_{\gamma_j}^2, \\ a &= \alpha + \sum_{j=1}^N \pi_{w_j}, b = N + 1 - \sum_{j=1}^N \pi_{w_j}, \\ \pi_{w_j} &= \frac{q_{j1}}{q_{j0} + q_{j1}},\end{aligned}$$

where

$$\begin{aligned}q_{j0} &= \exp[\psi(b) - \psi(a + b)], \\ q_{j1} &= \exp\left[-\frac{1}{2}\log(2\pi) - \frac{1}{2}\log(\sigma_{Y_j}^2 + \tau^2) - \frac{(\mu_\beta^2 + \sigma_\beta^2)(\mu_{\gamma_j}^2 + \sigma_{\gamma_j}^2) - 2\mu_\beta \mu_{\gamma_j} \hat{\Gamma}_j + \hat{\Gamma}_j^2}{2(\sigma_{Y_j}^2 + \tau^2)} + \psi(a) - \psi(a + b)\right].\end{aligned}$$

## A.2 M-step

We first evaluate the ELBO  $\mathcal{L} = \mathcal{L}(q, \boldsymbol{\theta})$ .

$$\begin{aligned}
\mathcal{L} &= \mathbb{E}_q[\log \Pr(\hat{\boldsymbol{\gamma}}, \hat{\boldsymbol{\Gamma}}, \mathbf{z} | \boldsymbol{\sigma}_X^2, \boldsymbol{\sigma}_Y^2, \boldsymbol{\theta}, \mathbf{h}_0)] - \mathbb{E}_q[\log q(\mathbf{z})] \\
&= \mathbb{E}_q[\log \Pr(\hat{\boldsymbol{\gamma}} | \boldsymbol{\sigma}_X^2, \boldsymbol{\gamma})] + \mathbb{E}_q[\log \Pr(\hat{\boldsymbol{\Gamma}} | \boldsymbol{\sigma}_Y^2, \beta, \boldsymbol{\gamma}, \mathbf{w}, \tau^2)] \\
&\quad + \mathbb{E}_q[\log \Pr(\beta | \sigma_0^2)] + \mathbb{E}_q[\log \Pr(\boldsymbol{\gamma} | \sigma^2)] + \mathbb{E}_q[\log \Pr(\mathbf{w} | \pi_1)] + \mathbb{E}_q[\log \Pr(\pi_1 | a_0)] \\
&\quad - \mathbb{E}_q[\log q(\beta)] - \mathbb{E}_q[\log q(\boldsymbol{\gamma})] - \mathbb{E}_q[\log q(\mathbf{w})] - \mathbb{E}_q[\log q(\pi_1)],
\end{aligned}$$

where

$$\begin{aligned}
&\mathbb{E}_q[\log \Pr(\hat{\boldsymbol{\gamma}} | \boldsymbol{\sigma}_X^2, \boldsymbol{\gamma})] \\
&= \mathbb{E}_q \left[ \sum_{j=1}^N \log \mathcal{N}(\hat{\gamma}_j | \gamma_j, \sigma_{X_j}^2) \right] \\
&= \mathbb{E}_q \left\{ \sum_{j=1}^N \left[ -\frac{1}{2} \log(\sigma_{X_j}^2) - \frac{1}{2\sigma_{X_j}^2} (\hat{\gamma}_j - \gamma_j)^2 \right] \right\} + \text{constant} \\
&= \sum_{j=1}^N \left\{ -\frac{1}{2} \log(\sigma_{X_j}^2) - \frac{1}{2\sigma_{X_j}^2} [(\hat{\gamma}_j - \mu_{\gamma_j})^2 + \sigma_{\gamma_j}^2] \right\} + \text{constant},
\end{aligned}$$

$$\begin{aligned}
&\mathbb{E}_q[\log \Pr(\hat{\boldsymbol{\Gamma}} | \boldsymbol{\sigma}_Y^2, \beta, \boldsymbol{\gamma}, \mathbf{w}, \tau^2)] \\
&= \mathbb{E}_q \left[ \log \prod_{j=1}^N \mathcal{N}(\hat{\Gamma}_j | \beta \gamma_j, \sigma_{Y_j}^2 + \tau^2)^{w_j} \right] \\
&= \mathbb{E}_q \left\{ \sum_{j=1}^N w_j \left[ -\frac{1}{2} \log(2\pi) - \frac{1}{2} \log(\sigma_{Y_j}^2 + \tau^2) - \frac{(\hat{\Gamma}_j - \beta \gamma_j)^2}{2(\sigma_{Y_j}^2 + \tau^2)} \right] \right\} + \text{constant} \\
&= \sum_{j=1}^N \pi_{w_j} \left[ -\frac{1}{2} \log(2\pi) - \frac{1}{2} \log(\sigma_{Y_j}^2 + \tau^2) \right] + \sum_{j=1}^N \pi_{w_j} \left[ -\frac{(\mu_\beta^2 + \sigma_\beta^2)(\mu_{\gamma_j}^2 + \sigma_{\gamma_j}^2) - 2\mu_\beta \mu_{\gamma_j} \hat{\Gamma}_j + \hat{\Gamma}_j^2}{2(\sigma_{Y_j}^2 + \tau^2)} \right] \\
&\quad + \text{constant},
\end{aligned}$$

$$\begin{aligned}
&\mathbb{E}_q[\log \Pr(\beta | \sigma_0^2)] \\
&= \mathbb{E}_q [\log \mathcal{N}(\beta | 0, \sigma_0^2)] \\
&= \mathbb{E}_q \left[ -\frac{1}{2} \log(\sigma_0^2) - \frac{1}{2\sigma_0^2} \beta^2 \right] + \text{constant} \\
&= -\frac{1}{2\sigma_0^2} (\mu_\beta^2 + \sigma_\beta^2) + \text{constant},
\end{aligned}$$

$$\begin{aligned}
& \mathbb{E}_q[\log \Pr(\boldsymbol{\gamma}|\sigma^2)] \\
&= \mathbb{E}_q \left[ \sum_{j=1}^N \log \mathcal{N}(\gamma_j|0, \sigma^2) \right] \\
&= \mathbb{E}_q \left\{ \sum_{j=1}^N \left[ -\frac{1}{2} \log(\sigma^2) - \frac{1}{2\sigma^2} \gamma_j^2 \right] \right\} + \text{constant} \\
&= -\frac{N}{2} \log(\sigma^2) - \frac{1}{2\sigma^2} \sum_{j=1}^N (\mu_{\gamma_j}^2 + \sigma_{\gamma_j}^2) + \text{constant},
\end{aligned}$$

$$\begin{aligned}
\mathbb{E}_q[\log \Pr(\mathbf{w}|\pi_1)] &= \mathbb{E}_q \left[ \sum_{j=1}^N \log \text{Bernoulli}(w_j|\pi_1) \right] \\
&= \mathbb{E}_q \left\{ \sum_{j=1}^N [w_j \log(\pi_1) + (1 - w_j) \log(1 - \pi_1)] \right\} \\
&= \sum_{j=1}^N \{ \pi_{w_j} [\psi(a) - \psi(a + b)] + (1 - \pi_{w_j}) [\psi(b) - \psi(a + b)] \},
\end{aligned}$$

$$\begin{aligned}
\mathbb{E}_q[\log \Pr(\pi_1|a_0)] &= \mathbb{E}_q[\log \text{Beta}(\pi_1|a_0, 1)] \\
&= \mathbb{E}_q[(a_0 - 1) \log(\pi_1)] + \text{constant} \\
&= (a_0 - 1) [\psi(a) - \psi(a + b)] + \text{constant},
\end{aligned}$$

$$\begin{aligned}
\mathbb{E}_q[\log q(\beta)] &= \mathbb{E}_q [\log \mathcal{N}(\beta|\mu_\beta, \sigma_\beta^2)] \\
&= \mathbb{E}_q \left[ -\frac{1}{2} \log(\sigma_\beta^2) - \frac{1}{2\sigma_\beta^2} (\beta - \mu_\beta)^2 \right] + \text{constant} \\
&= -\frac{1}{2} \log(\sigma_\beta^2) + \text{constant},
\end{aligned}$$

$$\begin{aligned}
\mathbb{E}_q[\log q(\boldsymbol{\gamma})] &= \mathbb{E}_q \left[ \sum_{j=1}^N \log \mathcal{N}(\gamma_j|\mu_{\gamma_j}, \sigma_{\gamma_j}^2) \right] \\
&= \mathbb{E}_q \left\{ \sum_{j=1}^N \left[ -\frac{1}{2} \log(\sigma_{\gamma_j}^2) - \frac{1}{2\sigma_{\gamma_j}^2} (\gamma_j - \mu_{\gamma_j})^2 \right] \right\} + \text{constant} \\
&= -\frac{1}{2} \sum_{j=1}^N \log(\sigma_{\gamma_j}^2) + \text{constant},
\end{aligned}$$

$$\begin{aligned}
\mathbb{E}_q[\log q(\mathbf{w})] &= \mathbb{E}_q \left[ \sum_{j=1}^N \log \text{Bernoulli}(w_j | \pi_{w_j}) \right] \\
&= \mathbb{E}_q \left\{ \sum_{j=1}^N [w_j \log(\pi_{w_j}) + (1 - w_j) \log(1 - \pi_{w_j})] \right\} \\
&= \sum_{j=1}^N [\pi_{w_j} \log(\pi_{w_j}) + (1 - \pi_{w_j}) \log(1 - \pi_{w_j})],
\end{aligned}$$

$$\begin{aligned}
\mathbb{E}_q[\log q(\pi_1)] &= \mathbb{E}_q[\log \text{Beta}(\pi_1 | a, b)] \\
&= \mathbb{E}_q \{ (a - 1) \log(\pi_1) + (b - 1) \log(1 - \pi_1) - \log[\text{B}(a, b)] \} \\
&= (a - 1)[\psi(a) - \psi(a + b)] + (b - 1)[\psi(b) - \psi(a + b)] - \log[\text{B}(a, b)].
\end{aligned}$$

Now we derive the updating equations for parameters  $\sigma^2$  and  $\tau^2$ .

For parameter  $\sigma^2$ , the ELBO  $\mathcal{L}$  terms with  $\sigma^2$  are given as

$$\mathcal{L}_{[\sigma^2]} = -\frac{N}{2} \log(\sigma^2) - \sum_{j=1}^N \left( \frac{\mu_{\gamma_j}^2 + \sigma_{\gamma_j}^2}{2\sigma^2} \right).$$

Then taking derivative of ELBO  $\mathcal{L}$  w.r.t.  $\sigma^2$

$$\frac{\partial \mathcal{L}}{\partial \sigma^2} = -\frac{N}{2\sigma^2} + \frac{1}{2(\sigma^2)^2} \sum_{j=1}^N (\mu_{\gamma_j}^2 + \sigma_{\gamma_j}^2).$$

and setting it to zero gives the updating equation for  $\sigma^2$  as

$$\sigma^2 = \frac{\sum_{j=1}^N (\mu_{\gamma_j}^2 + \sigma_{\gamma_j}^2)}{N}.$$

Similarly, for parameter  $\tau^2$ , we calculate the ELBO  $\mathcal{L}$  terms with  $\tau^2$  as

$$\mathcal{L}_{[\tau^2]} = \sum_{j=1}^N \left\{ \pi_{w_j} \left[ -\frac{1}{2} \log(\sigma_{Y_j}^2 + \tau^2) - \frac{(\mu_{\beta}^2 + \sigma_{\beta}^2)(\mu_{\gamma_j}^2 + \sigma_{\gamma_j}^2) - 2\mu_{\beta}\mu_{\gamma_j}\hat{\Gamma}_j + \hat{\Gamma}_j^2}{2(\sigma_{Y_j}^2 + \tau^2)} \right] \right\}.$$

However, directly taking derivative w.r.t.  $\tau^2$  and setting it to zero will not give a closed-form updating equation for  $\tau^2$ . Now we propose some tricks. Consider the function  $f(x, y) = \frac{x^2}{y}$  which is jointly convex in  $(x, y)$  for  $y > 0$  (This is known as ‘Quadratic over linear’). Now we consider function  $f(\sigma_{Y_j}^2 + (\tau^{(t)})^2, \sigma_{Y_j}^2 + \tau^2) = [\sigma_{Y_j}^2 + (\tau^{(t)})^2](\sigma_{Y_j}^2 + \tau^2)^{-1}[\sigma_{Y_j}^2 + (\tau^{(t)})^2]$ , and

we are going to make use of the convexity of  $f(x, y)$ :  $f(\lambda x_1 + (1 - \lambda)x_2, \lambda y_1 + (1 - \lambda)y_2) \leq \lambda f(x_1, y_1) + (1 - \lambda)f(x_2, y_2)$ . Denote

$$\begin{aligned}\lambda &= \frac{\sigma_{Y_j}^2}{\sigma_{Y_j}^2 + (\tau^{(\text{old})})^2}, & 1 - \lambda &= \frac{(\tau^{(\text{old})})^2}{\sigma_{Y_j}^2 + (\tau^{(\text{old})})^2}, \\ x_1 &= \frac{\sigma_{Y_j}^2 + (\tau^{(\text{old})})^2}{\sigma_{Y_j}^2} \sigma_{Y_j}^2, & x_2 &= \frac{\sigma_{Y_j}^2 + (\tau^{(\text{old})})^2}{(\tau^{(\text{old})})^2} (\tau^{(\text{old})})^2, \\ y_1 &= \frac{\sigma_{Y_j}^2 + (\tau^{(\text{old})})^2}{\sigma_{Y_j}^2} \sigma_{Y_j}^2, & y_2 &= \frac{\sigma_{Y_j}^2 + (\tau^{(\text{old})})^2}{(\tau^{(\text{old})})^2} \tau^2.\end{aligned}$$

Then we have

$$\begin{aligned}& [\sigma_{Y_j}^2 + (\tau^{(\text{old})})^2] (\sigma_{Y_j}^2 + \tau^2)^{-1} [\sigma_{Y_j}^2 + (\tau^{(\text{old})})^2] \\ &= [\lambda x_1 + (1 - \lambda)x_2] [\lambda y_1 + (1 - \lambda)y_2]^{-1} [\lambda x_1 + (1 - \lambda)x_2] \\ &= f(\lambda x_1 + (1 - \lambda)x_2, \lambda y_1 + (1 - \lambda)y_2) \\ &\leq \lambda f(x_1, y_1) + (1 - \lambda)f(x_2, y_2) \\ &= \lambda x_1 y_1^{-1} x_1 + (1 - \lambda)x_2 y_2^{-1} x_2\end{aligned}$$

It is easy to check

$$\begin{aligned}\lambda x_1 y_1^{-1} x_1 &= \sigma_{Y_j}^2, \\ (1 - \lambda)x_2 y_2^{-1} x_2 &= \frac{(\tau^{(\text{old})})^4}{\tau^2}.\end{aligned}$$

In summary, we derive the following inequality

$$(\sigma_{Y_j}^2 + \tau^2)^{-1} \leq [\sigma_{Y_j}^2 + (\tau^{(\text{old})})^2]^{-2} \left[ \sigma_{Y_j}^2 + \frac{(\tau^{(\text{old})})^4}{\tau^2} \right].$$

For the log term in  $\mathcal{L}_{[\tau^2]}$ , we also have a bound (first-order approximation to a concave function)

$$-\log(\sigma_{Y_j}^2 + \tau^2) \geq -\log[\sigma_{Y_j}^2 + (\tau^{(\text{old})})^2] - [\sigma_{Y_j}^2 + (\tau^{(\text{old})})^2]^{-1} [\tau^2 - (\tau^{(\text{old})})^2].$$

Using such two bounds, the ELBO  $\mathcal{L}$  terms containing  $\tau^2$  are bounded as

$$\mathcal{L}_{[\tau^2]} \geq \sum_{j=1}^N \left\{ -\frac{\pi_{w_j} [\tau^2 - (\tau^{(\text{old})})^2]}{2[\sigma_{Y_j}^2 + (\tau^{(\text{old})})^2]} - \frac{\pi_{w_j} [(\mu_\beta^2 + \sigma_\beta^2)(\mu_{\gamma_j}^2 + \sigma_{\gamma_j}^2) - 2\mu_\beta \mu_{\gamma_j} \hat{\Gamma}_j + \hat{\Gamma}_j^2]}{2} \frac{\sigma_{Y_j}^2 + \frac{[\tau^{(\text{old})}]^4}{\tau^2}}{[\sigma_{Y_j}^2 + (\tau^{(\text{old})})^2]^2} \right\} + \text{const}$$

Taking derivative of such bound of  $\mathcal{L}_{[\tau^2]}$  w.r.t.  $\tau^2$  and setting it to zero

$$\sum_{j=1}^N \left\{ -\frac{\pi_{w_j}}{2[\sigma_{Y_j}^2 + (\tau^{(\text{old})})^2]} + \frac{\pi_{w_j} [(\mu_\beta^2 + \sigma_\beta^2)(\mu_{\gamma_j}^2 + \sigma_{\gamma_j}^2) - 2\mu_\beta \mu_{\gamma_j} \hat{\Gamma}_j + \hat{\Gamma}_j^2] (\tau^{(\text{old})})^4}{2[\sigma_{Y_j}^2 + (\tau^{(\text{old})})^2]^2 \tau^4} \right\} = 0,$$

gives the following updating equation for  $\tau^2$ :

$$\tau^2 \leftarrow \sqrt{\frac{\sum_{j=1}^N \frac{\pi_{w_j} [(\mu_\beta^2 + \sigma_\beta^2)(\mu_{\gamma_j}^2 + \sigma_{\gamma_j}^2) - 2\mu_\beta \mu_{\gamma_j} \hat{\Gamma}_j + \hat{\Gamma}_j^2] (\tau^{(\text{old})})^4}{[\sigma_{Y_j}^2 + (\tau^{(\text{old})})^2]^2}}{\sum_{j=1}^N \frac{\pi_{w_j}}{\sigma_{Y_j}^2 + (\tau^{(\text{old})})^2}}}.$$

where  $(\tau^{(\text{old})})^2$  is the estimate of  $\tau^2$  at previous iteration.

## B Inference

With the mean field assumption, VEM algorithm can provide accurate posterior mean of  $\beta$  (Blei et al., 2017). However, MFVB often underestimates the posterior variance of latent variables (Blei et al., 2017). As inspired by the linear response methods (Giordano et al., 2015, 2018), in this section we propose an exact closed-form formula to correct the underestimated variance, yielding an accurate inference for  $\beta$ .

### B.1 An example showing the properties of MFVB

First we give a simple example to vividly show the properties of MFVB. Suppose the true posterior distribution is a multivariate normal distribution

$$p(\mathbf{z}) = \mathcal{N}(\boldsymbol{\mu}_0, \boldsymbol{\Sigma}_0),$$

where  $\mathbf{z} \in \mathbb{R}^{M \times 1}$ ,  $\boldsymbol{\mu}_0 \in \mathbb{R}^{M \times 1}$ ,  $\boldsymbol{\Sigma}_0 \in \mathbb{R}^{M \times M}$ . And we use the variational distribution  $q(\mathbf{z})$  to approximate it. According to MFVB, we assume that  $q(\mathbf{z})$  can be factorized as

$$q(\mathbf{z}) = \prod_{j=1}^M q(z_j).$$

Note that in the framework of VEM and MFVB, the optimal approximation  $q^*(\mathbf{z})$  of  $p(\mathbf{z})$  is obtained by maximizing ELBO w.r.t.  $q$ , which is equivalent to minimizing the Kullback-Leibler (KL) divergence  $KL(q(\mathbf{z})\|p(\mathbf{z}))$  w.r.t.  $q$ . We obtain

$$KL(q(\mathbf{z})\|p(\mathbf{z})) = \mathbb{E}_{q(\mathbf{z})} \left[ \log \frac{q(\mathbf{z})}{p(\mathbf{z})} \right] = \int \prod_{j=1}^M q(z_j) \left[ -\log p(\mathbf{z}) + \log \prod_{j=1}^M q(z_j) \right] d\mathbf{z}. \quad (18)$$

We now seek the minimum of  $KL(q(\mathbf{z})\|p(\mathbf{z}))$  by making optimization of  $KL(q(\mathbf{z})\|p(\mathbf{z}))$  w.r.t.  $q(z_j)$ ,  $j = 1, 2, \dots, M$ , in turn. Let  $\mathbf{z}_{-j} := \{z_i\}_{i \neq j}$  and  $q_{-j}(\mathbf{z}_{-j}) := \prod_{i \neq j} q(z_i)$ , then we re-arrange Eq. (18) as

$$\begin{aligned} KL(q(\mathbf{z})\|p(\mathbf{z})) &= \int q(z_j) \int q_{-j}(\mathbf{z}_{-j}) [-\log p(\mathbf{z}) + \log q_{-j}(\mathbf{z}_{-j}) + \log q(z_j)] d\mathbf{z}_{-j} dz_j \\ &= \int q(z_j) \int q_{-j}(\mathbf{z}_{-j}) [-\log p(\mathbf{z}) + \log q(z_j)] d\mathbf{z}_{-j} dz_j + \int q_{-j}(\mathbf{z}_{-j}) \log q_{-j}(\mathbf{z}_{-j}) d\mathbf{z}_{-j} \\ &= \int q(z_j) \left[ -\int q_{-j}(\mathbf{z}_{-j}) \log p(\mathbf{z}) d\mathbf{z}_{-j} + \log q(z_j) \right] dz_j + \int q_{-j}(\mathbf{z}_{-j}) \log q_{-j}(\mathbf{z}_{-j}) d\mathbf{z}_{-j}. \end{aligned}$$

By defining a new distribution  $\tilde{p}(z_j)$

$$\log \tilde{p}(z_j) := \int q_{-j}(\mathbf{z}_{-j}) \log p(\mathbf{z}) d\mathbf{z}_{-j} + \text{constant}, \quad (19)$$

we further derive

$$\begin{aligned} KL(q(\mathbf{z})\|p(\mathbf{z})) &= \int q(z_j) [-\log \tilde{p}(z_j) + \log q(z_j)] dz_j + \text{constant} \\ &= KL(q(z_j)\|\tilde{p}(z_j)) + \text{constant}. \end{aligned}$$

Given that the Kullback-Leibler (KL) divergence is nonnegative, we know that the optimal  $q(z_j)$  is given as

$$q(z_j) = \tilde{p}(z_j). \quad (20)$$

Thus, as  $p(\mathbf{z})$  is a multivariate normal distribution, it is reasonable to write the optimal  $q(z_j)$  as

$$q(z_j) = \mathcal{N}(\mu_j, \sigma_j^2). \quad (21)$$

Finally, from Eqs. (19,20,21), we derive

$$\mu_j = \boldsymbol{\mu}_0^{(j)}, \quad \sigma_j^2 = 1/[\boldsymbol{\Sigma}_0^{-1}]^{(j,j)},$$

where  $\boldsymbol{\mu}_0^{(j)}$  denotes the  $j$ -th element of  $\boldsymbol{\mu}_0$  and  $[\boldsymbol{\Sigma}_0^{-1}]^{(j,j)}$  denotes the element located in the  $j$ -th row and the  $j$ -th column of  $\boldsymbol{\Sigma}_0^{-1}$ . Therefore,

$$\begin{aligned} \hat{\boldsymbol{\mu}}_0^{(MFVB)} &= \boldsymbol{\mu}_0, \\ \hat{\boldsymbol{\Sigma}}_0^{(MFVB)} &= \text{diag} \left( 1/[\boldsymbol{\Sigma}_0^{-1}]^{(1,1)}, 1/[\boldsymbol{\Sigma}_0^{-1}]^{(2,2)}, \dots, 1/[\boldsymbol{\Sigma}_0^{-1}]^{(M,M)} \right). \end{aligned} \quad (22)$$

As can be seen from Eq. (22), MFVB gives accurate mean estimations while it provides no information of covariances between different variables and often gives underestimated variances.

## B.2 An example showing the intuition for linear response variational Bayes (LRVB)

We provide intuition for linear response variational Bayes (Giordano et al., 2015) by continuing the above example. For the sake of simplicity, we assume

$$\begin{aligned}
 p(\mathbf{z}) &= \mathcal{N}(\boldsymbol{\mu}_0, \boldsymbol{\Sigma}_0), \\
 \mathbf{z} &= (z_1, z_2), \\
 \boldsymbol{\mu}_0 &= (\mu_{0,1}, \mu_{0,2}), \\
 \boldsymbol{\Sigma}_0 &= \begin{bmatrix} a_{11} & a_{12} \\ a_{21} & a_{22} \end{bmatrix}, \quad \boldsymbol{\Sigma}_0^{-1} = \begin{bmatrix} r_{11} & r_{12} \\ r_{21} & r_{22} \end{bmatrix}. \\
 q(\mathbf{z}) &= q(z_1)q(z_2), \quad q(z_1) = \mathcal{N}(\mu_1, \sigma_1^2), \quad q(z_2) = \mathcal{N}(\mu_2, \sigma_2^2).
 \end{aligned}$$

and let  $\boldsymbol{\eta}$  be the collection of variational parameters, i.e.,

$$\boldsymbol{\eta} = \{\mu_1, \sigma_1^2, \mu_2, \sigma_2^2\}.$$

Here we denote  $p_0(\mathbf{z})$  as the true posterior of interest, i.e.,  $p_0(\mathbf{z}) = p(\mathbf{z})$ , and we define a perturbation of the posterior as

$$p_{\mathbf{t}}(\mathbf{z}) := \frac{p_0(\mathbf{z}) \exp(\mathbf{t}^T \mathbf{z})}{\int p_0(\mathbf{z}) \exp(\mathbf{t}^T \mathbf{z}) d\mathbf{z}}. \quad (23)$$

Recall that  $p_0(\mathbf{z}) = \mathcal{N}(\boldsymbol{\mu}_0, \boldsymbol{\Sigma}_0)$ , Eq. (23) implies

$$\begin{aligned}
 \log p_{\mathbf{t}}(\mathbf{z}) &= -\frac{1}{2}(\mathbf{z} - \boldsymbol{\mu}_0)^T \boldsymbol{\Sigma}_0^{-1}(\mathbf{z} - \boldsymbol{\mu}_0) + \mathbf{t}^T \mathbf{z} + \text{constant} \\
 &= -\frac{1}{2}\mathbf{z}^T \boldsymbol{\Sigma}_0^{-1} \mathbf{z} + (\boldsymbol{\mu}_0^T \boldsymbol{\Sigma}_0^{-1} + \mathbf{t}^T)\mathbf{z} + \text{constant} \\
 &= -\frac{1}{2}[\mathbf{z} - (\boldsymbol{\mu}_0 + \boldsymbol{\Sigma}_0 \mathbf{t})]^T \boldsymbol{\Sigma}_0^{-1} [\mathbf{z} - (\boldsymbol{\mu}_0 + \boldsymbol{\Sigma}_0 \mathbf{t})] + \text{constant}.
 \end{aligned} \quad (24)$$

The quadratic form in Eq. (24) yields

$$p_{\mathbf{t}}(\mathbf{z}) = \mathcal{N}(\boldsymbol{\mu}_0 + \boldsymbol{\Sigma}_0 \mathbf{t}, \boldsymbol{\Sigma}_0), \quad (25)$$

implying

$$\text{Cov}_{p(\mathbf{z})}[\mathbf{z}] = \boldsymbol{\Sigma}_0 = \left. \frac{\partial \mathbb{E}_{p_{\mathbf{t}}(\mathbf{z})}[\mathbf{z}]}{\partial \mathbf{t}^T} \right|_{\mathbf{t}=\mathbf{0}}. \quad (26)$$

Eq. (26) shows that the sensitivity of posterior mean at  $\mathbf{t} = \mathbf{0}$  can provide information about the true posterior variance.

We now introduce the key idea to approximate the posterior covariance matrix in Eq. (26) from MFVB. Let  $q_t(\mathbf{z})$  be the mean field approximation to  $p_t(\mathbf{z})$ , i.e.,

$$q_t(\mathbf{z}) := q(\mathbf{z}; \boldsymbol{\eta}_t^*) = \arg \min_q KL(q(\mathbf{z}; \boldsymbol{\eta}) \| p_t(\mathbf{z})).$$

Since MFVB often provides accurate inference on posterior mean (Blei et al., 2017), we assume the following conditions hold:

$$\begin{aligned} \text{Condition 1: } & \mathbb{E}_{q_t}[\mathbf{z}] \approx \mathbb{E}_{p_t}[\mathbf{z}] \text{ for all } \mathbf{t}, \text{ and} \\ \text{Condition 2: } & \left. \frac{\partial \mathbb{E}_{q_t}[\mathbf{z}]}{\partial \mathbf{t}^T} \right|_{\mathbf{t}=\mathbf{0}} \approx \left. \frac{\partial \mathbb{E}_{p_t}[\mathbf{z}]}{\partial \mathbf{t}^T} \right|_{\mathbf{t}=\mathbf{0}}. \end{aligned} \quad (27)$$

Condition 1 says that MFVB can provide good approximations to posterior means of all the perturbations. Condition 2 further requires the accuracy of the first order approximation at  $\mathbf{t} = \mathbf{0}$ . Consequently, from Eq. (26) and Condition 2 in Eq. (27), we know that the posterior covariance matrix  $\boldsymbol{\Sigma}_0$  can be approximated by

$$\boldsymbol{\Sigma}_0 \approx \left. \frac{\partial \mathbb{E}_{q_t}[\mathbf{z}]}{\partial \mathbf{t}} \right|_{\mathbf{t}=\mathbf{0}} = \left. \frac{d\mathbb{E}_{q_t}[\mathbf{z}]}{d\boldsymbol{\eta}} \right|_{\boldsymbol{\eta}=\boldsymbol{\eta}_0^*} \left. \frac{d\boldsymbol{\eta}_t^*}{d\mathbf{t}} \right|_{\mathbf{t}=\mathbf{0}}, \quad (28)$$

where  $\boldsymbol{\eta}_0^*$  is exactly the MFVB solution obtained in Section 2.1.

We now use properties of MFVB solution to calculate  $\left. \frac{d\boldsymbol{\eta}_t^*}{d\mathbf{t}} \right|_{\mathbf{t}=\mathbf{0}}$ . Importantly, note that  $KL(q(\mathbf{z}; \boldsymbol{\eta}) \| p_t(\mathbf{z}))$  can be viewed as a function of  $\mathbf{t}$ ,  $\boldsymbol{\eta}$ , and using  $q(\mathbf{z}; \boldsymbol{\eta})$  to approximate  $p_t(\mathbf{z})$  in the framework of MFVB is equivalent to minimizing  $KL(q(\mathbf{z}; \boldsymbol{\eta}) \| p_t(\mathbf{z}))$  w.r.t.  $\boldsymbol{\eta}$ . The minimization yields

$$\left. \frac{\partial KL(q(\mathbf{z}; \boldsymbol{\eta}) \| p_t(\mathbf{z}))}{\partial \boldsymbol{\eta}} \right|_{\boldsymbol{\eta}=\boldsymbol{\eta}_t^*} = \mathbf{0}.$$

By taking derivative w.r.t.  $\mathbf{t}$ , we then derive

$$\frac{d}{d\mathbf{t}} \left( \left. \frac{\partial KL(q(\mathbf{z}; \boldsymbol{\eta}) \| p_t(\mathbf{z}))}{\partial \boldsymbol{\eta}} \right|_{\boldsymbol{\eta}=\boldsymbol{\eta}_t^*} \right) = \mathbf{0},$$

yeilding

$$\left. \frac{\partial^2 KL(q(\mathbf{z}; \boldsymbol{\eta}) \| p_t(\mathbf{z}))}{\partial \boldsymbol{\eta} \partial \boldsymbol{\eta}^T} \right|_{\boldsymbol{\eta}=\boldsymbol{\eta}_t^*} \frac{d\boldsymbol{\eta}_t^*}{d\mathbf{t}} + \left. \frac{\partial^2 KL(q(\mathbf{z}; \boldsymbol{\eta}) \| p_t(\mathbf{z}))}{\partial \mathbf{t} \partial \boldsymbol{\eta}^T} \right|_{\boldsymbol{\eta}=\boldsymbol{\eta}_t^*} = \mathbf{0}. \quad (29)$$

The strict minimization of  $KL(q(\mathbf{z}; \boldsymbol{\eta}) \| p_t(\mathbf{z}))$  requires that  $\left. \frac{\partial^2 KL(q(\mathbf{z}; \boldsymbol{\eta}) \| p_t(\mathbf{z}))}{\partial \boldsymbol{\eta} \partial \boldsymbol{\eta}^T} \right|_{\boldsymbol{\eta}=\boldsymbol{\eta}_t^*}$  is a positive definite matrix. So we can evaluate Eq. (29) at  $\mathbf{t} = \mathbf{0}$  and solve it to find that

$$\left. \frac{d\boldsymbol{\eta}_t^*}{d\mathbf{t}^T} \right|_{\mathbf{t}=\mathbf{0}} = - \left( \left. \frac{\partial^2 KL(q(\mathbf{z}; \boldsymbol{\eta}) \| p_t(\mathbf{z}))}{\partial \boldsymbol{\eta} \partial \boldsymbol{\eta}^T} \right|_{\boldsymbol{\eta}=\boldsymbol{\eta}_0^*} \right)^{-1} \left. \frac{\partial^2 KL(q(\mathbf{z}; \boldsymbol{\eta}) \| p_t(\mathbf{z}))}{\partial \mathbf{t} \partial \boldsymbol{\eta}^T} \right|_{\boldsymbol{\eta}=\boldsymbol{\eta}_0^*, \mathbf{t}=\mathbf{0}}. \quad (30)$$

As the KL divergence is written as

$$KL(q(\mathbf{z}; \boldsymbol{\eta}) \| p_{\mathbf{t}}(\mathbf{z})) = \mathbb{E}_{q(\mathbf{z}; \boldsymbol{\eta})}[\log q(\mathbf{z}; \boldsymbol{\eta}) - \log p(\mathbf{z}) - \mathbf{t}^T \mathbf{z}] + \text{constant},$$

where the constant is not relevant to  $\boldsymbol{\eta}$ , the term  $\left. \frac{\partial^2 KL(q(\mathbf{z}; \boldsymbol{\eta}) \| p_{\mathbf{t}}(\mathbf{z}))}{\partial \mathbf{t} \partial \boldsymbol{\eta}^T} \right|_{\boldsymbol{\eta}=\boldsymbol{\eta}^*, \mathbf{t}=\mathbf{0}}$  can be further summarized as

$$\left. \frac{\partial^2 KL(q(\mathbf{z}; \boldsymbol{\eta}) \| p_{\mathbf{t}}(\mathbf{z}))}{\partial \mathbf{t} \partial \boldsymbol{\eta}^T} \right|_{\boldsymbol{\eta}=\boldsymbol{\eta}_0^*, \mathbf{t}=\mathbf{0}} = - \left. \frac{\partial \mathbb{E}_{q(\mathbf{z}; \boldsymbol{\eta})}[\mathbf{z}]}{\partial \boldsymbol{\eta}^T} \right|_{\boldsymbol{\eta}=\boldsymbol{\eta}_0^*}. \quad (31)$$

Finally, Eqs. (28,30,31) indicate an estimator of the posterior covariance matrix as

$$\hat{\Sigma}_0^{(LRVB)} := \left( \left. \frac{\partial \mathbb{E}_{q(\mathbf{z}; \boldsymbol{\eta})}[\mathbf{z}]}{\partial \boldsymbol{\eta}^T} \right|_{\boldsymbol{\eta}=\boldsymbol{\eta}_0^*} \right)^T \left( \left. \frac{\partial^2 KL(q(\mathbf{z}; \boldsymbol{\eta}) \| p(\mathbf{z}))}{\partial \boldsymbol{\eta} \partial \boldsymbol{\eta}^T} \right|_{\boldsymbol{\eta}=\boldsymbol{\eta}_0^*} \right)^{-1} \left( \left. \frac{\partial \mathbb{E}_{q(\mathbf{z}; \boldsymbol{\eta})}[\mathbf{z}]}{\partial \boldsymbol{\eta}^T} \right|_{\boldsymbol{\eta}=\boldsymbol{\eta}_0^*} \right).$$

In the above Gaussian example,  $KL(q(\mathbf{z}; \boldsymbol{\eta}) \| p(\mathbf{z}))$  is given as

$$\begin{aligned} KL(q(\mathbf{z}; \boldsymbol{\eta}) \| p(\mathbf{z})) &= \mathbb{E}_{q(\mathbf{z}; \boldsymbol{\eta})}[\log q(\mathbf{z}; \boldsymbol{\eta})] - \mathbb{E}_{q(\mathbf{z}; \boldsymbol{\eta})}[\log p(\mathbf{z})] \\ &= -\frac{1}{2} \log(\sigma_1^2) - \frac{1}{2} \log(\sigma_2^2) \\ &\quad + \frac{1}{2} r_{11} [(\mu_1 - \mu_{0,1})^2 + \sigma_1^2] + \frac{1}{2} r_{22} [(\mu_2 - \mu_{0,2})^2 + \sigma_2^2] + r_{12} (\mu_1 - \mu_{0,1})(\mu_2 - \mu_{0,2}) \\ &\quad + \text{constant}. \end{aligned}$$

Thus, in this case,

$$\left. \frac{\partial^2 KL(q(\mathbf{z}; \boldsymbol{\eta}) \| p(\mathbf{z}))}{\partial \boldsymbol{\eta} \partial \boldsymbol{\eta}^T} \right|_{\boldsymbol{\eta}=\boldsymbol{\eta}_0^*} = \begin{bmatrix} r_{11} & 0 & r_{12} & 0 \\ 0 & \frac{1}{2\sigma_1^4} & 0 & 0 \\ r_{21} & 0 & r_{22} & 0 \\ 0 & 0 & 0 & \frac{1}{2\sigma_2^4} \end{bmatrix}$$

Note that we already have

$$\sigma_1^2 = 1/r_{11}, \sigma_2^2 = 1/r_{22}, \begin{bmatrix} a_{11} & a_{12} \\ a_{21} & a_{22} \end{bmatrix} = \begin{bmatrix} r_{11} & r_{12} \\ r_{21} & r_{22} \end{bmatrix}^{-1} = \frac{1}{r_{11}r_{22} - r_{12}r_{21}} \begin{bmatrix} r_{22} & -r_{12} \\ -r_{21} & r_{11} \end{bmatrix}.$$

With

$$\left. \frac{\partial \mathbb{E}_{q(\mathbf{z}; \boldsymbol{\eta})}[\mathbf{z}]}{\partial \boldsymbol{\eta}^T} \right|_{\boldsymbol{\eta}=\boldsymbol{\eta}_0^*} = \begin{bmatrix} 1 & 0 & 0 & 0 \\ 0 & 0 & 1 & 0 \end{bmatrix}^T,$$

We finally calculate  $\hat{\Sigma}_0^{(LRVB)}$  as

$$\hat{\Sigma}_0^{(LRVB)} = \begin{bmatrix} 1 & 0 & 0 & 0 \\ 0 & 0 & 1 & 0 \end{bmatrix} \begin{bmatrix} r_{11} & 0 & r_{12} & 0 \\ 0 & \frac{1}{2\sigma_1^4} & 0 & 0 \\ r_{21} & 0 & r_{22} & 0 \\ 0 & 0 & 0 & \frac{1}{2\sigma_2^4} \end{bmatrix}^{-1} \begin{bmatrix} 1 & 0 & 0 & 0 \\ 0 & 0 & 1 & 0 \end{bmatrix}^T = \begin{bmatrix} a_{11} & a_{12} \\ a_{21} & a_{22} \end{bmatrix} = \Sigma_0.$$

This Gaussian example not only gives the intuition of LRVB, but also helps to show that LRVB can indeed correct the covariance estimation provided by MFVB.

### B.3 Inference of posterior variance of one specific latent variable

Note that, for BWMR model, in the inference part we only seek to derive the posterior variance of latent variable  $\beta$ , i.e., we only care about the inference of one specific latent variable among all latent variables. Before implementing inference for BWMR, we continue the Gaussian example to get more intuition.

Let  $\mathbf{t} = (t_1, 0)$  in  $p_{\mathbf{t}}(\mathbf{z}) = \mathcal{N}(\boldsymbol{\mu}_0 + \Sigma_0 \mathbf{t}, \Sigma_0)$  (Eq. (25)), we then have

$$p_{t_1}(\mathbf{z}) = \mathcal{N}((\mu_{0,1} + a_{11}t_1, \mu_{0,2} + a_{12}t_1), \Sigma_0). \quad (32)$$

It is not hard to find out that Eq. (32) corresponds to the perturbation

$$p_{t_1}(\mathbf{z}) = \frac{p(\mathbf{z}) \exp(t_1 z_1)}{\int p(\mathbf{z}) \exp(t_1 z_1) d\mathbf{z}}.$$

Eq. (32) indicates an approximation to  $\text{Var}(z_1)$ :

$$\text{Var}(z_1) = a_{11} = \left. \frac{d\mathbb{E}_{p_{t_1}}[z_1]}{dt_1} \right|_{t_1=0} \approx \left. \frac{d\mathbb{E}_{q_{t_1}}[z_1]}{dt_1} \right|_{t_1=0} = \widehat{\text{Var}}(z_1),$$

where  $q_{t_1}(\mathbf{z})$  is the optimal solution of variational distribution used to approximate  $p_{t_1}(\mathbf{z})$  in the framework of MFVB. Then

$$\widehat{\text{Var}}(z_1) = \left. \frac{\partial \mathbb{E}_{q_{t_1}}[z_1]}{\partial \boldsymbol{\eta}} \right|_{\boldsymbol{\eta}=\boldsymbol{\eta}_0^*} \left. \frac{d\boldsymbol{\eta}_{t_1}^*}{dt_1} \right|_{t_1=0}, \quad (33)$$

where  $\boldsymbol{\eta}_{t_1}^*$  is the optimal solution of  $\boldsymbol{\eta}$  when approximating  $p_{t_1}(\mathbf{z})$ , and  $\boldsymbol{\eta}_0^* = \boldsymbol{\eta}_{t_1}^*|_{t_1=0}$  still represents the optimal solution of  $\boldsymbol{\eta}$  when approximating true posterior  $p_0(\mathbf{z}) = p(\mathbf{z})$ .

To conveniently derive  $\left. \frac{d\boldsymbol{\eta}_{t_1}^*}{dt_1} \right|_{t_1=0}$ , similar as Eqs. (29,30), we now have

$$\left. \frac{\partial^2 KL(q(\mathbf{z}; \boldsymbol{\eta}) \| p_{t_1}(\mathbf{z}))}{\partial \boldsymbol{\eta} \partial \boldsymbol{\eta}^T} \right|_{\boldsymbol{\eta}=\boldsymbol{\eta}_{t_1}^*} \frac{d\boldsymbol{\eta}_{t_1}^*}{dt_1} + \left. \frac{\partial^2 KL(q(\mathbf{z}; \boldsymbol{\eta}) \| p_{t_1}(\mathbf{z}))}{\partial t_1 \partial \boldsymbol{\eta}^T} \right|_{\boldsymbol{\eta}=\boldsymbol{\eta}_{t_1}^*} = \mathbf{0},$$

indicating

$$\left. \frac{d\boldsymbol{\eta}_{t_1}^*}{dt_1} \right|_{t_1=0} = - \left( \left. \frac{\partial^2 KL(q(\mathbf{z}; \boldsymbol{\eta}) \| p_{t_1}(\mathbf{z}))}{\partial \boldsymbol{\eta} \partial \boldsymbol{\eta}^T} \right|_{\boldsymbol{\eta}=\boldsymbol{\eta}_0^*, t_1=0} \right)^{-1} \left. \frac{\partial^2 KL(q(\mathbf{z}; \boldsymbol{\eta}) \| p_{t_1}(\mathbf{z}))}{\partial t_1 \partial \boldsymbol{\eta}^T} \right|_{\boldsymbol{\eta}=\boldsymbol{\eta}_0^*, t_1=0}. \quad (34)$$

Then similar as the derivation of Eq. (31), given that now the KL divergence  $KL(q(\mathbf{z}; \boldsymbol{\eta}) \| p_{t_1}(\mathbf{z}))$  is written as

$$KL(q(\mathbf{z}; \boldsymbol{\eta}) \| p_{t_1}(\mathbf{z})) = \mathbb{E}_{q(\mathbf{z}; \boldsymbol{\eta})}[\log q(\mathbf{z}; \boldsymbol{\eta}) - \log p(\mathbf{z}) - t_1 z_1] + \text{constant},$$

where the constant is not relevant to  $\boldsymbol{\eta}$ , we summary the term  $\left. \frac{\partial^2 KL(q(\mathbf{z}; \boldsymbol{\eta}) \| p_{t_1}(\mathbf{z}))}{\partial t_1 \partial \boldsymbol{\eta}^T} \right|_{\boldsymbol{\eta}=\boldsymbol{\eta}_0^*, t_1=0}$  as

$$\left. \frac{\partial^2 KL(q(\mathbf{z}; \boldsymbol{\eta}) \| p_{t_1}(\mathbf{z}))}{\partial t_1 \partial \boldsymbol{\eta}^T} \right|_{\boldsymbol{\eta}=\boldsymbol{\eta}_0^*, t_1=0} = - \left. \frac{\partial \mathbb{E}_{q(\mathbf{z}; \boldsymbol{\eta})}[z_1]}{\partial \boldsymbol{\eta}^T} \right|_{\boldsymbol{\eta}=\boldsymbol{\eta}_0^*}. \quad (35)$$

From Eq. (33,34,35), we finally derive

$$\begin{aligned} \widehat{\text{Var}}(z_1) &= \left( \left. \frac{\partial \mathbb{E}_{q(\mathbf{z}; \boldsymbol{\eta})}[z_1]}{\partial \boldsymbol{\eta}^T} \right|_{\boldsymbol{\eta}=\boldsymbol{\eta}_0^*} \right)^T \left( \left. \frac{\partial^2 D_{KL}(q(\mathbf{z}; \boldsymbol{\eta}) \| p(\mathbf{z}))}{\partial \boldsymbol{\eta} \partial \boldsymbol{\eta}^T} \right|_{\boldsymbol{\eta}=\boldsymbol{\eta}_0^*} \right)^{-1} \left( \left. \frac{\partial \mathbb{E}_{q(\mathbf{z}; \boldsymbol{\eta})}[z_1]}{\partial \boldsymbol{\eta}^T} \right|_{\boldsymbol{\eta}=\boldsymbol{\eta}_0^*} \right) \\ &= [1, 0, 0, 0] \begin{bmatrix} r_{11} & 0 & r_{12} & 0 \\ 0 & \frac{1}{2\sigma_1^4} & 0 & 0 \\ r_{21} & 0 & r_{22} & 0 \\ 0 & 0 & 0 & \frac{1}{2\sigma_2^4} \end{bmatrix}^{-1} [1, 0, 0, 0]^T \\ &= a_{11} \\ &= \text{Var}(z_1). \end{aligned}$$

#### B.4 Detailed derivations for inference

For BWMR,  $\mathbf{z}$  denotes the latent variables and  $D$  denotes the input data. For notation convenience, we denote  $p_0(\mathbf{z})$  as the true posterior of interest, i.e.,  $p_0(\mathbf{z}) = \Pr(\mathbf{z}|D)$ . As we want to derive the accurate posterior variance of latent  $\beta$ , inspired by the inference of  $z_1$

in the Gaussian example, here we define a perturbation of the posterior  $p_0(\mathbf{z}) = \Pr(\mathbf{z}|D)$  in BWMR as

$$p_t(\mathbf{z}) := \frac{p_0(\mathbf{z}) \exp(t\beta)}{\int p_0(\mathbf{z}) \exp(t\beta) d\mathbf{z}}.$$

Let

$$C(t) := \log \int p_0(\mathbf{z}) \exp(t\beta) d\mathbf{z}. \quad (36)$$

Then the perturbation  $p_t(\mathbf{z})$  is written as

$$p_t(\mathbf{z}) = p_0(\mathbf{z}) \exp(t\beta - C(t)),$$

where  $C(t)$  normalizes  $p_t(\mathbf{z})$ .

- **use the cumulant generating properties**

We introduce a new variable  $u$  and seek to derive the cumulant generating function  $K_{p_t}(u)$  for  $p_t(\mathbf{z})$ . From the definition of the cumulant generating function as well as Eq. (36), we have

$$\begin{aligned} K_{p_t}(u) &= \log \mathbb{E}_{p_t}[\exp(u\beta)] \\ &= \log \int \exp(u\beta) p_0(\mathbf{z}) \exp(t\beta - C(t)) d\mathbf{z} \\ &= \log \int p_0(\mathbf{z}) \exp((u+t)\beta) d\mathbf{z} - C(t) \\ &= C(u+t) - C(t). \end{aligned}$$

The properties of the cumulant generating function implies

$$\begin{aligned} \mathbb{E}_{p_t}[\beta] &= \left. \frac{\partial K_{p_t}(u)}{\partial u} \right|_{u=0} = \frac{dC(t)}{dt}, \\ \text{Var}_{p_t}[\beta] &= \left. \frac{\partial^2 K_{p_t}(u)}{\partial u^2} \right|_{u=0} = \frac{d^2 C(t)}{dt^2}. \end{aligned}$$

Therefore we get

$$\text{Var}_{\Pr(\mathbf{z}|D)}[\beta] = \text{Var}_{p_0}[\beta] = \text{Var}_{p_t}[\beta]|_{t=0} = \left. \frac{d\mathbb{E}_{p_t}[\beta]}{dt} \right|_{t=0}. \quad (37)$$

- **use the properties of MFVB solution**

Eq. (37) provides insight of using the accurate mean estimation from MFVB to correct the posterior variance inference. However, in practice we seek to only implement VEM

and MFVB once without any perturbations of the posterior. The usage of MFVB solution properties helps to address this problem.

The variational distributions from MFVB is

$$q(\mathbf{z}) = q(\beta)q(\pi_1) \prod_{j=1}^N q(\gamma_j) \prod_{j=1}^N q(w_j),$$

with

$$\begin{aligned} q(\beta) &= \mathcal{N}(\mu_\beta, \sigma_\beta^2), \quad q(\gamma_j) = \mathcal{N}(\mu_{\gamma_j}, \sigma_{\gamma_j}^2), \\ q(w_j) &= \text{Bernoulli}(\pi_{w_j}), \quad q(\pi_1) = \text{Beta}(a, b). \end{aligned}$$

We now use the variational distribution

$$q(\mathbf{z}; \boldsymbol{\eta}) = q(\mathbf{z}),$$

with the collection of variational parameters

$$\boldsymbol{\eta} = \{\mu_\beta, \sigma_\beta^2, \mu_{\gamma_1}, \sigma_{\gamma_1}^2, \pi_{w_1}, \dots, \mu_{\gamma_j}, \sigma_{\gamma_j}^2, \pi_{w_j}, \dots, \mu_{\gamma_N}, \sigma_{\gamma_N}^2, \pi_{w_N}, a, b\}$$

to approximate the perturbation  $p_t(\mathbf{z})$  of the posterior  $p_0(\mathbf{z}) = \Pr(\mathbf{z}|D)$ . Let  $q_t(\mathbf{z}) = q(\mathbf{z}; \boldsymbol{\eta}_t^*)$  denotes the optimal solution of variational distribution in MFVB when inferring  $p_t(\mathbf{z}|D)$ , with  $\boldsymbol{\eta}_t^*$  denoting the corresponding optimal solution of  $\boldsymbol{\eta}$ . Note that  $\Pr(\mathbf{z}|D) = p_t(\mathbf{z})|_{t=0}$ . Let  $q_0(\mathbf{z}) = q_t(\mathbf{z})|_{t=0}$  and  $\boldsymbol{\eta}_0^* = \boldsymbol{\eta}_t^*|_{t=0}$  refer to the optimal solution in the VEM algorithm for BWMR. Since MFVB often provides accurate inference on posterior mean, similar as in the Gaussian example, here we assume the following conditions hold:

Condition 1:  $\mathbb{E}_{q_t}[\beta] \approx \mathbb{E}_{p_t}[\beta]$  for all  $t$ , and

Condition 2:  $\left. \frac{d\mathbb{E}_{q_t}[\beta]}{dt} \right|_{t=0} \approx \left. \frac{d\mathbb{E}_{p_t}[\beta]}{dt} \right|_{t=0}$ .

Then we now have

$$\begin{aligned} \text{Var}_{\Pr(\mathbf{z}|D)}[\beta] &= \left. \frac{d\mathbb{E}_{p_t}[\beta]}{dt} \right|_{t=0} \approx \left. \frac{d\mathbb{E}_{q_t}[\beta]}{dt} \right|_{t=0} =: \widehat{\text{Var}}_{\Pr(\mathbf{z}|D)}[\beta], \\ \widehat{\text{Var}}_{\Pr(\mathbf{z}|D)}[\beta] &= \left. \frac{\partial \mathbb{E}_{q(\mathbf{z}; \boldsymbol{\eta})}[\beta]}{\partial \boldsymbol{\eta}} \right|_{\boldsymbol{\eta}=\boldsymbol{\eta}_0^*} \left. \frac{d\boldsymbol{\eta}_t^*}{dt} \right|_{t=0}. \end{aligned} \tag{38}$$

Similar as Eq. (34) and Eq. (35), we can derive

$$\begin{aligned} \left. \frac{d\boldsymbol{\eta}_t^*}{dt} \right|_{t=0} &= - \left( \left. \frac{\partial^2 KL(q(\mathbf{z}; \boldsymbol{\eta}) \| p_t(\mathbf{z}|D))}{\partial \boldsymbol{\eta} \partial \boldsymbol{\eta}^T} \right|_{\boldsymbol{\eta}=\boldsymbol{\eta}_0^*, t=0} \right)^{-1} \left. \frac{\partial^2 KL(q(\mathbf{z}; \boldsymbol{\eta}) \| p_t(\mathbf{z}|D))}{\partial t \partial \boldsymbol{\eta}^T} \right|_{\boldsymbol{\eta}=\boldsymbol{\eta}_0^*, t=0}, \\ \left. \frac{\partial^2 KL(q(\mathbf{z}; \boldsymbol{\eta}) \| p_t(\mathbf{z}|D))}{\partial t \partial \boldsymbol{\eta}^T} \right|_{\boldsymbol{\eta}=\boldsymbol{\eta}_0^*, t=0} &= - \left. \frac{\partial \mathbb{E}_{q(\mathbf{z}; \boldsymbol{\eta})}[\beta]}{\partial \boldsymbol{\eta}} \right|_{\boldsymbol{\eta}=\boldsymbol{\eta}_0^*}. \end{aligned} \quad (39)$$

Recall that the ELBO  $\mathcal{L}$  in VEM algorithm can be written as

$$\mathcal{L} = -KL(q(\mathbf{z}; \boldsymbol{\eta}) \| \Pr(\mathbf{z}|D)) + \text{constant},$$

where the constant is not relevant to  $\boldsymbol{\eta}$ , indicating

$$\frac{\partial^2 KL(q(\mathbf{z}; \boldsymbol{\eta}) \| \Pr(\mathbf{z}|D))}{\partial \boldsymbol{\eta} \partial \boldsymbol{\eta}^T} = - \frac{\partial^2 \mathcal{L}}{\partial \boldsymbol{\eta} \partial \boldsymbol{\eta}^T}. \quad (40)$$

Combining Eqs. (38, 39, 40), we finally derive the estimator of posterior variance of  $\beta$  as

$$\widehat{\text{Var}}_{\Pr(\mathbf{z}|D)}(\beta) = -\mathbf{g}^T \mathbf{H}^{-1} \mathbf{g}, \quad (41)$$

where

$$\mathbf{g} = \left. \frac{\partial \mathbb{E}_{q(\mathbf{z}; \boldsymbol{\eta})}[\beta]}{\partial \boldsymbol{\eta}^T} \right|_{\boldsymbol{\eta}=\boldsymbol{\eta}_0^*}, \quad \mathbf{H} = \left. \frac{\partial^2 \mathcal{L}}{\partial \boldsymbol{\eta} \partial \boldsymbol{\eta}^T} \right|_{\boldsymbol{\eta}=\boldsymbol{\eta}_0^*}. \quad (42)$$

- calculate the matrix  $\mathbf{H}$

The first derivatives of ELBO  $\mathcal{L}$  is given as

$$\begin{aligned} \frac{\partial \mathcal{L}}{\partial \mu_\beta} &= - \left( \sum_{j=1}^N \pi_{w_j} \frac{\mu_\beta (\mu_{\gamma_j}^2 + \sigma_{\gamma_j}^2) - \mu_{\gamma_j} \hat{\Gamma}_j}{\sigma_{Y_j}^2 + \tau^2} \right) - \frac{\mu_\beta}{\sigma_0^2}, \\ \frac{\partial \mathcal{L}}{\partial \sigma_\beta^2} &= - \left( \sum_{j=1}^N \frac{\pi_{w_j} (\mu_{\gamma_j}^2 + \sigma_{\gamma_j}^2)}{2(\sigma_{Y_j}^2 + \tau^2)} \right) - \frac{1}{2\sigma_0^2} + \frac{1}{2\sigma_\beta^2}, \\ \frac{\partial \mathcal{L}}{\partial \mu_{\gamma_j}} &= - \frac{\mu_{\gamma_j} - \hat{\gamma}_j}{\sigma_{X_j}^2} - \pi_{w_j} \frac{\mu_{\gamma_j} (\mu_\beta^2 + \sigma_\beta^2) - \mu_\beta \hat{\Gamma}_j}{\sigma_{Y_j}^2 + \tau^2} - \frac{\mu_{\gamma_j}}{\sigma^2}, \\ \frac{\partial \mathcal{L}}{\partial \sigma_{\gamma_j}^2} &= - \frac{1}{2\sigma_{X_j}^2} - \frac{\pi_{w_j} (\mu_\beta^2 + \sigma_\beta^2)}{2(\sigma_{Y_j}^2 + \tau^2)} - \frac{1}{2\sigma^2} + \frac{1}{2\sigma_{\gamma_j}^2}, \end{aligned}$$

$$\frac{\partial \mathcal{L}}{\partial \pi_{w_j}} = -\frac{\log(2\pi)}{2} - \frac{\log(\sigma_{Y_j}^2 + \tau^2)}{2} - \frac{(\mu_\beta^2 + \sigma_\beta^2)(\mu_{\gamma_j}^2 + \sigma_{\gamma_j}^2) - 2\mu_\beta \mu_{\gamma_j} \hat{\Gamma}_j + \hat{\Gamma}_j^2}{2(\sigma_{Y_j}^2 + \tau^2)} + \psi(a) - \psi(b) + \log\left(\frac{1 - \pi_{w_j}}{\pi_{w_j}}\right),$$

$$\frac{\partial \mathcal{L}}{\partial a} = \psi'(a)(a_0 - a + \sum_{j=1}^N \pi_{w_j}) + \psi'(a+b)(a+b-1-N-a_0),$$

$$\frac{\partial \mathcal{L}}{\partial b} = \psi'(b)(N+1-b - \sum_{j=1}^N \pi_{w_j}) + \psi'(a+b)(a+b-1-N-a_0).$$

Among the second derivatives of ELBO  $\mathcal{L}$ , those do not have zero-values, are written

as

$$\begin{aligned} \frac{\partial^2 \mathcal{L}}{\partial \mu_\beta \partial \mu_\beta} &= -\left(\sum_{j=1}^N \frac{\pi_{w_j}(\mu_{\gamma_j}^2 + \sigma_{\gamma_j}^2)}{\sigma_{Y_j}^2 + \tau^2}\right) - \frac{1}{\sigma_0^2}, \\ \frac{\partial^2 \mathcal{L}}{\partial \mu_\beta \partial \mu_{\gamma_j}} &= \frac{\partial^2 \mathcal{L}}{\partial \mu_{\gamma_j} \partial \mu_\beta} = -\frac{\pi_{w_j}(2\mu_\beta \mu_{\gamma_j} - \hat{\Gamma}_j)}{\sigma_{Y_j}^2 + \tau^2}, \\ \frac{\partial^2 \mathcal{L}}{\partial \mu_\beta \partial \sigma_{\gamma_j}^2} &= \frac{\partial^2 \mathcal{L}}{\partial \sigma_{\gamma_j}^2 \partial \mu_\beta} = -\frac{\pi_{w_j} \mu_\beta}{\sigma_{Y_j}^2 + \tau^2}, \\ \frac{\partial^2 \mathcal{L}}{\partial \mu_\beta \partial \pi_{w_j}} &= \frac{\partial^2 \mathcal{L}}{\partial \pi_{w_j} \partial \mu_\beta} = -\frac{\mu_\beta(\mu_{\gamma_j}^2 + \sigma_{\gamma_j}^2) - \mu_{\gamma_j} \hat{\Gamma}_j}{\sigma_{Y_j}^2 + \tau^2}, \\ \frac{\partial^2 \mathcal{L}}{\partial \sigma_\beta^2 \partial \sigma_\beta^2} &= -\frac{1}{2(\sigma_\beta^2)^2}, \\ \frac{\partial^2 \mathcal{L}}{\partial \sigma_\beta^2 \partial \mu_{\gamma_j}} &= \frac{\partial^2 \mathcal{L}}{\partial \mu_{\gamma_j} \partial \sigma_\beta^2} = -\frac{\pi_{w_j} \mu_{\gamma_j}}{\sigma_{Y_j}^2 + \tau^2}, \\ \frac{\partial^2 \mathcal{L}}{\partial \sigma_\beta^2 \partial \sigma_{\gamma_j}^2} &= \frac{\partial^2 \mathcal{L}}{\partial \sigma_{\gamma_j}^2 \partial \sigma_\beta^2} = -\frac{\pi_{w_j}}{2(\sigma_{Y_j}^2 + \tau^2)}, \quad \frac{\partial^2 \mathcal{L}}{\partial \sigma_\beta^2 \partial \pi_{w_j}} = \frac{\partial^2 \mathcal{L}}{\partial \pi_{w_j} \partial \sigma_\beta^2} = -\frac{\mu_{\gamma_j}^2 + \sigma_{\gamma_j}^2}{2(\sigma_{Y_j}^2 + \tau^2)}, \\ \frac{\partial^2 \mathcal{L}}{\partial \mu_{\gamma_j} \partial \mu_{\gamma_j}} &= -\frac{1}{\sigma_{X_j}^2} - \frac{\pi_{w_j}(\mu_\beta^2 + \sigma_\beta^2)}{\sigma_{Y_j}^2 + \tau^2} - \frac{1}{\sigma^2}, \\ \frac{\partial^2 \mathcal{L}}{\partial \mu_{\gamma_j} \partial \pi_{w_j}} &= \frac{\partial^2 \mathcal{L}}{\partial \pi_{w_j} \partial \mu_{\gamma_j}} = -\frac{\mu_{\gamma_j}(\mu_\beta^2 + \sigma_\beta^2) - \mu_\beta \hat{\Gamma}_j}{\sigma_{Y_j}^2 + \tau^2}, \\ \frac{\partial^2 \mathcal{L}}{\partial \sigma_{\gamma_j}^2 \partial \sigma_{\gamma_j}^2} &= -\frac{1}{2(\sigma_{\gamma_j}^2)^2}, \\ \frac{\partial^2 \mathcal{L}}{\partial \sigma_{\gamma_j}^2 \partial \pi_{w_j}} &= \frac{\partial^2 \mathcal{L}}{\partial \pi_{w_j} \partial \sigma_{\gamma_j}^2} = -\frac{\mu_\beta^2 + \sigma_\beta^2}{2(\sigma_{Y_j}^2 + \tau^2)}, \\ \frac{\partial^2 \mathcal{L}}{\partial \pi_{w_j} \partial \pi_{w_j}} &= -\frac{1}{\pi_{w_j}} - \frac{1}{1 - \pi_{w_j}}, \end{aligned}$$

$$\frac{\partial^2 \mathcal{L}}{\partial \pi_{w_j} \partial a} = \frac{\partial^2 \mathcal{L}}{\partial a \partial \pi_{w_j}} = \psi'(a),$$

$$\frac{\partial^2 \mathcal{L}}{\partial \pi_{w_j} \partial b} = \frac{\partial^2 \mathcal{L}}{\partial b \partial \pi_{w_j}} = -\psi'(b),$$

$$\frac{\partial^2 \mathcal{L}}{\partial a \partial a} = \psi''(a)(a_0 - a + \sum_{j=1}^N \pi_{w_j}) - \psi'(a) + \psi''(a+b)(a+b - a_0 - 1 - N) + \psi'(a+b),$$

$$\frac{\partial^2 \mathcal{L}}{\partial a \partial b} = \frac{\partial^2 \mathcal{L}}{\partial b \partial a} = \psi''(a+b)(a+b - a_0 - 1 - N) + \psi'(a+b),$$

$$\frac{\partial^2 \mathcal{L}}{\partial b \partial b} = \psi''(b)(N+1-b - \sum_{j=1}^N \pi_{w_j}) - \psi'(b) + \psi''(a+b)(a+b - a_0 - 1 - N) + \psi'(a+b).$$

- calculate the vector  $\mathbf{g}$

$$\mathbf{g} = \left. \frac{\partial \mathbb{E}_{q(\mathbf{z}; \boldsymbol{\eta})}[\beta]}{\partial \boldsymbol{\eta}} \right|_{\boldsymbol{\eta}=\boldsymbol{\eta}_0^*} = \left. \frac{\partial \mu_\beta}{\partial \boldsymbol{\eta}} \right|_{\boldsymbol{\eta}=\boldsymbol{\eta}_0^*} = [1, 0, 0, \dots, 0, 0]^T.$$

- Numerical problem of the matrix  $\mathbf{H}$

When the variational parameter  $\pi_{w_j}$  is close to its boundary 0, 1, the term  $\frac{\partial^2 \mathcal{L}}{\partial \pi_{w_j} \partial \pi_{w_j}} = -\frac{1}{\pi_{w_j}} - \frac{1}{1-\pi_{w_j}}$  makes the matrix  $\mathbf{H}$  numerically not invertible.

- Address the numerical problem by a reparameterized trick

Note that

$$\frac{\partial^2 \mathcal{L}}{\partial \pi_{w_j} \partial \pi_{w_j}} = -\frac{1}{\pi_{w_j}} - \frac{1}{1-\pi_{w_j}} = \frac{\partial^2 \mathbb{E}_{q(\mathbf{z}; \boldsymbol{\eta})}[-\log q(\mathbf{z}; \boldsymbol{\eta})]}{\partial \pi_{w_j} \partial \pi_{w_j}}.$$

The numerical problem is deal with the term  $\left. \frac{\partial^2 \mathbb{E}_{q(\mathbf{z}; \boldsymbol{\eta})}[-\log q(\mathbf{z}; \boldsymbol{\eta})]}{\partial \boldsymbol{\eta} \partial \boldsymbol{\eta}^T} \right|_{\boldsymbol{\eta}=\boldsymbol{\eta}_0^*}$ . Next we introduce a reparameterized trick to address the numerical problem.

The variational distribution  $q(\mathbf{z}; \boldsymbol{\eta})$

$$q(\mathbf{z}; \boldsymbol{\eta}) = q(\beta; \boldsymbol{\eta}) q(\pi_1; \boldsymbol{\eta}) \prod_{j=1}^N q(\gamma_j; \boldsymbol{\eta}) \prod_{j=1}^N q(w_j; \boldsymbol{\eta}),$$

with

$$\begin{aligned} q(\beta; \boldsymbol{\eta}) &= \mathcal{N}(\mu_\beta, \sigma_\beta^2), \quad q(\gamma_j; \boldsymbol{\eta}) = \mathcal{N}(\mu_{\gamma_j}, \sigma_{\gamma_j}^2), \\ q(w_j; \boldsymbol{\eta}) &= \text{Bernoulli}(\pi_{w_j}), \quad q(\pi_1; \boldsymbol{\eta}) = \text{Beta}(a, b), \\ \boldsymbol{\eta} &= \{\mu_\beta, \sigma_\beta^2, \mu_{\gamma_1}, \sigma_{\gamma_1}^2, \pi_{w_1}, \dots, \mu_{\gamma_j}, \sigma_{\gamma_j}^2, \pi_{w_j}, \dots, \mu_{\gamma_N}, \sigma_{\gamma_N}^2, \pi_{w_N}, a, b\}, \end{aligned}$$

is in an exponential family, i.e., the variational distribution can be written in the following form:

$$q(\mathbf{z}; \boldsymbol{\eta}) = \exp(\boldsymbol{\zeta}^T \mathbf{z}_s - A(\boldsymbol{\zeta})),$$

where  $\mathbf{z}_s = T(\mathbf{z})$  are the sufficient statistics,  $\boldsymbol{\zeta} = h(\boldsymbol{\eta})$ ,  $h(\cdot)$  and  $A(\cdot)$  are known functions. Then the entropy  $\mathbb{E}_{q(\mathbf{z}; \boldsymbol{\eta})}[-\log q(\mathbf{z}; \boldsymbol{\eta})]$  can be written as

$$\mathbb{E}_{q(\mathbf{z}; \boldsymbol{\eta})}[-\log q(\mathbf{z}; \boldsymbol{\eta})] = -\boldsymbol{\zeta}^T \mathbb{E}_{q(\mathbf{z}; \boldsymbol{\eta})}[\mathbf{z}_s] + A(\boldsymbol{\zeta}). \quad (43)$$

Moreover, using the cumulant generating properties again yields

$$\begin{aligned} \mathbb{E}_{q(\mathbf{z}; \boldsymbol{\eta})}[\mathbf{z}_s] &= \frac{\partial A(\boldsymbol{\zeta})}{\partial \boldsymbol{\zeta}}, \\ \text{Cov}_{q(\mathbf{z}; \boldsymbol{\eta})}[\mathbf{z}_s] &= \frac{\partial^2 A(\boldsymbol{\zeta})}{\partial \boldsymbol{\zeta}^T \partial \boldsymbol{\zeta}}, \end{aligned}$$

indicating

$$\text{Cov}_{q(\mathbf{z}; \boldsymbol{\eta})}[\mathbf{z}_s] = \frac{\partial \mathbb{E}_{q(\mathbf{z}; \boldsymbol{\eta})}[\mathbf{z}_s]}{\partial \boldsymbol{\zeta}}. \quad (44)$$

For notation convenience, let

$$\mathbf{m} := \mathbb{E}_{q(\mathbf{z}; \boldsymbol{\eta})}[\mathbf{z}_s]. \quad (45)$$

Then combining Eqs. (43,44,45), we derive

$$\begin{aligned} \frac{\partial \mathbb{E}_{q(\mathbf{z}; \boldsymbol{\eta})}[-\log q(\mathbf{z}; \boldsymbol{\eta})]}{\partial \mathbf{m}} &= \frac{\partial[-\boldsymbol{\zeta}^T \mathbf{m} + A(\boldsymbol{\zeta})]}{\partial \boldsymbol{\zeta}^T} \frac{\partial \boldsymbol{\zeta}}{\partial \mathbf{m}} + \frac{\partial[-\boldsymbol{\zeta}^T \mathbf{m} + A(\boldsymbol{\zeta})]}{\partial \mathbf{m}} \\ &= \left( -\mathbf{m} + \frac{\partial A(\boldsymbol{\zeta})}{\partial \boldsymbol{\zeta}} \right) \frac{\partial \boldsymbol{\zeta}}{\partial \mathbf{m}} - \boldsymbol{\zeta} \\ &= -\boldsymbol{\zeta}, \end{aligned}$$

and

$$\frac{\partial^2 \mathbb{E}_{q(\mathbf{z}; \boldsymbol{\eta})}[-\log q(\mathbf{z}; \boldsymbol{\eta})]}{\partial \mathbf{m} \partial \mathbf{m}^T} = -\frac{\partial \boldsymbol{\zeta}}{\partial \mathbf{m}} = -\left( \frac{\partial \mathbf{m}}{\partial \boldsymbol{\zeta}} \right)^{-1} = -(\text{Cov}_{q(\mathbf{z}; \boldsymbol{\eta})}[\mathbf{z}_s])^{-1}. \quad (46)$$

Note that  $q(\beta)$ ,  $q(\gamma_j)$ ,  $q(w_j)$ ,  $q(\pi_1)$  can be written in exponential family forms as

$$\begin{aligned} q(\beta) &= \frac{1}{\sqrt{2\pi\sigma_\beta^2}} \exp\left(-\frac{1}{2\sigma_\beta^2}(\beta - \mu_\beta)^2\right) = \frac{1}{\sqrt{2\pi\sigma_\beta^2}} \exp\left(-\frac{\mu_\beta}{2\sigma_\beta^2}\right) \exp\left(\frac{\mu_\beta}{\sigma_\beta^2}\beta - \frac{1}{2\sigma_\beta^2}\beta^2\right), \\ q(\gamma_j) &= \frac{1}{\sqrt{2\pi\sigma_{\gamma_j}^2}} \exp\left(-\frac{1}{2\sigma_{\gamma_j}^2}(\gamma_j - \mu_{\gamma_j})^2\right) = \frac{1}{\sqrt{2\pi\sigma_{\gamma_j}^2}} \exp\left(-\frac{\mu_{\gamma_j}}{2\sigma_{\gamma_j}^2}\right) \exp\left(\frac{\mu_{\gamma_j}}{\sigma_{\gamma_j}^2}\gamma_j - \frac{1}{2\sigma_{\gamma_j}^2}\gamma_j^2\right), \\ q(w_j) &= \pi_{w_j}^{w_j} (1 - \pi_{w_j})^{1-w_j} = (1 - \pi_{w_j}) \exp[(\log \pi_{w_j} - \log(1 - \pi_{w_j}))w_j], \\ q(\pi_1) &= \frac{\pi_1^{a-1} (1 - \pi_1)^{b-1}}{\text{B}(a, b)} = \frac{1}{\text{B}(a, b)} \exp[(a-1)\log \pi_1 + (b-1)\log(1 - \pi_1)], \end{aligned}$$

where  $B(\cdot, \cdot)$  denotes the beta function. Clearly, we get the sufficient statistics of latent variables as

$$\begin{aligned} T(\beta) &= (\beta, \beta^2), T(\gamma_j) = (\gamma_j, \gamma_j^2) \\ T(w_j) &= w_j, T(\pi_1) = (\log \pi_1, \log(1 - \pi_1)), \end{aligned}$$

implying

$$\begin{aligned} \mathbf{z}_s &= T(\mathbf{z}) \\ &= (T(\beta), T(\gamma_1), T(w_1), \dots, T(\gamma_j), T(w_j), \dots, T(\gamma_N), T(w_N), T(\pi_1)) \\ &= (\beta, \beta^2, \gamma_1, \gamma_1^2, w_1, \dots, \gamma_j, \gamma_j^2, w_j, \dots, \gamma_N, \gamma_N^2, w_N, \log \pi_1, \log(1 - \pi_1)). \end{aligned}$$

Then we derive  $\mathbf{m}$  as

$$\begin{aligned} \mathbf{m} &= \mathbb{E}_q[\mathbf{z}_s] \\ &= (m_{\beta,1}, m_{\beta,2}, m_{\gamma_{1,1}}, m_{\gamma_{1,2}}, m_{w_1}, \dots, m_{\gamma_{j,1}}, m_{\gamma_{j,2}}, m_{w_j}, \dots, m_{\gamma_{N,1}}, m_{\gamma_{N,2}}, m_{w_N}, m_{\pi_{1,1}}, m_{\pi_{1,2}}), \end{aligned}$$

with

$$\begin{aligned} m_{\beta,1} &:= \mathbb{E}_q[\beta] = \mu_\beta, m_{\beta,2} := \mathbb{E}_q[\beta^2] = \mu_\beta^2 + \sigma_\beta^2, \\ m_{\gamma_{j,1}} &:= \mathbb{E}_q[\gamma_j] = \mu_{\gamma_j}, m_{\gamma_{j,2}} := \mathbb{E}_q[\gamma_j^2] = \mu_{\gamma_j}^2 + \sigma_{\gamma_j}^2 \\ m_{w_j} &:= \mathbb{E}_q[w_j] = \pi_{w_j}, \\ m_{\pi_{1,1}} &:= \mathbb{E}_q[\log \pi_1] = \psi(a) - \psi(a + b), m_{\pi_{1,2}} := \mathbb{E}_q[\log(1 - \pi_1)] = \psi(b) - \psi(a + b). \end{aligned}$$

Importantly, note that the variational distribution  $q(\mathbf{z}) = q(\mathbf{z}; \boldsymbol{\eta})$  can also be parameterized by the vector  $\mathbf{m}$ , here adopt this reparameterized trick and let  $q(\mathbf{z}) = q(\mathbf{z}; \mathbf{m})$  represents the variational distribution parameterized by  $\mathbf{m}$ . We assume that the parameters  $\boldsymbol{\eta}_0^*$  (optimal solution of  $\boldsymbol{\eta}$ ) and  $\mathbf{m}_0^*$  (optimal solution of  $\mathbf{m}$ ) in MFVB from the VEM algorithm are in the interior of their feasible space. Then under the same conditions (Condition 1, 2), similar as the result in Eqs. (41, 42), i.e.,

$$\widehat{\text{Var}}_{\text{Pr}(\mathbf{z}|D)}(\beta) = -\mathbf{g}^T \mathbf{H}^{-1} \mathbf{g},$$

where

$$\mathbf{g} = \left. \frac{\partial \mathbb{E}_{q(\mathbf{z}; \boldsymbol{\eta})}[\beta]}{\partial \boldsymbol{\eta}^T} \right|_{\boldsymbol{\eta} = \boldsymbol{\eta}_0^*}, \mathbf{H} = \left. \frac{\partial^2 \mathcal{L}}{\partial \boldsymbol{\eta} \partial \boldsymbol{\eta}^T} \right|_{\boldsymbol{\eta} = \boldsymbol{\eta}_0^*},$$

with the reparameterization we now have

$$\widehat{\text{Var}}_{\text{Pr}(\mathbf{z}|D)}(\beta) = -\mathbf{g}_m^T (\mathbf{H}_{mm})^{-1} \mathbf{g}_m,$$

where

$$\mathbf{g}_{\mathbf{m}} = \frac{\partial \mathbb{E}_{q(\mathbf{z}; \mathbf{m})}[\beta]}{\partial \mathbf{m}^T} \Big|_{\mathbf{m}=\mathbf{m}_0^*}, \quad \mathbf{H}_{\mathbf{m}\mathbf{m}} = \frac{\partial^2 \mathcal{L}}{\partial \mathbf{m} \partial \mathbf{m}^T} \Big|_{\mathbf{m}=\mathbf{m}_0^*}.$$

Note that the

$$\mathcal{L} = \mathbb{E}_{q(\mathbf{z}; \mathbf{m})}[\log \Pr(\hat{\gamma}, \hat{\Gamma}, \mathbf{z} | \sigma_X^2, \sigma_Y^2; \boldsymbol{\theta}; \mathbf{h}_0)] + \mathbb{E}_{q(\mathbf{z}; \mathbf{m})}[-\log q(\mathbf{z}; \mathbf{m})],$$

and that the results given in Eq. (46) as

$$\frac{\partial^2 \mathbb{E}_{q(\mathbf{z}; \mathbf{m})}[-\log q(\mathbf{z}; \mathbf{m})]}{\partial \mathbf{m} \partial \mathbf{m}^T} = -(\text{Cov}_{q(\mathbf{z}; \mathbf{m})}[\mathbf{z}_s])^{-1}.$$

Let

$$\mathbf{H}_{\mathbf{m}\mathbf{m}}^1 := \frac{\partial^2 \mathbb{E}_{q(\mathbf{z}; \mathbf{m})}[\log \Pr(\hat{\gamma}, \hat{\Gamma}, \mathbf{z} | \sigma_X^2, \sigma_Y^2; \boldsymbol{\theta}; \mathbf{h}_0)]}{\partial \mathbf{m} \partial \mathbf{m}^T} \Big|_{\mathbf{m}=\mathbf{m}_0^*}, \quad \mathbf{V} := \text{Cov}_{q(\mathbf{z}; \mathbf{m})}[\mathbf{z}_s] \Big|_{\mathbf{m}=\mathbf{m}_0^*}.$$

Then we can write  $(\mathbf{H}_{\mathbf{m}\mathbf{m}})^{-1}$  as

$$(\mathbf{H}_{\mathbf{m}\mathbf{m}})^{-1} = (\mathbf{H}_{\mathbf{m}\mathbf{m}}^1 - \mathbf{V}^{-1})^{-1} = (\mathbf{V}\mathbf{H}_{\mathbf{m}\mathbf{m}}^1 - \mathbf{I})^{-1}\mathbf{V}.$$

Calculating  $(\mathbf{H}_{\mathbf{m}\mathbf{m}})^{-1}$  in this way can prevent the numerical instability in practice, because the term corresponding to  $-\frac{1}{w_j} - \frac{1}{1-w_j} = -\frac{1}{w_j(1-w_j)}$  becomes  $w_j(1-w_j)$  in matrix  $\mathbf{V}$ .

- **calculate matrix  $\mathbf{V}$**

Recall that  $\mathbf{V} = \text{Cov}_{q(\mathbf{z}; \mathbf{m})}[\mathbf{z}_s] \Big|_{\mathbf{m}=\mathbf{m}_0^*}$ . As MFVB provides no information of covariances between different latent variables, we only need to calculate the covariance matrices  $\text{Cov}_{q(\mathbf{z})}[T(\beta)]$ ,  $\text{Cov}_{q(\mathbf{z})}[T(\gamma_j)]$ ,  $\text{Cov}_{q(\mathbf{z})}[T(w_j)]$ ,  $\text{Cov}_{q(\mathbf{z})}[T(\pi_1)]$ . Intuitively, we give a illustrative diagram for matrix  $\mathbf{V}$  in the following Figure.

As  $q(\beta)$  and  $q(\gamma_j)$  are normal distributions, the covariance matrices  $\text{Cov}_{q(\mathbf{z})}[T(\beta)]$ ,  $\text{Cov}_{q(\mathbf{z})}[T(\gamma_j)]$  are given as

$$\text{Cov}_{q(\mathbf{z})}[T(\beta)] = \begin{bmatrix} \text{Var}_q(\beta) & \text{Cov}_q(\beta, \beta^2) \\ \text{Cov}_q(\beta^2, \beta) & \text{Var}_q(\beta^2) \end{bmatrix},$$

$$\text{Cov}_{q(\mathbf{z})}[T(\gamma_j)] = \begin{bmatrix} \text{Var}_q(\gamma_j) & \text{Cov}_q(\gamma_j, \gamma_j^2) \\ \text{Cov}_q(\gamma_j^2, \gamma_j) & \text{Var}_q(\gamma_j^2) \end{bmatrix}.$$

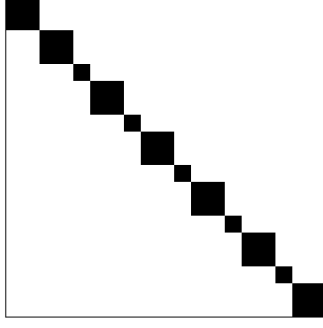


Figure 5: Sparsity pattern for the  $(3N + 4) \times (3N + 4)$  matrix  $\mathbf{V}$ . For simplicity, here we choose  $N = 5$  as an example.

Recall that  $q(\beta) = \mathcal{N}(\mu_\beta, \sigma_\beta^2)$ , and that if  $\xi \sim \mathcal{N}(\xi|0, 1)$  then

$$\mathbb{E}(\xi^k) = \begin{cases} (k-1)!!, & k = 2n, n \in \mathbb{N}_+, \\ 0, & k = 2n-1, n \in \mathbb{N}_+. \end{cases}$$

To use this property, we rewrite  $\beta$  as  $\beta = \sigma_\beta \left( \frac{\beta - \mu_\beta}{\sigma_\beta} + \frac{\mu_\beta}{\sigma_\beta} \right) = \sigma_\beta \left( \xi + \frac{\mu_\beta}{\sigma_\beta} \right)$ . Therefore, we have

$$\mathbb{E}_q(\beta^2) = \mu_\beta^2 + \sigma_\beta^2,$$

$$\mathbb{E}_q(\beta^3) = \mathbb{E} \left[ \sigma_\beta^3 \left( \xi + \frac{\mu_\beta}{\sigma_\beta} \right)^3 \right] = \sigma_\beta^3 \mathbb{E} \left[ \xi^3 + 3 \frac{\mu_\beta}{\sigma_\beta} \xi^2 + 3 \left( \frac{\mu_\beta}{\sigma_\beta} \right)^2 \xi + \left( \frac{\mu_\beta}{\sigma_\beta} \right)^3 \right] = 3\mu_\beta \sigma_\beta^2 + \mu_\beta^3,$$

$$\mathbb{E}_q(\beta^4) = \mathbb{E} \left[ \sigma_\beta^4 \left( \xi + \frac{\mu_\beta}{\sigma_\beta} \right)^4 \right] = \sigma_\beta^4 \mathbb{E} \left[ \xi^4 + 4 \frac{\mu_\beta}{\sigma_\beta} \xi^3 + 6 \left( \frac{\mu_\beta}{\sigma_\beta} \right)^2 \xi^2 + 4 \left( \frac{\mu_\beta}{\sigma_\beta} \right)^3 \xi + \left( \frac{\mu_\beta}{\sigma_\beta} \right)^4 \right] = 3\sigma_\beta^4 + 6\mu_\beta^2 \sigma_\beta^2 +$$

Then, we derive

$$\text{Var}_q(\beta^2) = \mathbb{E}(\beta^4) - \mathbb{E}^2(\beta^2) = 3\sigma_\beta^4 + 6\mu_\beta^2 \sigma_\beta^2 + \mu_\beta^4 - (\sigma_\beta^2 + \mu_\beta^2)^2 = 2\sigma_\beta^4 + 4\mu_\beta^2 \sigma_\beta^2,$$

$$\text{Cov}(\beta^2, \beta) = \mathbb{E}(\beta^3) - \mathbb{E}(\beta^2)\mathbb{E}(\beta) = 3\mu_\beta \sigma_\beta^2 + \mu_\beta^3 - (\sigma_\beta^2 + \mu_\beta^2)\mu_\beta = 2\mu_\beta \sigma_\beta^2,$$

yielding

$$\text{Cov}_{q(\mathbf{z})}[T(\beta)] = \begin{bmatrix} \sigma_\beta^2 & 2\mu_\beta \sigma_\beta^2 \\ 2\mu_\beta \sigma_\beta^2 & 2\sigma_\beta^4 + 4\mu_\beta^2 \sigma_\beta^2 \end{bmatrix}.$$

Similarly, we have

$$\text{Cov}_{q(\mathbf{z})}[T(\gamma_j)] = \begin{bmatrix} \sigma_{\gamma_j}^2 & 2\mu_{\gamma_j} \sigma_{\gamma_j}^2 \\ 2\mu_{\gamma_j} \sigma_{\gamma_j}^2 & 2\sigma_{\gamma_j}^4 + 4\mu_{\gamma_j}^2 \sigma_{\gamma_j}^2 \end{bmatrix}.$$

Given that  $q(w_j) = \text{Bernoulli}(\pi_{w_j})$ , the variance of  $w_j$  is given as

$$\text{Var}_{q(\mathbf{z})}[T(w_j)] = \mathbb{E}_q(w_j^2) - \mathbb{E}_q^2(w_j) = \pi_{w_j} - \pi_{w_j}^2.$$

Recall that  $q(\pi_1) = \text{Beta}(a, b)$  and  $T(\pi_1) = (\log \pi_1, \log(1 - \pi_1))$ , then we know

$$\text{Cov}_{q(\mathbf{z})}[T(\pi_1)] = \begin{bmatrix} \text{Var}_q(\log \pi_1) & \text{Cov}_q(\log \pi_1, \log(1 - \pi_1)) \\ \text{Cov}_q(\log(1 - \pi_1), \log \pi_1) & \text{Var}_q(\log(1 - \pi_1)) \end{bmatrix}. \quad (47)$$

It is not hard to derive

$$\text{Var}_q(\log \pi_1) = \psi_1(a) - \psi_1(a + b),$$

where  $\psi_1(\cdot)$  represents the trigamma function. Note that  $(1 - \pi_1) \sim \text{Beta}(b, a)$ , then we know

$$\text{Var}_q(\log(1 - \pi_1)) = \psi_1(b) - \psi_1(a + b).$$

To calculate  $\text{Cov}_q(\log(1 - \pi_1), \log \pi_1)$ , we need to find  $\mathbb{E}_q[\log \pi_1 \log(1 - \pi_1)]$  firstly:

$$\mathbb{E}_q[\log \pi_1 \log(1 - \pi_1)] = \int_0^1 \log x \log(1 - x) \frac{x^{a-1}(1-x)^{b-1}}{\text{B}(a, b)} dx.$$

Note that,

$$\frac{\partial^2[x^{a-1}(1-x)^{b-1}]}{\partial a \partial b} = \frac{\partial^2[x^{a-1}(1-x)^{b-1}]}{\partial b \partial a} = \log x \log(1-x) x^{a-1}(1-x)^{b-1}.$$

Therefore,

$$\begin{aligned} \mathbb{E}_q[\log \pi_1 \log(1 - \pi_1)] &= \frac{1}{\text{B}(a, b)} \int_0^1 \frac{\partial^2[x^{a-1}(1-x)^{b-1}]}{\partial a \partial b} dx \\ &= \frac{1}{\text{B}(a, b)} \frac{\partial^2}{\partial a \partial b} \int_0^1 x^{a-1}(1-x)^{b-1} dx \\ &= \frac{1}{\text{B}(a, b)} \frac{\partial^2 \text{B}(a, b)}{\partial a \partial b}. \end{aligned}$$

With detailed derivations as

$$\begin{aligned} \frac{\partial \text{B}(a, b)}{\partial a} &= \frac{\partial}{\partial a} \left[ \frac{\Gamma(a)\Gamma(b)}{\Gamma(a+b)} \right] \\ &= \Gamma(b) \frac{\Gamma'(a)\Gamma(a+b) - \Gamma(a)\Gamma'(a+b)}{\Gamma^2(a+b)} \\ &= \frac{\Gamma(a)\Gamma(b)}{\Gamma(a+b)} \left[ \frac{\Gamma'(a)}{\Gamma(a)} - \frac{\Gamma'(a+b)}{\Gamma(a+b)} \right] \\ &= \text{B}(a, b)[\psi(a) - \psi(a+b)] \end{aligned}$$

and

$$\begin{aligned}
\frac{\partial^2 B(a, b)}{\partial b \partial a} &= \frac{\partial B(a, b)}{\partial b} [\psi(a) - \psi(a + b)] + B(a, b) \frac{\partial}{\partial b} [\psi(a) - \psi(a + b)] \\
&= B(a, b) [\psi(b) - \psi(a + b)] [\psi(a) - \psi(a + b)] - B(a, b) \psi_1(a + b) \\
&= B(a, b) \{ [\psi(b) - \psi(a + b)] [\psi(a) - \psi(a + b)] - \psi_1(a + b) \},
\end{aligned}$$

we finally derive

$$\mathbb{E}_q[\log \pi_1 \log(1 - \pi_1)] = [\psi(a) - \psi(a + b)] [\psi(b) - \psi(a + b)] - \psi_1(a + b). \quad (48)$$

Further considering that  $\mathbb{E}_q[\log \pi_1] = \psi(a) - \psi(a + b)$ ,  $\mathbb{E}_q[\log(1 - \pi_1)] = \psi(b) - \psi(a + b)$  and Eq. (48), we have

$$\begin{aligned}
\text{Cov}_q(\log \pi_1, \log(1 - \pi_1)) &= \mathbb{E}_q[\log p(\pi_1) \log p(1 - \pi_1)] - \mathbb{E}_q[\log p(\pi_1)] \mathbb{E}_q[\log p(1 - \pi_1)] \\
&= [\psi(a) - \psi(a + b)] [\psi(b) - \psi(a + b)] - \psi_1(a + b) \\
&\quad - [\psi(a) - \psi(a + b)] [\psi(b) - \psi(a + b)] \\
&= -\psi_1(a + b),
\end{aligned}$$

i.e.,

$$\text{Cov}_{q(\mathbf{z})}(\log \pi_1, \log(1 - \pi_1)) = \text{Cov}_{q(\mathbf{z})}(\log(1 - \pi_1), \log \pi_1) = -\psi_1(a + b).$$

Thus, we derive

$$\text{Cov}_{q(\mathbf{z})}[T(\pi_1)] = \begin{bmatrix} \psi_1(a) - \psi_1(a + b) & -\psi_1(a + b) \\ -\psi_1(a + b) & \psi_1(b) - \psi_1(a + b) \end{bmatrix}.$$

- calculate matrix  $\mathbf{H}_{\mathbf{m}\mathbf{m}}^1$

Recall that  $\mathbf{H}_{\mathbf{m}\mathbf{m}}^1 = \left. \frac{\partial^2 \mathbb{E}_q[\log \Pr(\hat{\gamma}, \hat{\Gamma}, \mathbf{z} | \sigma_X^2, \sigma_Y^2; \boldsymbol{\theta}; \mathbf{h}_0)]}{\partial \mathbf{m}^T \partial \mathbf{m}} \right|_{\mathbf{m}=\mathbf{m}_0^*}$ . To calculate matrix  $\mathbf{H}_{\mathbf{m}\mathbf{m}}^1$ , we summa-

size the terms with  $\mathbf{m}$  in  $\mathbb{E}_q[\log \Pr(\hat{\gamma}, \hat{\Gamma}, \mathbf{z} | \sigma_X^2, \sigma_Y^2; \boldsymbol{\theta}; \mathbf{h}_0)]$  as:

$$\begin{aligned}
& \mathbb{E}_q[\log \Pr(\hat{\gamma}, \hat{\Gamma}, \mathbf{z} | \sigma_X^2, \sigma_Y^2; \boldsymbol{\theta}; \mathbf{h}_0)] \\
&= \sum_{j=1}^N \left( -\frac{m_{\gamma_{j,2}} - 2\hat{\gamma}_j m_{\gamma_{j,1}}}{2\sigma_{X_j}^2} \right) \\
&+ \sum_{j=1}^N m_{w_j} \left[ -\frac{1}{2} \log(2\pi) - \frac{1}{2} \log(\sigma_{Y_j}^2 + \tau^2) - \frac{m_{\beta,2} m_{\gamma_{j,2}} - 2m_{\beta,1} \hat{\Gamma}_j m_{\gamma_{j,1}} + \hat{\Gamma}_j^2}{2(\sigma_{Y_j}^2 + \tau^2)} \right] \\
&- \frac{m_{\beta,2}}{2\sigma_0^2} \\
&+ \sum_{j=1}^N \left( -\frac{m_{\gamma_{j,2}}}{2\sigma^2} \right) \\
&+ \sum_{j=1}^N [m_{w_j} m_{\pi_{1,1}} + (1 - m_{w_j}) m_{\pi_{1,2}}] \\
&+ (a_0 - 1) m_{\pi_{1,1}} \\
&+ \text{constant.}
\end{aligned}$$

Therefore we can calculate  $\frac{\partial^2 \mathbb{E}_q[\log \Pr(\hat{\gamma}, \hat{\Gamma}, \mathbf{z} | \sigma_X^2, \sigma_Y^2; \boldsymbol{\theta}; \mathbf{h}_0)]}{\partial \mathbf{m}^T \partial \mathbf{m}}$  as follows. The first derivatives are given as

$$\begin{aligned}
\frac{\partial \mathbb{E}_q[\log \Pr(\hat{\gamma}, \hat{\Gamma}, \mathbf{z} | \sigma_X^2, \sigma_Y^2; \boldsymbol{\theta}; \mathbf{h}_0)]}{\partial m_{\beta,1}} &= \sum_{j=1}^N \frac{m_{w_j} \hat{\Gamma}_j m_{\gamma_{j,1}}}{\sigma_{Y_j}^2 + \tau^2}, \\
\frac{\partial \mathbb{E}_q[\log \Pr(\hat{\gamma}, \hat{\Gamma}, \mathbf{z} | \sigma_X^2, \sigma_Y^2; \boldsymbol{\theta}; \mathbf{h}_0)]}{\partial m_{\beta,2}} &= - \sum_{j=1}^N \left[ \frac{m_{w_j} m_{\gamma_{j,2}}}{2(\sigma_{Y_j}^2 + \tau^2)} \right] - \frac{1}{2\sigma_0^2}, \\
\frac{\partial \mathbb{E}_q[\log \Pr(\hat{\gamma}, \hat{\Gamma}, \mathbf{z} | \sigma_X^2, \sigma_Y^2; \boldsymbol{\theta}; \mathbf{h}_0)]}{\partial m_{\gamma_{j,1}}} &= \frac{\hat{\gamma}_j}{\sigma_{X_j}^2} + \frac{m_{w_j} m_{\beta,1} \hat{\Gamma}_j}{\sigma_{Y_j}^2 + \tau^2}, \\
\frac{\partial \mathbb{E}_q[\log \Pr(\hat{\gamma}, \hat{\Gamma}, \mathbf{z} | \sigma_X^2, \sigma_Y^2; \boldsymbol{\theta}; \mathbf{h}_0)]}{\partial m_{\gamma_{j,2}}} &= -\frac{1}{2\sigma_{X_j}^2} - \frac{m_{w_j} m_{\beta,2}}{2(\sigma_{Y_j}^2 + \tau^2)} - \frac{1}{2\sigma^2}, \\
\frac{\partial \mathbb{E}_q[\log \Pr(\hat{\gamma}, \hat{\Gamma}, \mathbf{z} | \sigma_X^2, \sigma_Y^2; \boldsymbol{\theta}; \mathbf{h}_0)]}{\partial m_{w_j}} &= -\frac{1}{2} \log(2\pi) - \frac{1}{2} \log(\sigma_{Y_j}^2 + \tau^2) \\
&- \frac{m_{\beta,2} m_{\gamma_{j,2}} - 2m_{\beta,1} \hat{\Gamma}_j m_{\gamma_{j,1}} + \hat{\Gamma}_j^2}{2(\sigma_{Y_j}^2 + \tau^2)} + m_{\pi_{1,1}} - m_{\pi_{1,2}},
\end{aligned}$$

$$\frac{\partial \mathbb{E}_q[\log \Pr(\hat{\gamma}, \hat{\Gamma}, \mathbf{z} | \sigma_X^2, \sigma_Y^2; \boldsymbol{\theta}; \mathbf{h}_0)]}{\partial m_{\pi,1}} = (a_0 - 1) + \sum_{j=1}^N m_{w_j},$$

$$\frac{\partial \mathbb{E}_q[\log \Pr(\hat{\gamma}, \hat{\Gamma}, \mathbf{z} | \sigma_X^2, \sigma_Y^2; \boldsymbol{\theta}; \mathbf{h}_0)]}{\partial m_{\pi,2}} = N - \sum_{j=1}^N m_{w_j}.$$

Among the second derivatives, those which do not have zero values are:

$$\frac{\partial^2 \mathbb{E}_q[\log \Pr(\hat{\gamma}, \hat{\Gamma}, \mathbf{z} | \sigma_X^2, \sigma_Y^2; \boldsymbol{\theta}; \mathbf{h}_0)]}{\partial m_{\beta,1} \partial m_{\gamma_j,1}} = \frac{\partial^2 \mathbb{E}_q[\log \Pr(\hat{\gamma}, \hat{\Gamma}, \mathbf{z} | \sigma_X^2, \sigma_Y^2; \boldsymbol{\theta}; \mathbf{h}_0)]}{\partial m_{\gamma_j,1} \partial m_{\beta,1}} = \frac{m_{w_j} \hat{\Gamma}_j}{\sigma_{Y_j}^2 + \tau^2},$$

$$\frac{\partial^2 \mathbb{E}_q[\log \Pr(\hat{\gamma}, \hat{\Gamma}, \mathbf{z} | \sigma_X^2, \sigma_Y^2; \boldsymbol{\theta}; \mathbf{h}_0)]}{\partial m_{\beta,1} \partial m_{w_j}} = \frac{\partial^2 \mathbb{E}_q[\log \Pr(\hat{\gamma}, \hat{\Gamma}, \mathbf{z} | \sigma_X^2, \sigma_Y^2; \boldsymbol{\theta}; \mathbf{h}_0)]}{\partial m_{w_j} \partial m_{\beta,1}} = \frac{m_{\gamma_j,1} \hat{\Gamma}_j}{\sigma_{Y_j}^2 + \tau^2},$$

$$\frac{\partial^2 \mathbb{E}_q[\log \Pr(\hat{\gamma}, \hat{\Gamma}, \mathbf{z} | \sigma_X^2, \sigma_Y^2; \boldsymbol{\theta}; \mathbf{h}_0)]}{\partial m_{\beta,2} \partial m_{\gamma_j,2}} = \frac{\partial^2 \mathbb{E}_q[\log \Pr(\hat{\gamma}, \hat{\Gamma}, \mathbf{z} | \sigma_X^2, \sigma_Y^2; \boldsymbol{\theta}; \mathbf{h}_0)]}{\partial m_{\gamma_j,2} \partial m_{\beta,2}} = -\frac{m_{w_j}}{2(\sigma_{Y_j}^2 + \tau^2)},$$

$$\frac{\partial^2 \mathbb{E}_q[\log \Pr(\hat{\gamma}, \hat{\Gamma}, \mathbf{z} | \sigma_X^2, \sigma_Y^2; \boldsymbol{\theta}; \mathbf{h}_0)]}{\partial m_{\beta,2} \partial m_{w_j}} = \frac{\partial^2 \mathbb{E}_q[\log \Pr(\hat{\gamma}, \hat{\Gamma}, \mathbf{z} | \sigma_X^2, \sigma_Y^2; \boldsymbol{\theta}; \mathbf{h}_0)]}{\partial m_{w_j} \partial m_{\beta,2}} = -\frac{m_{\gamma_j,2}}{2(\sigma_{Y_j}^2 + \tau^2)},$$

$$\frac{\partial^2 \mathbb{E}_q[\log \Pr(\hat{\gamma}, \hat{\Gamma}, \mathbf{z} | \sigma_X^2, \sigma_Y^2; \boldsymbol{\theta}; \mathbf{h}_0)]}{\partial m_{\gamma_j,1} \partial m_{w_j}} = \frac{\partial^2 \mathbb{E}_q[\log \Pr(\hat{\gamma}, \hat{\Gamma}, \mathbf{z} | \sigma_X^2, \sigma_Y^2; \boldsymbol{\theta}; \mathbf{h}_0)]}{\partial m_{w_j} \partial m_{\gamma_j,1}} = \frac{m_{\beta,1} \hat{\Gamma}_j}{\sigma_{Y_j}^2 + \tau^2},$$

$$\frac{\partial^2 \mathbb{E}_q[\log \Pr(\hat{\gamma}, \hat{\Gamma}, \mathbf{z} | \sigma_X^2, \sigma_Y^2; \boldsymbol{\theta}; \mathbf{h}_0)]}{\partial m_{\gamma_j,2} \partial m_{w_j}} = \frac{\partial^2 \mathbb{E}_q[\log \Pr(\hat{\gamma}, \hat{\Gamma}, \mathbf{z} | \sigma_X^2, \sigma_Y^2; \boldsymbol{\theta}; \mathbf{h}_0)]}{\partial m_{w_j} \partial m_{\gamma_j,2}} = -\frac{m_{\beta,2}}{2(\sigma_{Y_j}^2 + \tau^2)},$$

$$\frac{\partial^2 \mathbb{E}_q[\log \Pr(\hat{\gamma}, \hat{\Gamma}, \mathbf{z} | \sigma_X^2, \sigma_Y^2; \boldsymbol{\theta}; \mathbf{h}_0)]}{\partial m_{\pi,1} \partial m_{w_j}} = \frac{\partial^2 \mathbb{E}_q[\log \Pr(\hat{\gamma}, \hat{\Gamma}, \mathbf{z} | \sigma_X^2, \sigma_Y^2; \boldsymbol{\theta}; \mathbf{h}_0)]}{\partial m_{w_j} \partial m_{\pi,1}} = 1,$$

$$\frac{\partial^2 \mathbb{E}_q[\log \Pr(\hat{\gamma}, \hat{\Gamma}, \mathbf{z} | \sigma_X^2, \sigma_Y^2; \boldsymbol{\theta}; \mathbf{h}_0)]}{\partial m_{\pi,2} \partial m_{w_j}} = \frac{\partial^2 \mathbb{E}_q[\log \Pr(\hat{\gamma}, \hat{\Gamma}, \mathbf{z} | \sigma_X^2, \sigma_Y^2; \boldsymbol{\theta}; \mathbf{h}_0)]}{\partial m_{w_j} \partial m_{\pi,2}} = -1.$$

We finally derive the matrix  $\mathbf{H}_{\text{mm}}^1$ . Intuitively, we give a illustrative diagram for matrix  $\mathbf{H}_{\text{mm}}^1$  in the following figure:

- calculate the vector  $\mathbf{g}_m$

$$\mathbf{g}_m = \frac{\partial \mathbb{E}_q[\mathbf{z} | \beta]}{\partial \mathbf{m}} \Big|_{\boldsymbol{\eta} = \boldsymbol{\eta}_0^*} = \frac{\partial m_{\beta,1}}{\partial \mathbf{m}} \Big|_{\mathbf{m} = \mathbf{m}_0^*} = [1, 0, 0, \dots, 0]^T.$$

- calculate the standard error of  $\beta$

Finally, the standard error of  $\beta$  is provided as the element in the first row and the first column of the matrix  $\mathbf{H}_{\text{mm}} = (\mathbf{V} \mathbf{H}_{\text{mm}}^1 - \mathbf{I})^{-1} \mathbf{V}$ .

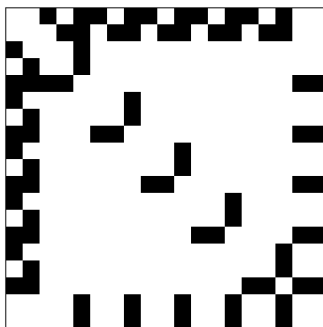


Figure 6: Sparsity pattern for the  $(3N + 4) \times (3N + 4)$  matrix  $\mathbf{H}_{\text{mmm}}^1$ . For simplicity, here we choose  $N = 5$  as an example.

## C Comparison of different MR Methods

Methods like Egger and GSMR are closely related to standard Inverse Variance Weighted (IVW) meta analysis approach. The development of these MR methods put more efforts to address the issue of horizontal pleiotropy. To connect these methods, we first introduce the IVW method here.

Assuming that the involved genetic variants satisfy the conditions of instrumental variables (see Methods section in main text), the IVW approach serves as a standard approach for Mendelian Randomization analysis, which can also be viewed as a meta analysis of single causal estimates (Bowden et al., 2015). Let  $\{G_j\}_{j=1}^N$  be  $N$  independent variants which serve as valid instrumental variables (IVs). For a single variant  $G_j$ , the causal effect of exposure on the outcome can be estimated as  $\hat{\beta}_j = \frac{\hat{\Gamma}_j}{\hat{\gamma}_j}$ , where  $\hat{\gamma}_j$  and  $\hat{\Gamma}_j$  are the estimated SNP-exposure and SNP-outcome effects, respectively (Lawlor et al., 2008). Since the variants are selected to be strongly associated with exposure, the variance of  $\hat{\beta}_j$  can be given as:  $\frac{\sigma_{Y_j}^2}{\hat{\gamma}_j^2}$ , where the estimation errors  $\sigma_{X_j}^2$  are ignored.

Therefore, the IVW estimator based on the  $N$  IVs is given as,

$$\hat{\beta}_{IVW} = \frac{\sum_{j=1}^N \hat{\Gamma}_j \hat{\gamma}_j \sigma_{Y_j}^{-2}}{\sum_{j=1}^N \hat{\gamma}_j^2 \sigma_{Y_j}^{-2}}. \quad (49)$$

In fact, this can be obtained by solving the following weighted least square problem where  $\sigma_{Y_j}^{-2}, j = 1, \dots, N$  are the weights,

$$\hat{\beta}_{IVW} = \arg \min_{\beta} \sum_{j=1}^N \frac{(\hat{\Gamma}_j - \beta \hat{\gamma}_j)^2}{\sigma_{Y_j}^2}. \quad (50)$$

Then the standard error of  $\hat{\beta}_{IVW}$  is given as,

$$SE(\hat{\beta}_{IVW}) = \sqrt{\frac{\hat{\sigma}^2}{\sum_{j=1}^N \hat{\gamma}_j^2 \sigma_{Y_j}^{-2}}}. \quad (51)$$

where  $\hat{\sigma}^2$  is the variance of residuals from the weighed regression.

The Egger method extends the IVW method by introducing an intercept term  $\beta_0$  to address the influence of horizontal pleiotropy (Bowden et al., 2015),

$$\hat{\beta}_{Egger} = \arg \min_{\beta} \sum_{j=1}^N \frac{(\hat{\Gamma}_j - \beta_0 - \beta \hat{\gamma}_j)^2}{\sigma_{Y_j}^2}. \quad (52)$$

Then the standard error of the Egger estimate can be obtained by

$$SE(\hat{\beta}_{Egger}) = \sqrt{\frac{\hat{\sigma}^2}{\sum_{j=1}^N (\hat{\gamma}_j - \bar{\gamma}_w)^2 \sigma_{Y_j}^2}}. \quad (53)$$

where  $\bar{\gamma}_w$  is the weighted average of the estimated exposure effects that  $\bar{\gamma}_w = \frac{\sum_{i=1}^N \hat{\gamma}_i \sigma_{Y_i}^{-2}}{\sum_{i=1}^N \sigma_{Y_i}^{-2}}$ .

From the model assumption of Egger, we can see that Egger may not have a satisfactory performance in the presence of weak but non-constant pleiotropic effects. In addition, Egger may not be robust if there exist a few strong pleiotropic effects (i.e., outliers).

Unlike Egger, GSMR introduces an outlier detection procedure (called HEIDI-outlier) to reduce the strong effects of horizontal pleiotropy. It further takes into account the measurement error of the SNP-exposure effect and weak LD between SNPs (Zhu et al., 2018). Let  $\hat{\boldsymbol{\beta}} = (\hat{\beta}_1, \hat{\beta}_2, \dots, \hat{\beta}_N)$  be the vector of single variant MR estimates and  $\mathbf{U}$  be the variance covariance matrix of  $\hat{\boldsymbol{\beta}}$ , then we have  $\hat{\boldsymbol{\beta}} \sim N(\beta \mathbf{1}, \mathbf{U})$ . Notice that, if variants are correlated, the non-diagonal elements in matrix  $\mathbf{U}$  is non zero. The generalized least square approach is then applied to estimate the causal effect, yielding  $\hat{\beta}_{GSMR} = (\mathbf{1}^T \mathbf{U}^{-1} \mathbf{1})^{-1} \mathbf{1}^T \mathbf{U}^{-1} \hat{\boldsymbol{\beta}}$ . In the special case that uncorrelated and strong variants are used as IVs (now  $\mathbf{U}$  is a diagonal matrix), the GSMR estimator can be written as follows:

$$\hat{\beta}_{GSMR} = \arg \min_{\beta} \sum_{j=1}^N \frac{(\hat{\Gamma}_j - \beta \gamma_j)^2}{\sigma_{Y_j}^2 + \hat{\beta}_j^2 \sigma_{X_j}^2}, \quad (54)$$

Then the corresponding standard error is

$$SE(\hat{\beta}_{GSMR}) = \frac{1}{\sum_{j=1}^N \hat{\gamma}_j^2 / (\sigma_{Y_j}^2 + \hat{\beta}_j^2 \sigma_{X_j}^2)}. \quad (55)$$

To deal with horizontal pleiotropy, the HEIDI-outlier method firstly chooses a variant as the target, and then tests the estimated causal effect of the target variant and each of other variants. The variants that are significantly different from the target variant will be considered as outliers and then be removed in model fitting (54, 55). To avoid choosing a potential pleiotropic outlier as the target variant, the HEIDI-outlier method adopts an ad-hoc way: it chooses the top exposure-associated variant among those with the corresponding causal effect estimates in the third quintile (41% to 60%) of the single causal variant estimates  $(\hat{\beta}_1, \dots, \hat{\beta}_N)$ . The HEIDI-outlier method has the risk of selecting an inappropriate variant as the target variant leading to biased estimate or inflated type I errors.

RAPS uses a random effects model to model the weak Horizontal pleiotropy that  $\alpha_j \sim N(0, \tau^2)$  with a variance component  $\tau^2$  and the measurement error of  $\hat{\gamma}_j$  is also taken into account:

$$\hat{\Gamma}_j \sim N(\beta\gamma_j, \tau^2 + \sigma_{Y_j}^2), \quad \hat{\gamma}_j \sim N(\gamma_j, \sigma_{X_j}^2). \quad (56)$$

Parameter estimation of RAPS is obtained by maximizing the profile likelihood and in which  $\gamma_1, \dots, \gamma_N$  are considered as nuisance parameters being profiled out. The profile likelihood function is given as follows:

$$l(\beta, \tau) = -\frac{1}{2} \sum_{j=1}^N \frac{(\hat{\Gamma}_j - \beta\gamma_j)^2}{\sigma_{Y_j}^2 + \tau^2 + \beta^2 \sigma_{X_j}^2} + \log(\sigma_{Y_j}^2 + \tau^2). \quad (57)$$

An adjusted profile score (APS) (McCullagh and Tibshirani, 1990) is used in RAPS to obtain an consistent estimator of  $\beta$  and  $\tau$ . To reduce the influence of the large pleiotropic effects ( i.e. outliers) , robust loss functions, like the Huber loss and Tukey's biweight loss functions, are suggested to replace the  $l_2$  loss in (57).

Clearly, if we set  $\tau = 0$  , the optimum obtained by maximizing (57) w.r.t.  $\beta$  equals to an IVW estimate with weights:  $w(\beta) = 1/(\sigma_{Y_j}^2 + \beta^2 \sigma_{X_j}^2)$ , which is a function of the true causal effect  $\beta$ . From this perspective, the estimates from IVW (50) and Egger (52)

estimates correspond to setting  $\sigma_{X_j} = 0$  in  $w(\beta)$ , while the estimates from GSMR (54) are obtained by replacing the unknown true effect size  $\beta$  with  $\hat{\beta}_j$ .

Compared with RAPS in (57), we conclude that GSMR ignores weak pleiotropic effects ( $\tau^2 = 0$ ) which could lead to its inflated type I errors, as shown in simulation study and real data analysis.

## D More simulation results

### D.1 Summary-level simulations

We simulated summary-level data  $D = \{\hat{\gamma}, \hat{\Gamma}, \sigma_X, \sigma_Y\}$  to test the robustness of BWMR and its related methods. We first generated  $\Gamma_j$  and  $\gamma_j$  in the following five cases:

- Case-1:  $\gamma_j \stackrel{\text{i.i.d.}}{\sim} \mathcal{N}(0, \sigma^2)$ ,  $\alpha_j \stackrel{\text{i.i.d.}}{\sim} \mathcal{N}(0, \tau^2)$ ,  $\Gamma_j = \beta\gamma_j + \alpha_j$ .
- Case-2:  $\gamma_j \stackrel{\text{i.i.d.}}{\sim} \mathcal{N}(0, \sigma^2)$ ,  $\alpha_j \stackrel{\text{i.i.d.}}{\sim} \mathcal{N}(0, \tau^2)$ ,

$$\Gamma_j = \begin{cases} \beta\gamma_j + \alpha_j, & j = 1, 2, \dots, (N \times C), \\ \beta_c\gamma_j + \alpha_j, & j = (N \times C + 1), \dots, N, \end{cases}$$

with  $\beta_c$  denoting corrupted value of  $\beta$  and  $C$  denoting the corresponding corrupted rate.

- Case-3:  $\gamma_j \stackrel{\text{i.i.d.}}{\sim} \mathcal{N}(0, \sigma^2)$ ,  $\Gamma_j = \beta\gamma_j + \alpha_j$  and

$$\alpha_j \stackrel{\text{i.i.d.}}{\sim} \begin{cases} \mathcal{N}(0, \tau^2), & j = 1, 2, \dots, (N \times C), \\ \mathcal{N}(0, \tau_c^2), & j = (N \times C + 1), \dots, N, \end{cases}$$

with  $\tau_c^2$  denoting corrupted value of  $\tau^2$ .

- Case-4:  $\gamma_j \stackrel{\text{i.i.d.}}{\sim} (1 - R)\mathcal{N}(0, \sigma^2) + R\mathcal{N}(0, 10\sigma^2)$ ,  $\alpha_j \stackrel{\text{i.i.d.}}{\sim} \mathcal{N}(0, \tau^2)$  and  $\Gamma_j = \beta\gamma_j + \alpha_j$ , where  $0 < R < 1$ .
- Case-5:  $\gamma_j \stackrel{\text{i.i.d.}}{\sim} \mathcal{N}(0, \sigma^2)$ ,  $\Gamma_j = \beta\gamma_j + \alpha_j$  and  $\alpha_j \stackrel{\text{i.i.d.}}{\sim} \tau\text{Laplace}(r)$ , where  $\text{Laplace}(r)$  represents Laplace (double exponential) distribution with the rate  $r$ .

With  $\Gamma_j$  and  $\gamma_j$  generated above, we simulated  $\hat{\Gamma}_j$  and  $\hat{\gamma}_j$  from  $\hat{\gamma}_j|\gamma_j \sim \mathcal{N}(\gamma_j, \sigma_{X_j}^2)$ ,  $\hat{\Gamma}_j|\Gamma_j \sim \mathcal{N}(\Gamma_j, \sigma_{Y_j}^2)$ , where  $\sigma_{X_j}$  and  $\sigma_{Y_j}$  were i.i.d. from the uniform distribution  $U[c, d]$ .

- Summary-level simulation results in Case-1

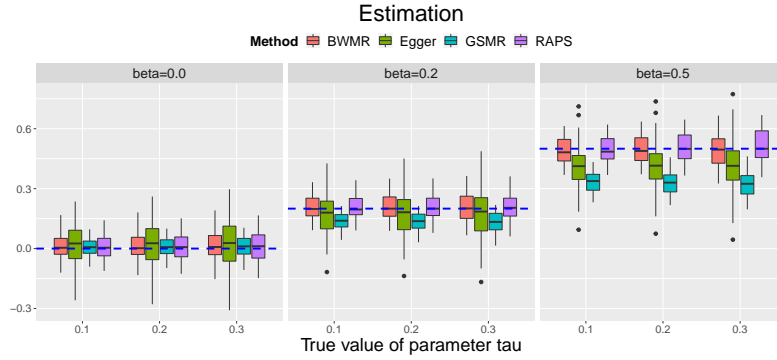


Figure 7: Comparison of estimation accuracy of BWMR, Egger, GSMR and RAPS in Case-1 of the summary-level data simulation. The simulation parameters were varied in the following range:  $\beta \in \{0.0, 0.2, 0.5\}$ ,  $\tau \in \{0.1, 0.2, 0.3\}$ ,  $\sigma = 0.8$ ,  $[c, d] = [0.3, 0.5]$ . The results were summarized from 50 replications.

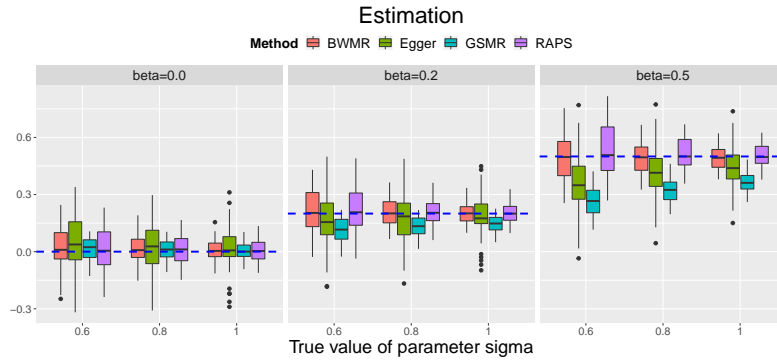


Figure 8: Comparison of estimation accuracy of BWMR, Egger, GSMR and RAPS in Case-1 of the summary-level data simulation. The simulation parameters were varied in the following range:  $\beta \in \{0.0, 0.2, 0.5\}$ ,  $\sigma \in \{0.6, 0.8, 1.0\}$ ,  $\tau = 0.2$ ,  $[c, d] = [0.3, 0.5]$ . The results were summarized from 50 replications.

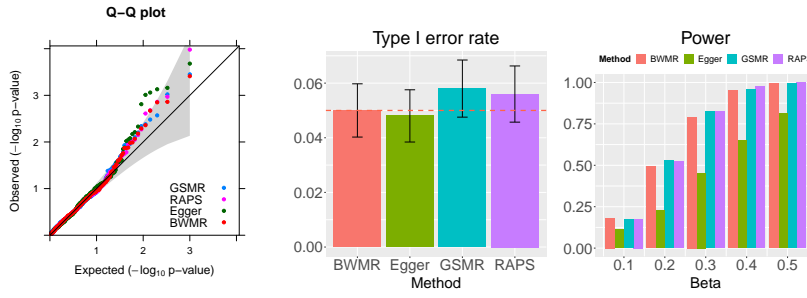


Figure 9: Comparison of type I error control and statistical power of BWMR, Egger, GSMR and RAPS in Case-1 of the summary-level data simulation. The simulation parameters were varied in the following range:  $\beta \in \{0.0, 0.1, 0.2, 0.3, 0.4, 0.5\}$ ,  $\tau = 0.3$ ,  $\sigma = 0.8$ ,  $[c, d] = [0.3, 0.5]$ . We evaluated the empirical type I error rate and power by controlling type I error rates at the nominal level 0.05. The results were summarized from 500 replications.

- Summary-level simulation results in Case-2

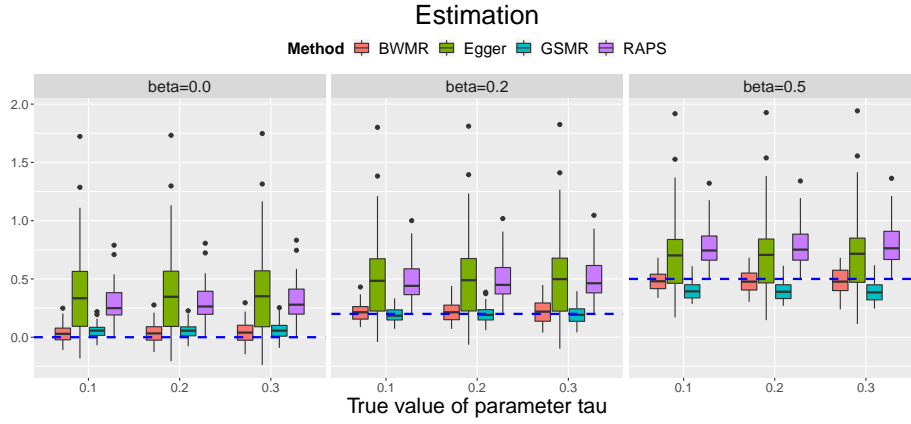


Figure 10: Comparison of estimation accuracy of BWMR, Egger, GSMR and RAPS in Case-2 of the summary-level data simulation. The simulation parameters were varied in the following range:  $\beta \in \{0.0, 0.2, 0.5\}$ ,  $\tau \in \{0.1, 0.2, 0.3\}$ ,  $\sigma = 0.8$ ,  $[c, d] = [0.3, 0.5]$ ,  $\beta_c = 3$ ,  $C = 0.2$ . The results were summarized from 50 replications.

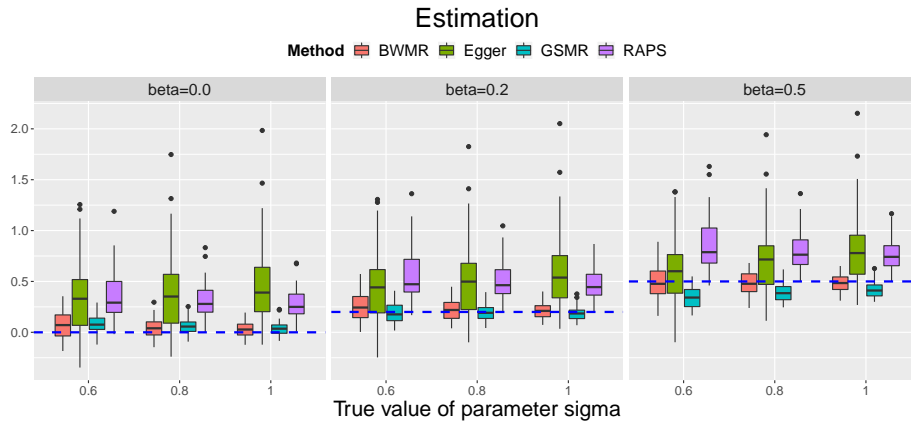


Figure 11: Comparison of estimation accuracy of BWMR, Egger, GSMR and RAPS in Case-2 of the summary-level data simulation. The simulation parameters were varied in the following range:  $\beta \in \{0.0, 0.2, 0.5\}$ ,  $\sigma \in \{0.6, 0.8, 1.0\}$ ,  $\tau = 0.2$ ,  $[c, d] = [0.3, 0.5]$ ,  $\beta_c = 3$ ,  $C = 0.2$ . The results were summarized from 50 replications.

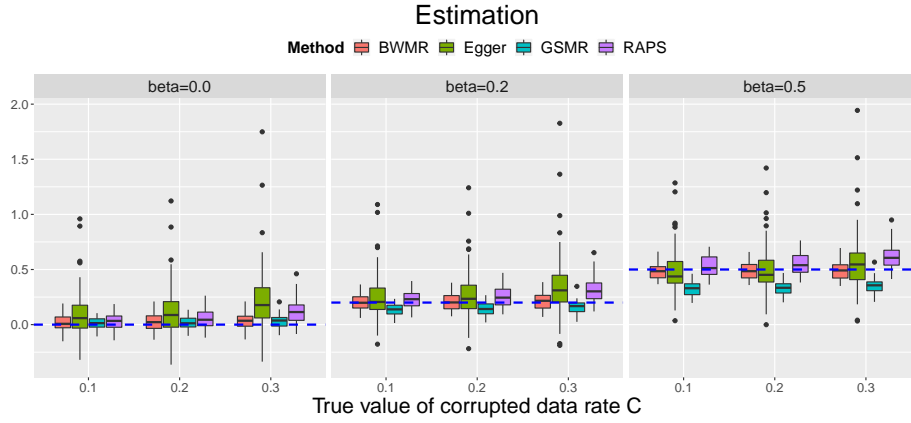


Figure 12: Comparison of estimation accuracy of BWMR, Egger, GSMR and RAPS in Case-2 of the summary-level data simulation. The simulation parameters were varied in the following range:  $\beta \in \{0.0, 0.2, 0.5\}$ ,  $C \in \{0.1, 0.2, 0.3\}$ ,  $\tau = 0.2$ ,  $\sigma = 0.8$ ,  $[c, d] = [0.3, 0.5]$ ,  $\beta_c = 3$ . The results were summarized from 50 replications.

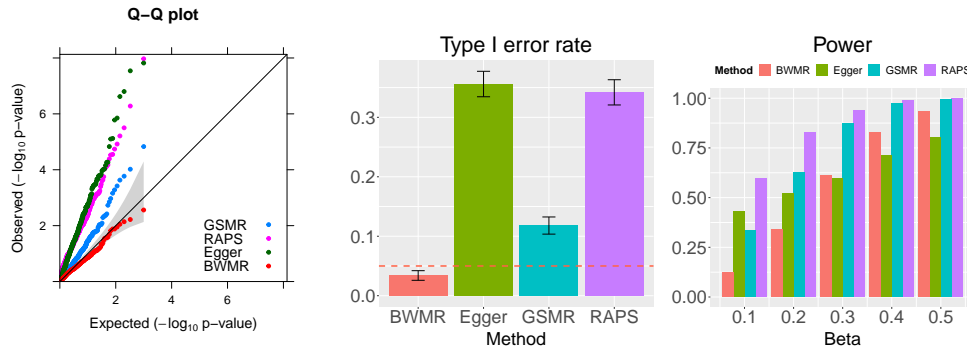


Figure 13: Comparison of type I error control and statistical power of BWMR, Egger, GSMR and RAPS in Case-2 of the summary-level data simulation. The simulation parameters were varied in the following range:  $\beta \in \{0.0, 0.1, 0.2, 0.3, 0.4, 0.5\}$ ,  $\tau = 0.3$ ,  $\sigma = 0.8$ ,  $[c, d] = [0.3, 0.5]$ ,  $\beta_c = 3$ ,  $C = 0.2$ . We evaluated the empirical type I error rate and power by controlling type I error rates at the nominal level 0.05. The results were summarized from 500 replications.

- Summary-level simulation results in Case-3

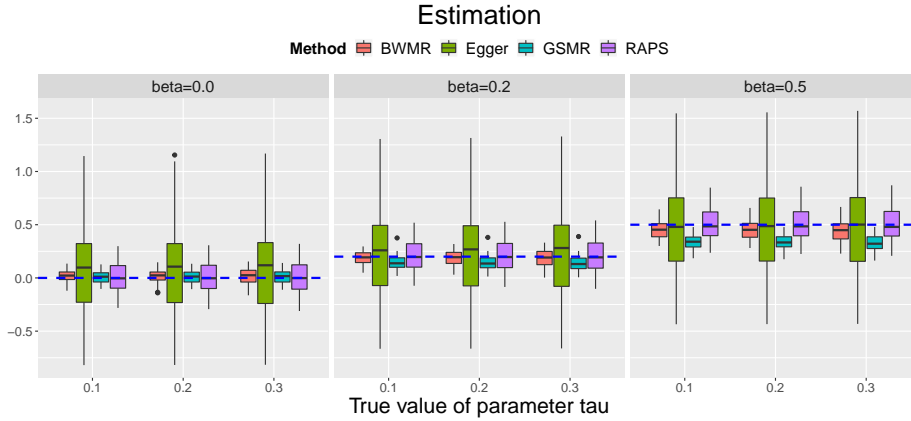


Figure 14: Comparison of estimation accuracy of BWMR, Egger, GSMR and RAPS in Case-3 of the summary-level data simulation. The simulation parameters were varied in the following range:  $\beta \in \{0.0, 0.2, 0.5\}$ ,  $\tau \in \{0.1, 0.2, 0.3\}$ ,  $\sigma = 0.8$ ,  $[c, d] = [0.3, 0.5]$ ,  $\tau_c = 3$ ,  $C = 0.2$ . The results were summarized from 50 replications.

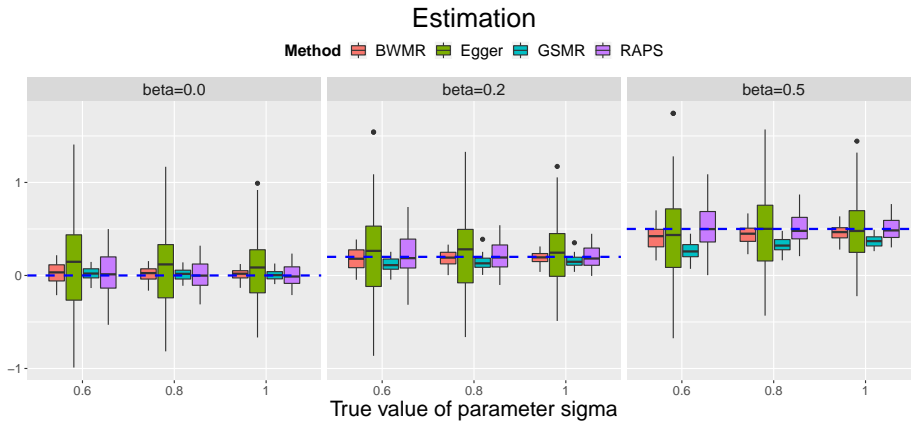


Figure 15: Comparison of estimation accuracy of BWMR, Egger, GSMR and RAPS in Case-3 of the summary-level data simulation. The simulation parameters were varied in the following range:  $\beta \in \{0.0, 0.2, 0.5\}$ ,  $\sigma \in \{0.6, 0.8, 1.0\}$ ,  $\tau = 0.2$ ,  $[c, d] = [0.3, 0.5]$ ,  $\tau_c = 3$ ,  $C = 0.2$ . The results were summarized from 50 replications.

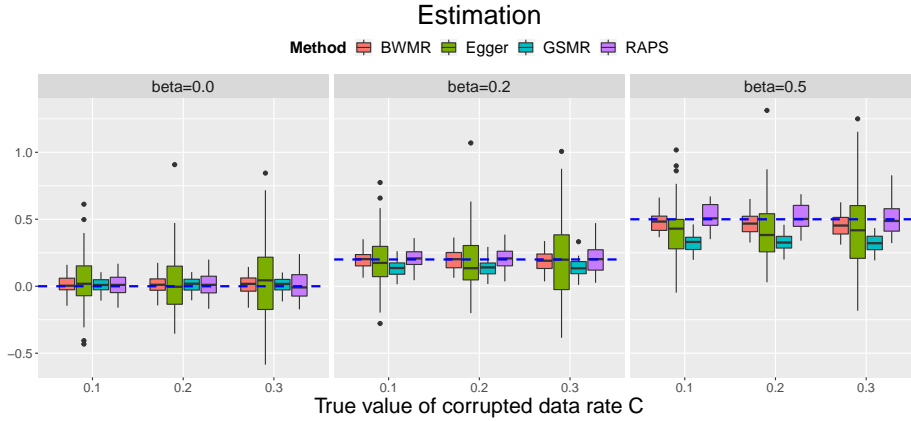


Figure 16: Comparison of estimation accuracy of BWMR, Egger, GSMR and RAPS in Case-3 of the summary-level data simulation. The simulation parameters were varied in the following range:  $\beta \in \{0.0, 0.2, 0.5\}$ ,  $C \in \{0.1, 0.2, 0.3\}$ ,  $\tau = 0.2$ ,  $\sigma = 0.8$ ,  $[c, d] = [0.3, 0.5]$ ,  $\tau_c = 3$ . The results were summarized from 50 replications.

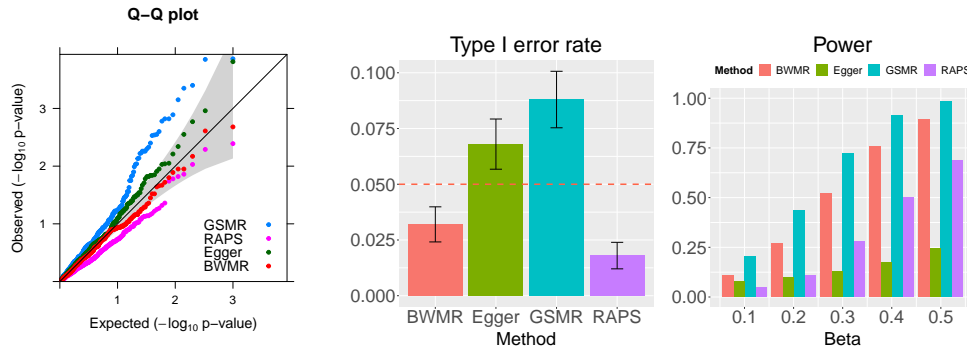


Figure 17: Comparison of type I error control and statistical power of BWMR, Egger, GSMR and RAPS in Case-3 of the summary-level data simulation. The simulation parameters were varied in the following range:  $\beta \in \{0.0, 0.1, 0.2, 0.3, 0.4, 0.5\}$ ,  $\tau = 0.3$ ,  $\sigma = 0.8$ ,  $[c, d] = [0.3, 0.5]$ ,  $\tau_c = 3$ ,  $C = 0.2$ . We evaluated the empirical type I error rate and power by controlling type I error rates at the nominal level 0.05. The results were summarized from 500 replications.

- Summary-level simulation results in Case-4

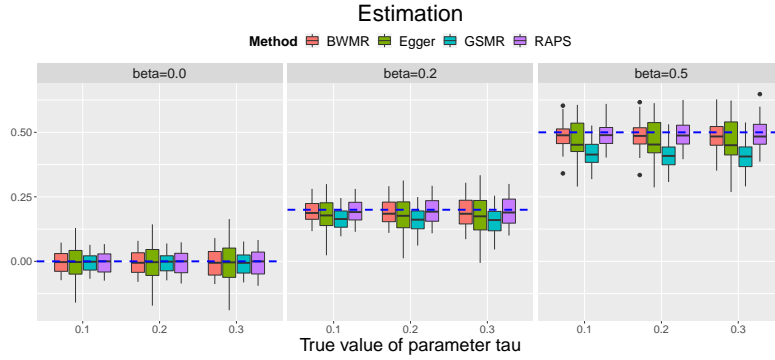


Figure 18: Comparison of estimation accuracy of BWMR, Egger, GSMR and RAPS in Case-4 of the summary-level data simulation. The simulation parameters were varied in the following range:  $\beta \in \{0.0, 0.2, 0.5\}$ ,  $\tau \in \{0.1, 0.2, 0.3\}$ ,  $\sigma = 0.8$ ,  $[c, d] = [0.3, 0.5]$ ,  $R = 0.2$ . The results were summarized from 50 replications.

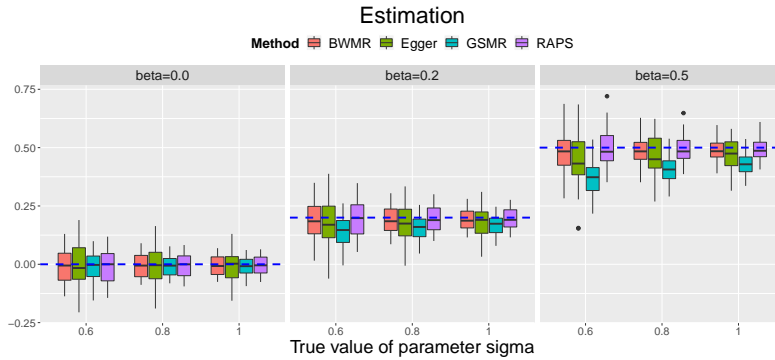


Figure 19: Comparison of estimation accuracy of BWMR, Egger, GSMR and RAPS in Case-4 of the summary-level data simulation. The simulation parameters were varied in the following range:  $\beta \in \{0.0, 0.2, 0.5\}$ ,  $\sigma \in \{0.6, 0.8, 1.0\}$ ,  $\tau = 0.2$ ,  $[c, d] = [0.3, 0.5]$ ,  $R = 0.2$ . The results were summarized from 50 replications.

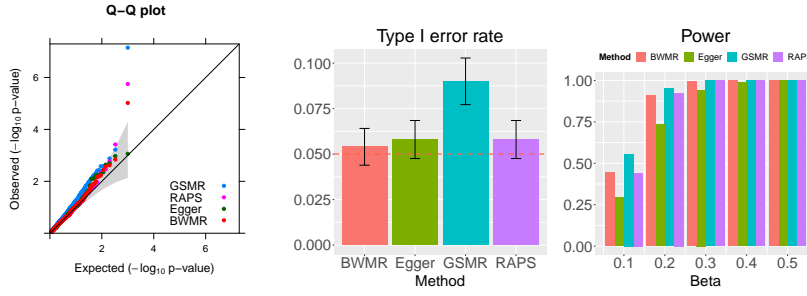


Figure 20: Comparison of type I error control and statistical power of BWMR, Egger, GSMR and RAPS in Case-4 of the summary-level data simulation. The simulation parameters were varied in the following range:  $\beta \in \{0.0, 0.1, 0.2, 0.3, 0.4, 0.5\}$ ,  $\tau = 0.3$ ,  $\sigma = 0.8$ ,  $[c, d] = [0.3, 0.5]$ ,  $R = 0.2$ . We evaluated the empirical type I error rate and power by controlling type I error rates at the nominal level 0.05. The results were summarized from 500 replications.

- Summary-level simulation results in Case-5

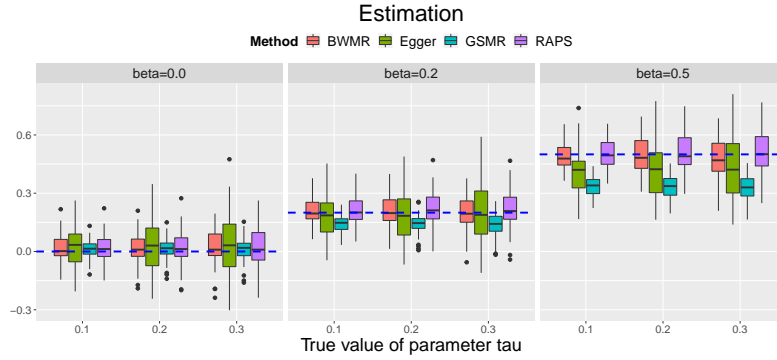


Figure 21: Comparison of estimation accuracy of BWMR, Egger, GSMR and RAPS in Case-5 of the summary-level data simulation. The simulation parameters were varied in the following range:  $\beta \in \{0.0, 0.2, 0.5\}$ ,  $\tau \in \{0.1, 0.2, 0.3\}$ ,  $\sigma = 0.8$ ,  $[c, d] = [0.3, 0.5]$ ,  $r = 1$ . The results were summarized from 50 replications.

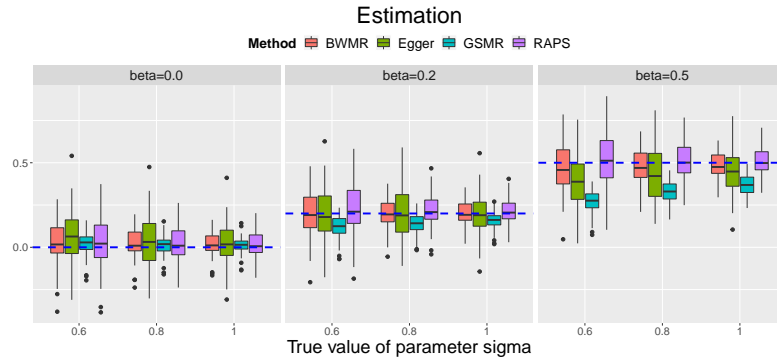


Figure 22: Comparison of estimation accuracy of BWMR, Egger, GSMR and RAPS in Case-5 of the summary-level data simulation. The simulation parameters were varied in the following range:  $\beta \in \{0.0, 0.2, 0.5\}$ ,  $\sigma \in \{0.6, 0.8, 1.0\}$ ,  $\tau = 0.2$ ,  $[c, d] = [0.3, 0.5]$ ,  $r = 1$ . The results were summarized from 50 replications.

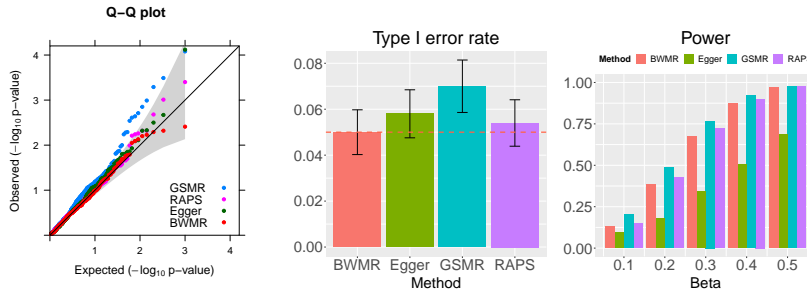


Figure 23: Comparison of type I error control and statistical power of BWMR, Egger, GSMR and RAPS in Case-5 of the summary-level data simulation. The simulation parameters were varied in the following range:  $\beta \in \{0.0, 0.1, 0.2, 0.3, 0.4, 0.5\}$ ,  $\tau = 0.3$ ,  $\sigma = 0.8$ ,  $[c, d] = [0.3, 0.5]$ ,  $r = 1$ . We evaluated the empirical type I error rate and power by controlling type I error rates at the nominal level 0.05. The results were summarized from 500 replications.

## D.2 Individul-level simulations

- Individual-level simulations discussing the selection bias in MR

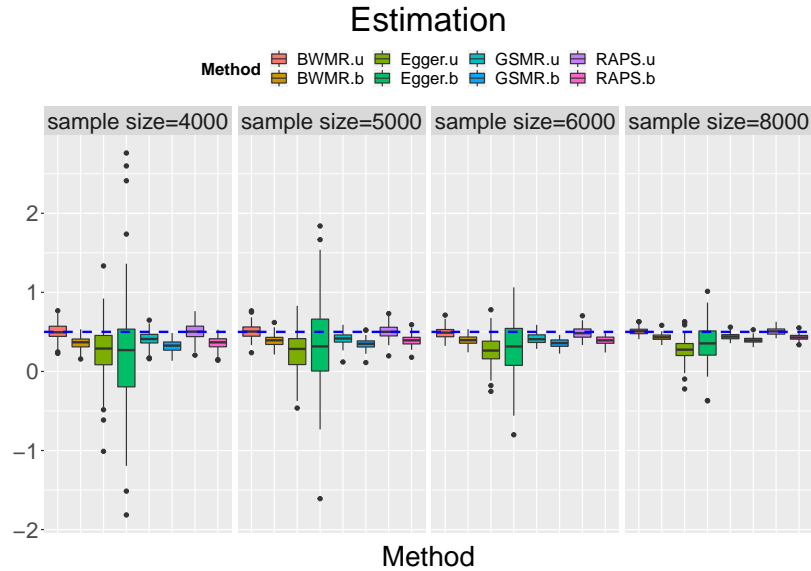


Figure 24: Comparison of BWMR, Egger, GSMR and RAPS in the individual-level data simulation, with / without selection bias, under the choices of  $\beta \in \{0.0, 0.1, 0.2, 0.3, 0.4, 0.5\}$ ,  $N_0 = 10,000$ ,  $n_1 = n_2 \in \{4,000, 5,000, 6,000, 8,000\}$ ,  $\pi_{11} = 0.02$ ,  $\pi_{10} = 0.08$ ,  $\pi_{01} = 0.08$ ,  $\pi_{00} = 0.82$ ,  $SNR_1 = SNR_2 = 1 : 1$ , and  $p$ -value threshold =  $1 \times 10^{-5}$ . Let “.u” denote simulations without selection bias (unbias), let “.b” denote simulations with selection bias. The results were summarized from 100 replications.

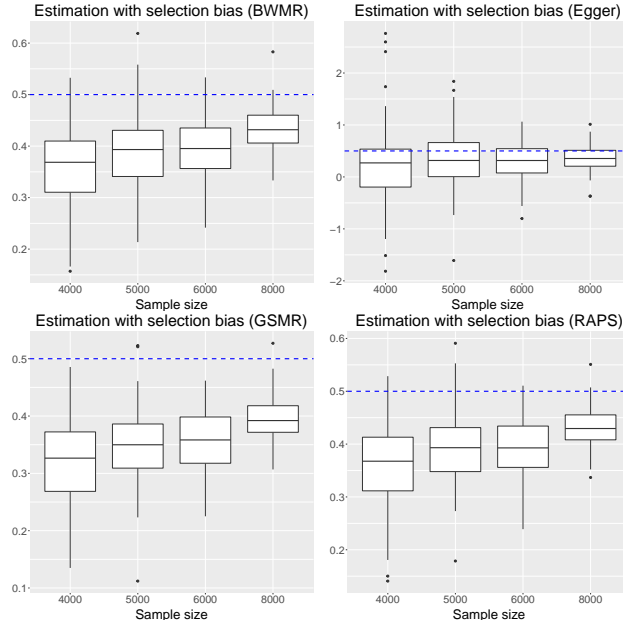


Figure 25: Comparison of individual-level data simulation with selection bias using different sample sizes, under the choices of  $\beta \in \{0.0, 0.1, 0.2, 0.3, 0.4, 0.5\}$ ,  $N_0 = 10,000$ ,  $n_1 = n_2 \in \{4,000, 5,000, 6,000, 8,000\}$ ,  $\pi_{11} = 0.02$ ,  $\pi_{10} = 0.08$ ,  $\pi_{01} = 0.08$ ,  $\pi_{00} = 0.82$ ,  $SNR_1 = SNR_2 = 1 : 1$ , and  $p$ -value threshold  $= 1 \times 10^{-5}$ . The results were summarized from 100 replications.

## E Real data analysis

### E.1 Data sources

Table 1: Supplementary Table for GWAS sources of metabolites

Metabolite	# Sample Size	Reference
123 Blood metabolites from multiple metabolic pathways	up to 24925	(Kettunen et al., 2016)
Fasting glucose	up to 122,743	(Dupuis et al., 2010)
Vitamin D levels	up to 41,274	(Manousaki et al., 2017)
Serum Urate	up to 14,000	(Köttgen et al., 2013)
Total Cholesterol	up to 188,577	(Willer et al., 2013)
Triglycerides	up to 188,577	(Willer et al., 2013)
HDL cholesterol	up to 188,577	(Willer et al., 2013)
LDL cholesterol	up to 188,577	(Willer et al., 2013)

Table 2: Supplementary Table for GWAS sources of complex human traits and diseases

Category	Name	# Sample Size	Reference
Anthropometric Trait	Body mass index	339,224	(Locke et al., 2015)
Anthropometric Trait	Body fat percentage	100,716	(Lu et al., 2016)
Anthropometric Trait	Height	253,288	(Wood et al., 2014)
Anthropometric Trait	Hip circumference	224,459	(Shungin et al., 2015)
Anthropometric Trait	Waist circumference	224,459	(Shungin et al., 2015)
Anthropometric Trait	Waist hip ratio	224,459	(Shungin et al., 2015)
Anthropometric Trait	Birth length	28,459	(van der Valk et al., 2015)
Anthropometric Trait	Birth weight	153,781	(Horikoshi et al., 2016)
Anthropometric Trait	Childhood obesity	13,848	(Bradfield et al., 2012)
Anthropometric Trait	Infant head circumference	10,768	(Taal et al., 2012)
Cardiovascular measure	Diastolic blood pressure	120,473	(Liu et al., 2016)
Cardiovascular measure	Hypertension	120,473	(Liu et al., 2016)
Cardiovascular measure	Mean arterial pressure	120,473	(Liu et al., 2016)
Cardiovascular measure	Pulse pressure	120,473	(Liu et al., 2016)
Cardiovascular measure	Systolic blood pressure	120,473	(Liu et al., 2016)
Cardiovascular measure	Coronary artery disease	184,305	(Nikpay et al., 2015)
Cardiovascular measure	Heart rate	181,171	(Den Hoed et al., 2013)
Cardiovascular measure	Heart rate variability pVRS	53,174	(Nolte et al., 2017)
Cardiovascular measure	Heart rate variability RMSSD	53,174	(Nolte et al., 2017)
Cardiovascular measure	Heart rate variability SDNN	53,174	(Nolte et al., 2017)
Cardiovascular measure	Peripheral vascular disease	53,991	(Zhu et al., 2018)

Category	Name	# Sample Size	Reference
Immune system disorder	Atopic dermatitis	103,066	(Paternoster et al., 2015)
Immune system disorder	Crohn's disease	20,883	(Liu et al., 2015)
Immune system disorder	Inflammatory bowel disease	34,652	(Liu et al., 2015)
Immune system disorder	Ulcerative colitis	34,652	(Liu et al., 2015)
Immune system disorder	Celiac disease	15,283	(Dubois et al., 2010)
Immune system disorder	Eczema	40,835	(Paternoster et al., 2015)
Immune system disorder	Multiple sclerosis	27,098	(Sawcer et al., 2011)
Immune system disorder	Primary biliary cirrhosis	13,239	(Cordell et al., 2015)
Immune system disorder	Rheumatoid arthritis	58,284	(Okbay et al., 2016)
Immune system disorder	Systemic lupus erythematosus	23,210	(Bentham et al., 2015)
Immune system disorder	Type 1 diabetes	14,741	(Censin et al., 2017)
Metabolic Trait	Age at menarche	182,416	(Perry et al., 2014)
Metabolic Trait	Age at natural menopause	69,360	(Day et al., 2015)
Metabolic Trait	Dyslipidemia	53,991	(Zhu et al., 2018)
Metabolic Trait	Estimated glomerular filtration rate	111,666	(Li et al., 2017)
Metabolic Trait	Fasting insulin	51,750	(Manning et al., 2012)
Metabolic Trait	Fasting proinsulin	10,701	(Strawbridge et al., 2011)
Metabolic Trait	Glycated haemoglobin levels	123,665	(Wheeler et al., 2017)
Metabolic Trait	Gout	69,374	(Köttgen et al., 2013)
Metabolic Trait	Hemoglobin A1c	123,665	(Wheeler et al., 2017)
Metabolic Trait	Hemorrhoids	53,991	(Zhu et al., 2018)
Metabolic Trait	Iron deficiency	53,991	(Zhu et al., 2018)
Metabolic Trait	Type 2 diabetes	69,033	(Morris et al., 2012)
Metabolic Trait	Urinary albumin to creatinine ratio	54,450	(Teumer et al., 2016)
Metabolic Trait	Varicose veins	53,991	(Zhu et al., 2018)
Neurodegenerative disease	Alzheimer's disease	54,162	(Lambert et al., 2013)
Neurodegenerative disease	Amyotrophic lateral sclerosis	36,052	(Benyamin et al., 2017)
Neurodegenerative disease	Age related macular degeneration	53,991	(Zhu et al., 2018)
Neurodegenerative disease	Parkinson	8,477	(Pankratz et al., 2012)
Other complex trait	Asthma	26,475	(Moffatt et al., 2010)
Other complex trait	Breast cancer	2,287	(Hunter et al., 2007)
Other complex trait	Dermatophytosis	53,991	(Zhu et al., 2018)
Other complex trait	Leptin	32,161	(Kilpeläinen et al., 2016)
Other complex trait	Leptin adjusted for BMI	32,161	(Kilpeläinen et al., 2016)
Other complex trait	Osteoarthritis	53,991	(Zhu et al., 2018)
Other complex trait	Osteoporosis	53,991	(Zhu et al., 2018)
Psychiatric disorder	Angst	18,000	(Otowa et al., 2016)
Psychiatric disorder	Bipolar disorder	16,731	(Sklar et al., 2011)
Psychiatric disorder	Attention deficit hyperactivity disorder	5,422	*
Psychiatric disorder	Autism spectrum disorder	10,763	*
Psychiatric disorder	Major depressive disorder	16,610	*
Psychiatric disorder	Schizophrenia	17,115	*
Psychiatric disorder	Depress	53,991	(Zhu et al., 2018)

\*: (Cross-Disorder Group of the Psychiatric Genomics Consortium et al., 2013)

Category	Name	# Sample Size	Reference
Psychiatric disorder	Child aggressive behaviour	18,988	(Pappa et al., 2016)
Psychiatric disorder	Anorexia nervosa	14,477	(Duncan et al., 2017)
Psychiatric disorder	Loneliness	10,760	(Gao et al., 2017)
Psychiatric disorder	Obsessive compulsive disorder	9,995	(Stewart et al., 2013)
Psychiatric disorder	Post-traumatic stress disorder	9,954	(Duncan et al., 2017)
Psychiatric disorder	Stress	53,991	(Zhu et al., 2018)
Social Trait	Alcohol continuous	70,460	(Schumann et al., 2016)
Social Trait	Alcohol light heavy	74,711	(Schumann et al., 2016)
Social Trait	Cognitive performance	106,736	(Rietveld et al., 2014)
Social Trait	Chronotype	127,898	(Jones et al., 2016)
Social Trait	Oversleepers	127,573	(Jones et al., 2016)
Social Trait	Sleep duration	127,573	(Jones et al., 2016)
Social Trait	Undersleepers	127,573	(Jones et al., 2016)
Social Trait	Insomnia complaints	113,006	(Hammerschlag et al., 2017)
Social Trait	Educational attainment college	95,429	(Rietveld et al., 2013)
Social Trait	Educational attainment eduyears	101,069	(Rietveld et al., 2013)
Social Trait	Agreeableness	17,375	(De Moor et al., 2012)
Social Trait	Conscientiousness	17,375	(De Moor et al., 2012)
Social Trait	Extraversion	17,375	(De Moor et al., 2012)
Social Trait	Neuroticism	17,375	(De Moor et al., 2012)
Social Trait	Openness	17,375	(De Moor et al., 2012)
Social Trait	Intelligence	78,308	(Sniekers et al., 2017)
Social Trait	Depressive symptoms	161,460	(Okbay et al., 2016)
Social Trait	Neuroticism	170,911	(Okbay et al., 2016)
Social Trait	Subjective well being	298,420	(Okbay et al., 2016)
Social Trait	Age onset	47,961	(Furberg et al., 2010)
Social Trait	Cigarette per day	68,028	(Furberg et al., 2010)
Social Trait	Ever smoked	74,035	(Furberg et al., 2010)
Social Trait	Former smoker	41,969	(Furberg et al., 2010)

## E.2 MR implementation

The  $p$ -value threshold for selecting IVs was set to be  $5 \times 10^{-8}$ . The LD clumping was implemented by using PLINK (Purcell et al., 2007) with a  $r^2$  threshold of 0.001 and a window size of 1Mb. Before implementing MR methods, we harmonised the alleles for the exposure and the outcome by using the R package “TwoSampleMR” (Hemani et al., 2018), and standardised the SNP-exposure and SNP-outcome effects by using the R package “gsmr” (Zhu et al., 2018). Egger and RAPS were implemented with the R package “TwoSampleMR”, GSMR was implemented with its R package “gsmr”, and BWMR was implemented with our R package “BWMR”.

### E.3 Examination of selection bias

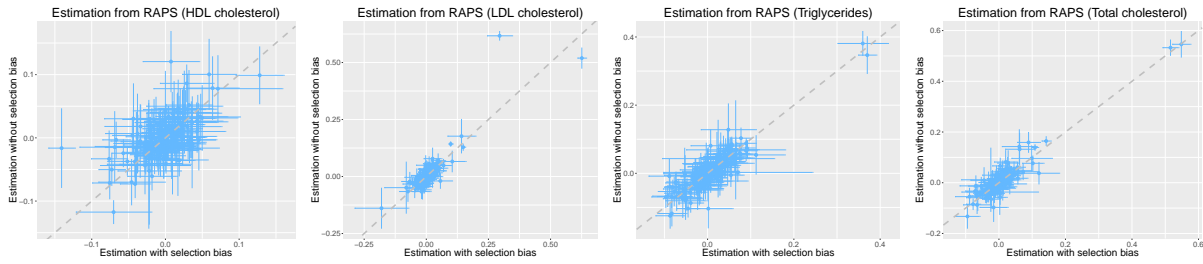


Figure 26: Comparisons of analysis results provided by RAPS with selection bias ( $x$ -axis) and without selection bias ( $y$ -axis). The dots represent estimated causal effect sizes  $\hat{\beta}$  and the bars represent their standard errors  $se(\hat{\beta})$ . The diagonal is indicated by the dashed line.

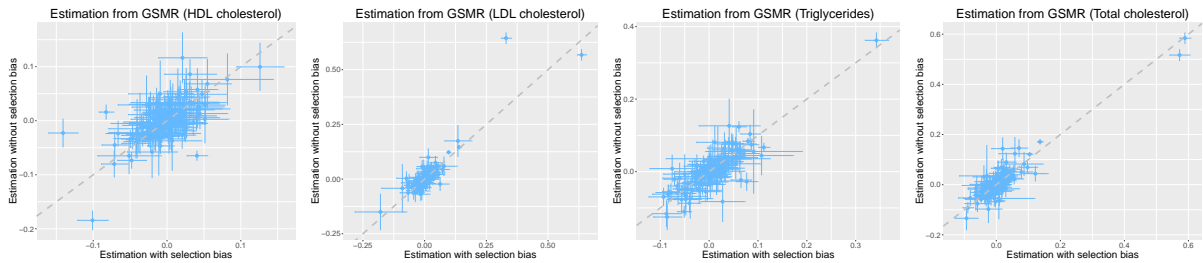


Figure 27: Comparisons of analysis results provided by GSMR with selection bias ( $x$ -axis) and without selection bias ( $y$ -axis). The dots represent estimated causal effect sizes  $\hat{\beta}$  and the bars represent their standard errors  $se(\hat{\beta})$ . The diagonal is indicated by the dashed line.

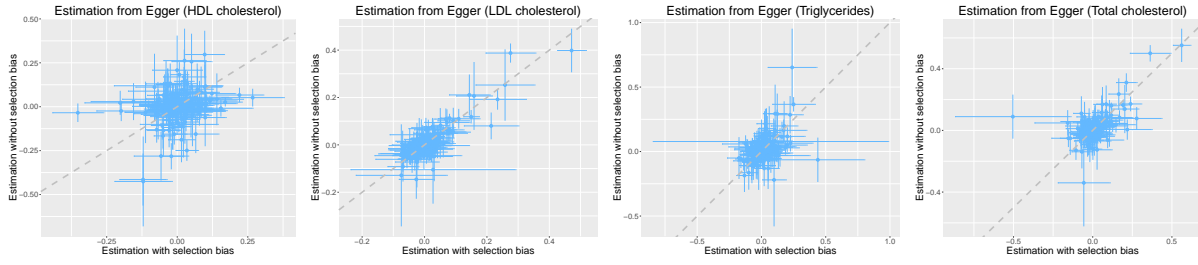


Figure 28: Comparisons of analysis results provided by Egger with selection bias ( $x$ -axis) and without selection bias ( $y$ -axis). The dots represent estimated causal effect sizes  $\hat{\beta}$  and the bars represent their standard errors  $se(\hat{\beta})$ . The diagonal is indicated by the dashed line.

#### E.4 Consistency of analysis results

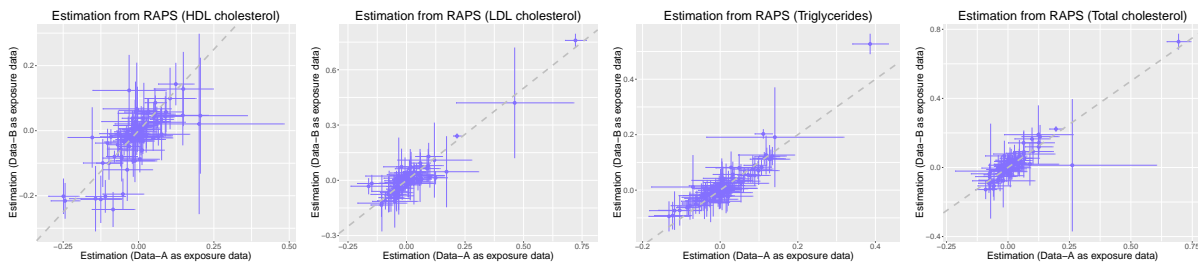


Figure 29: Comparisons of analysis results provided by RAPS using Data-A as exposure data ( $x$ -axis) and using Data-B as exposure data ( $y$ -axis). The dots represent estimated causal effect sizes  $\hat{\beta}$  and the bars represent their standard errors  $se(\hat{\beta})$ . The diagonal is indicated by the dashed line.

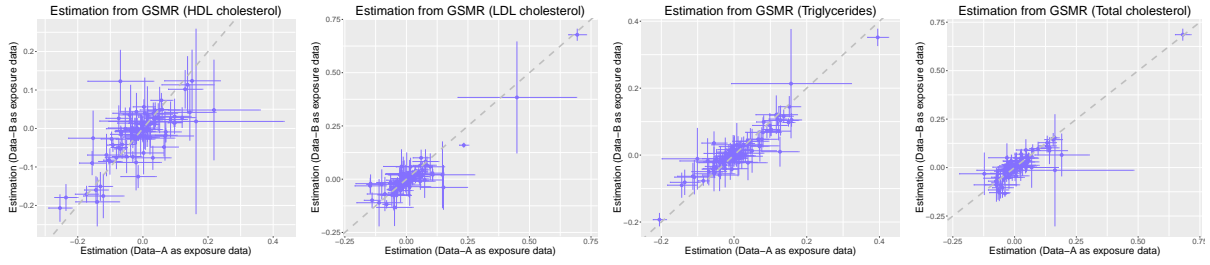


Figure 30: Comparisons of analysis results provided by GSMR using Data-A as exposure data ( $x$ -axis) and using Data-B as exposure data ( $y$ -axis). The dots represent estimated causal effect sizes  $\hat{\beta}$  and the bars represent their standard errors  $se(\hat{\beta})$ . The diagonal is indicated by the dashed line.

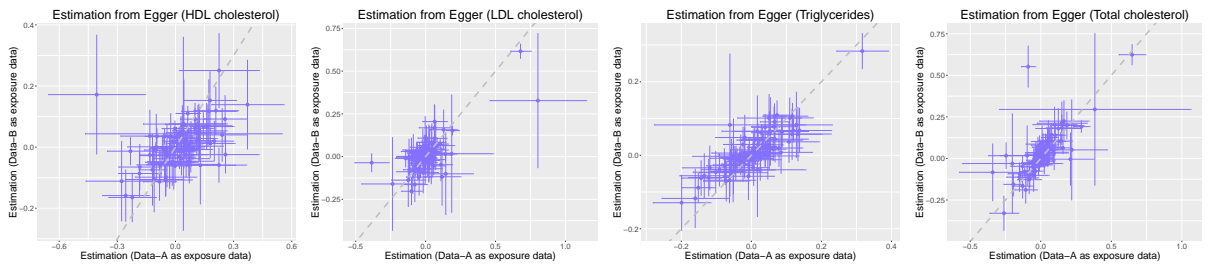


Figure 31: Comparisons of analysis results provided by Egger using Data-A as exposure data ( $x$ -axis) and using Data-B as exposure data ( $y$ -axis). The dots represent estimated causal effect sizes  $\hat{\beta}$  and the bars represent their standard errors  $se(\hat{\beta})$ . The diagonal is indicated by the dashed line.

## E.5 Some illustrative examples in real data analysis

- exposure: LDL cholesterol; outcome: height.

Table 3: MR results of “LDL cholesterol - height”

method	$\hat{\beta}$	$\hat{se}$	$p$ -value
BWMR	-0.0295	0.0164	0.0721
Egger	-0.0135	0.0378	0.7222
GSMR	-0.0655	0.0088	$7.8146 \times 10^{-14}$
RAPS	-0.0290	0.0169	0.0856

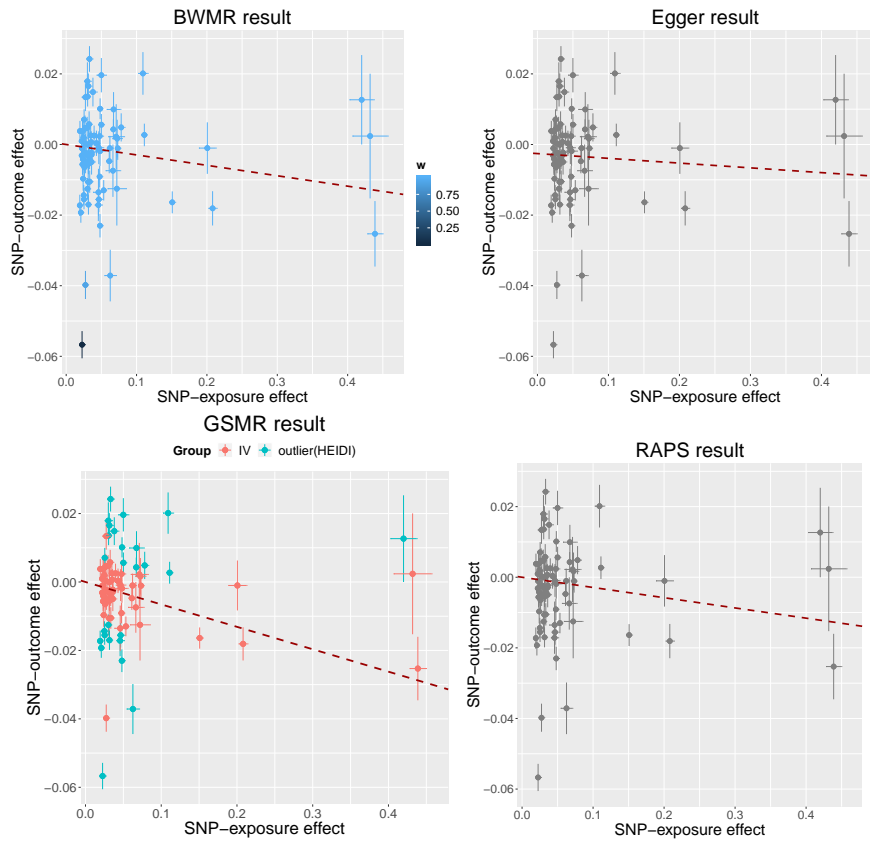


Figure 32: Comparisons of causal inference results when estimating the causal effect of LDL cholesterol on height. We use this example to show that GSMR may suffer from inflated type I error rate when IVs are affected by weak horizontal pleiotropic effects, and the HEIDI outlier method in GSMR has a risk of selecting an inappropriate SNP (e.g., pleiotropic IV) as the top variant leading to false discovery.

- exposure: Gp; outcome: Crohn’s disease.

Table 4: MR results of “Gp - Crohn’s disease”

method	$\hat{\beta}$	$\hat{se}$	$p$ -value
BWMR	0.0711	0.0678	0.2946
Egger	-0.0781	0.1668	0.6521
GSMR	0.1483	0.0417	0.0004
RAPS	0.0691	0.0700	0.3242

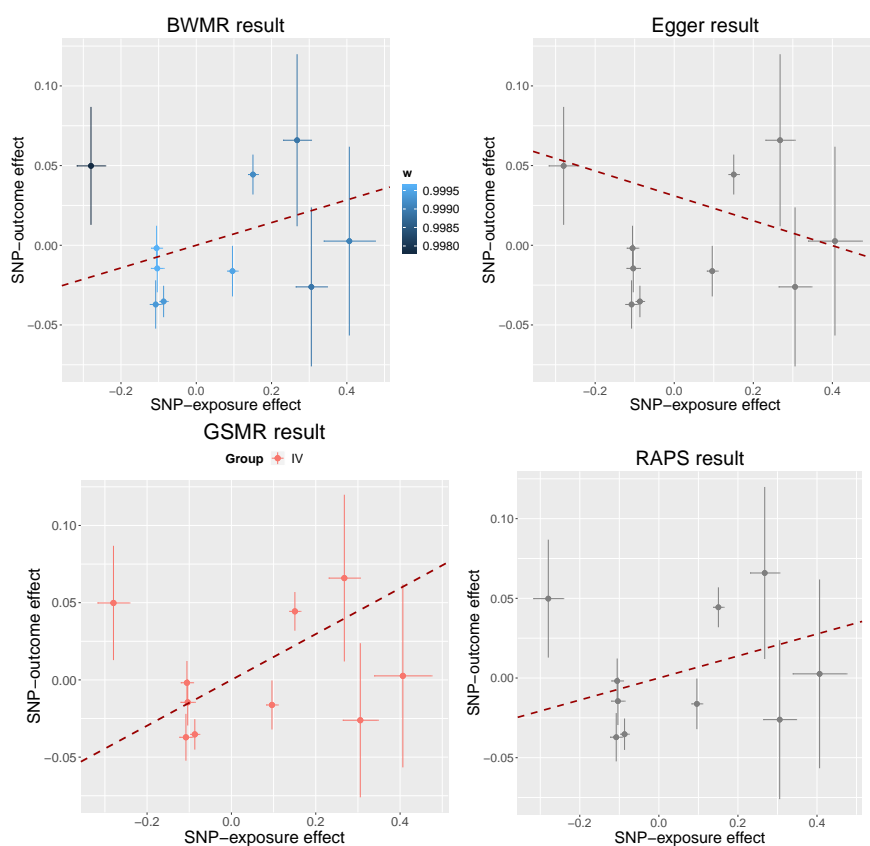


Figure 33: Comparisons of causal inference results when estimating the causal effect of Gp on Crohn’s disease. We use this example to show that GSMR may suffer from inflated type I error rate when IVs are affected by weak horizontal pleiotropic effects, leading to false discovery.

- exposure: waist circumference; outcome: L.LDL.L.

Table 5: MR results of “waist circumference - L.LDL.L”

method	$\hat{\beta}$	$\hat{se}$	$p$ -value
BWMR	-0.005	0.0632	0.9334
Egger	0.2431	0.2574	0.3482
GSMR	0.0002	0.0587	0.9968
RAPS	0.0004	0.0625	0.9461

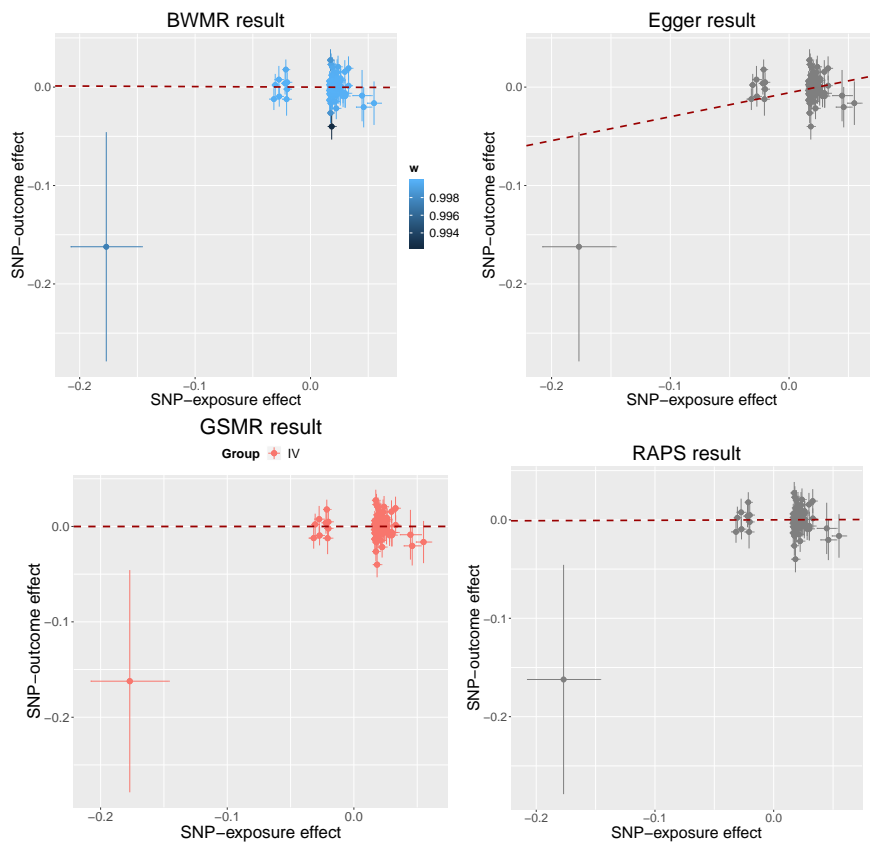


Figure 34: Comparisons of causal inference results when estimating the causal effect of waist circumference on L.LDL.L. We use this example to show that Egger is sensitive to outliers due to a few large pleiotropic effects.

- exposure: age at menarche; outcome: S.VLDL.C.

Table 6: MR results of “age at menarche - S.VLDL.C”

method	$\hat{\beta}$	$\hat{se}$	$p$ -value
BWMR	-0.0163	0.0463	0.7251
Egger	-0.6315	0.1917	0.0015
GSMR	-0.0155	0.0436	0.7212
RAPS	-0.0069	0.0472	0.8838

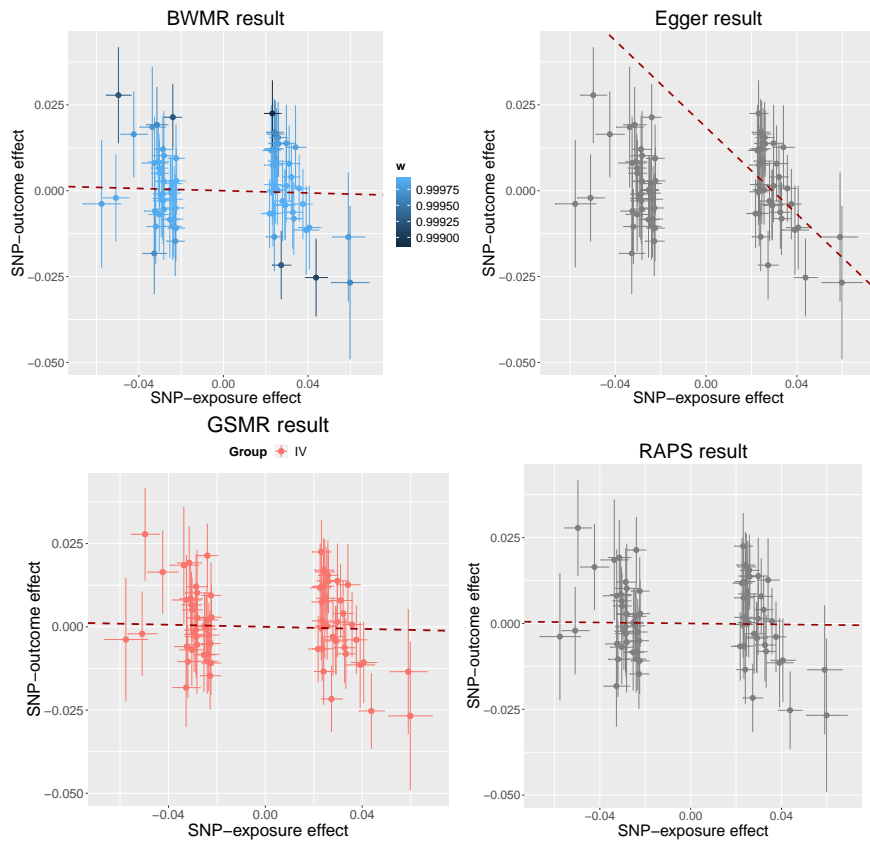


Figure 35: Comparisons of causal inference results when estimating the causal effect of age at menarche on S.VLDL.C. We use this example to show that Egger may mistakenly detect pleiotropic IVs or outliers, leading to biased estimates. Indeed, the two components in summary statistics are due to the phenomenon of selection bias.

- exposure: CAD; outcome: M.LDL.C.

Table 7: MR results of “CAD - M.LDL.C”

method	$\hat{\beta}$	$\hat{se}$	$p$ -value
BWMR	0.0668	0.0978	0.4946
Egger	0.5445	0.5994	0.3690
GSMR	-0.0393	0.0647	0.5433
RAPS	0.3317	0.1734	0.0557

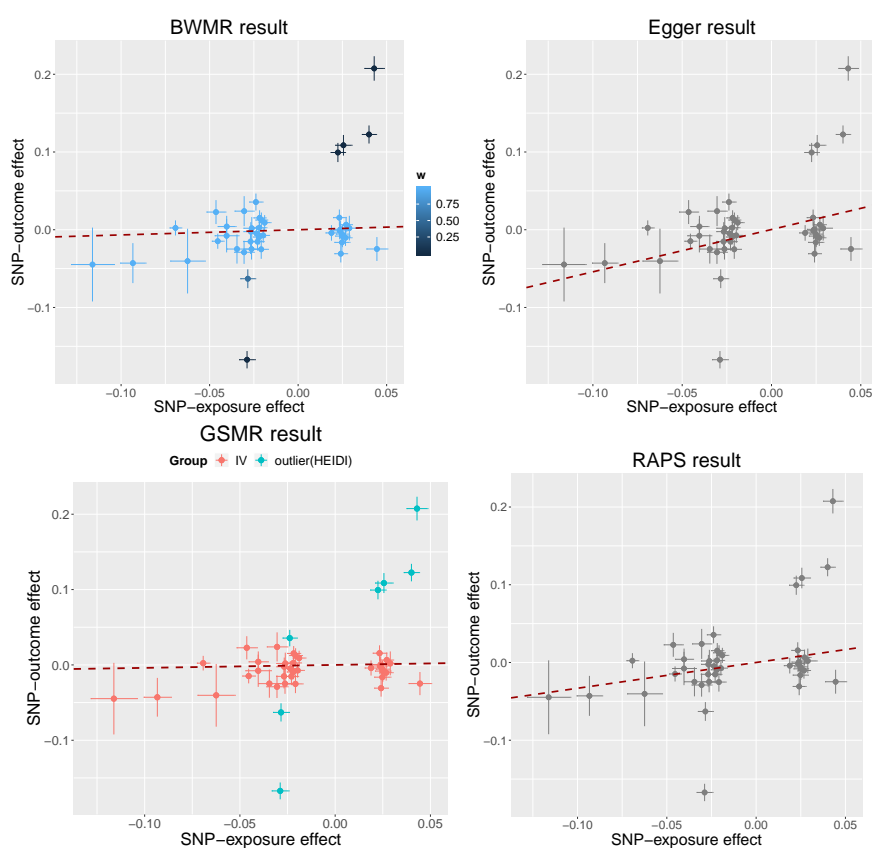


Figure 36: Comparisons of causal inference results when estimating the causal effect of CAD on M.LDL.C. We use this example to show that RAPS may not be robust to pleiotropic IVs when the horizontal pleiotropic effects have correlation with SNP-exposure effects.





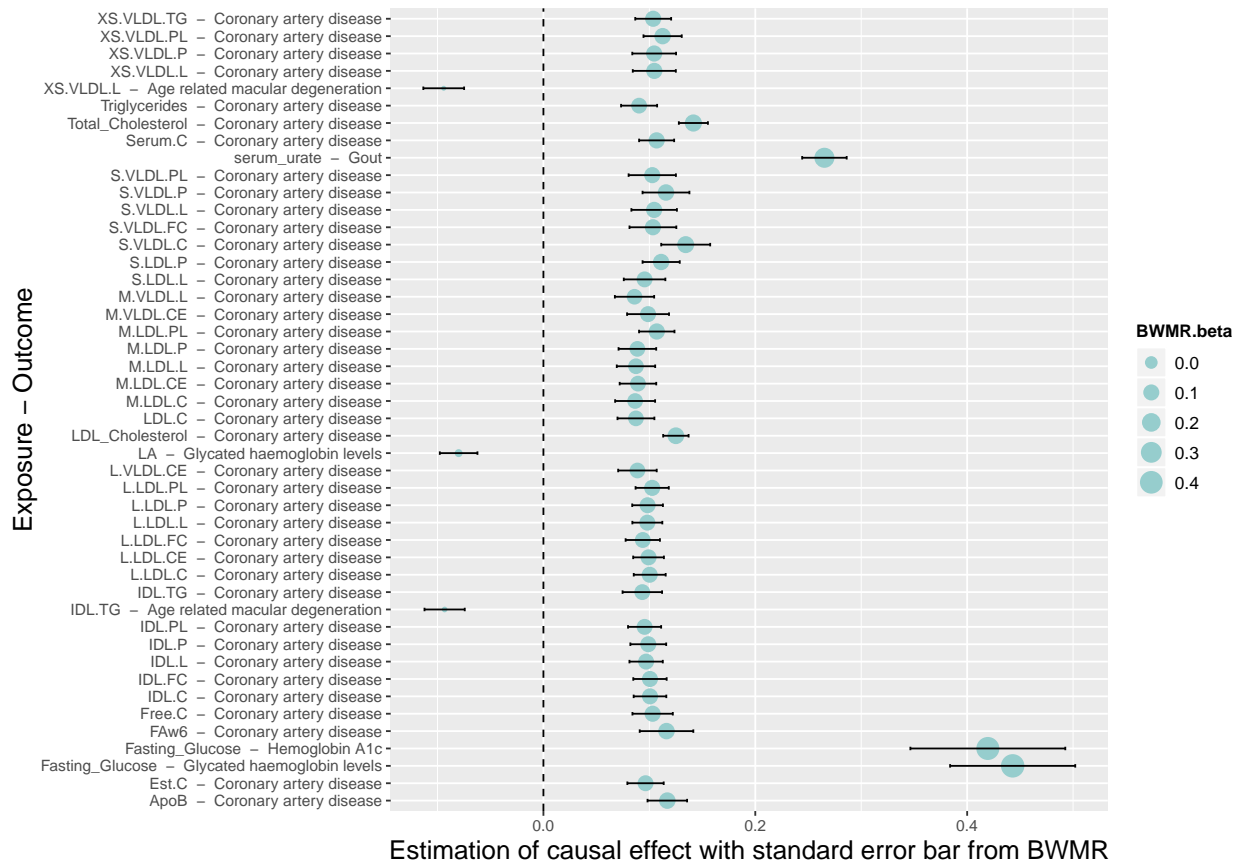


Figure 39: Significant causal effects of metabolites on complex human traits estimated by BWMR. We selected SNPs as IVs by the  $p$ -value threshold  $5 \times 10^{-8}$  and controlled the type I error rate after Bonferroni correction at level 0.05.



Figure 40: Significant causal effects of complex human traits on metabolites estimated by BWMR. We selected SNPs as IVs by the  $p$ -value threshold  $5 \times 10^{-8}$  and controlled the type I error rate after Bonferroni correction at level 0.05.

- Detailed results from RAPS

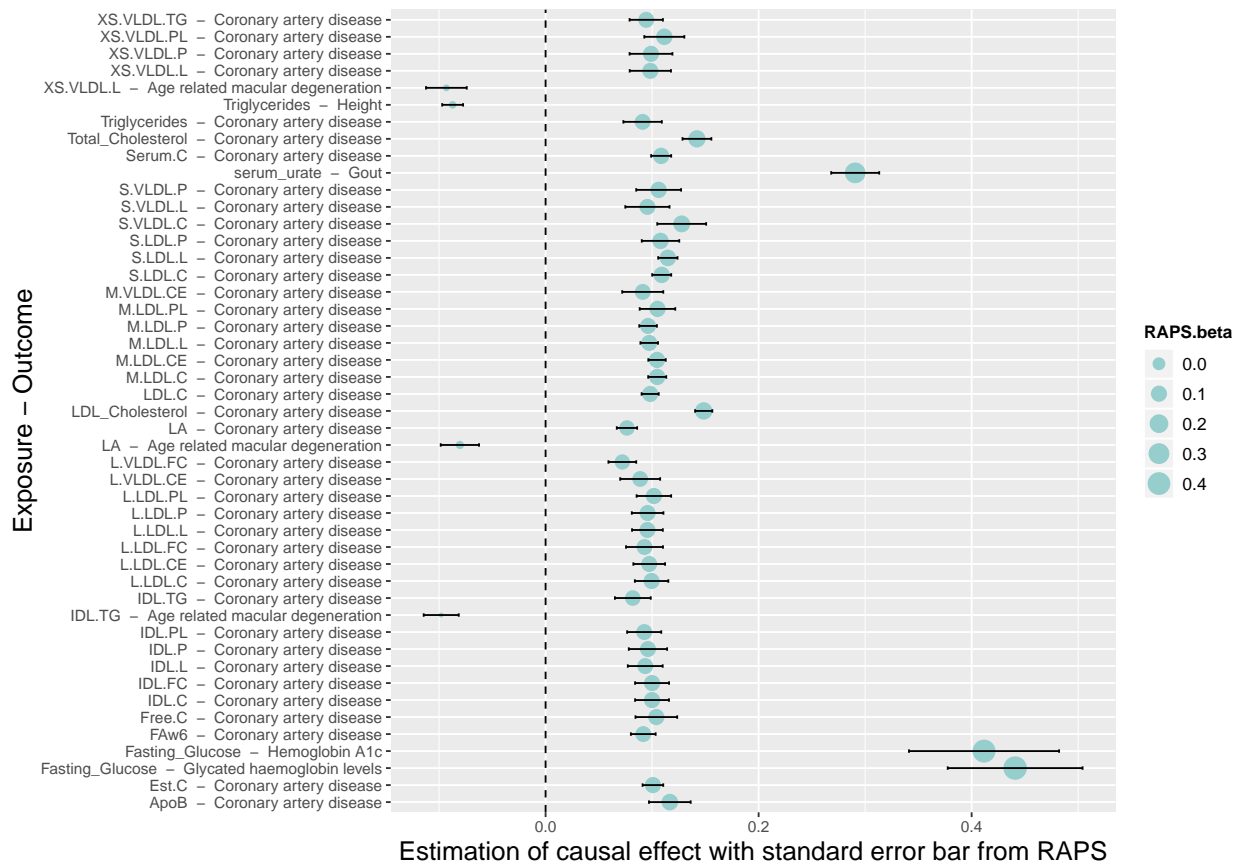


Figure 41: Significant causal effects of metabolites on complex human traits estimated by RAPS. We selected SNPs as IVs by the  $p$ -value threshold  $5 \times 10^{-8}$  and controlled the type I error rate after Bonferroni correction at level 0.05.



Figure 42: Significant causal effects of complex human traits on metabolites estimated by RAPS. We selected SNPs as IVs by the  $p$ -value threshold  $5 \times 10^{-8}$  and controlled the type I error rate after Bonferroni correction at level 0.05.

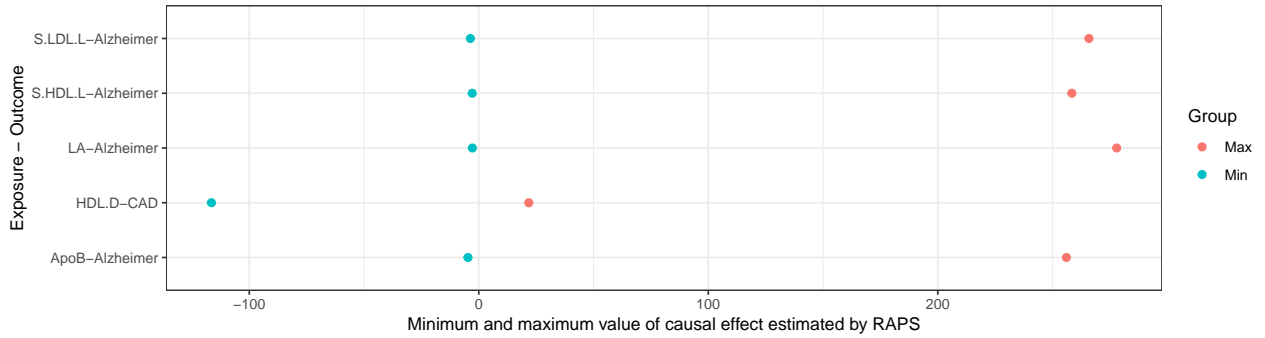


Figure 43: Numerical instability of RAPS. We implemented the method RAPS to estimate the causal effects of metabolites on human traits. To test the stability of the method, we repeated 300 times for each pair of exposure and outcome. The plot shows the cases that estimations from RAPS are not the same (maximum value – minimum value > 50).

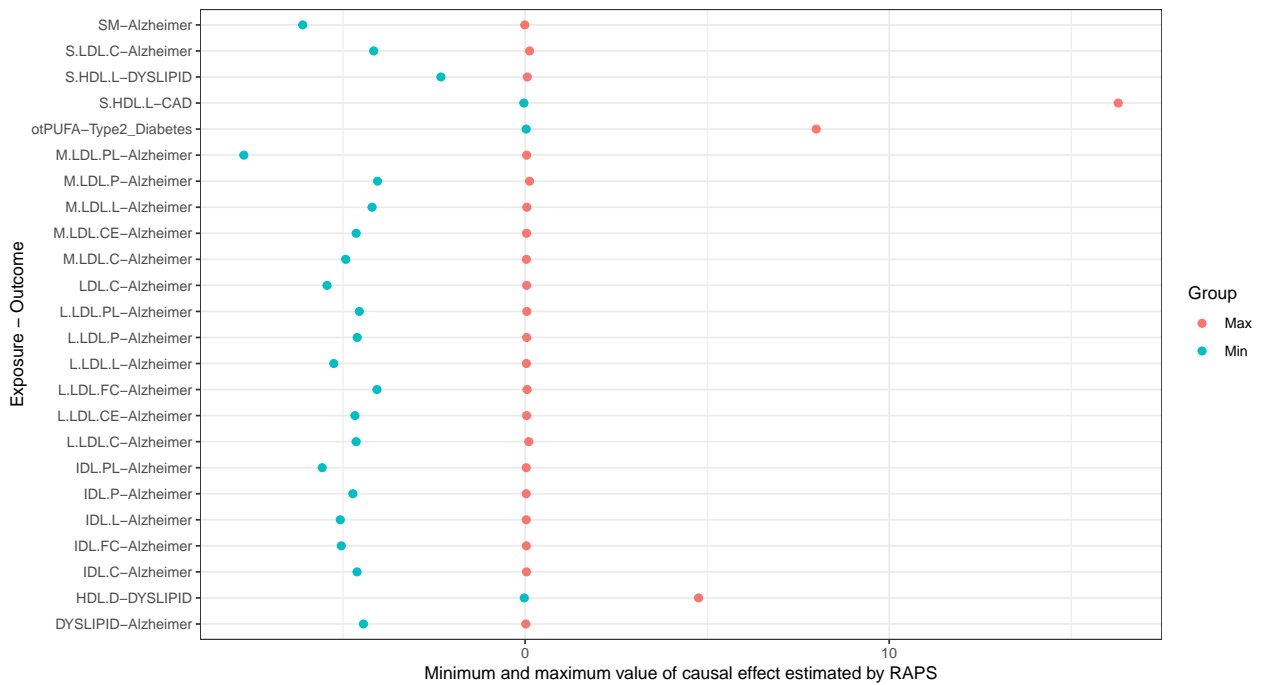


Figure 44: Numerical instability of RAPS. We implemented the method RAPS to estimate the causal effects of metabolites on human traits. To test the stability of the method, we repeated 300 times for each pair of exposure and outcome. The plot shows the cases that estimations from RAPS are not the same ( $2 < \text{maximum value} - \text{minimum value} < 50$ ).

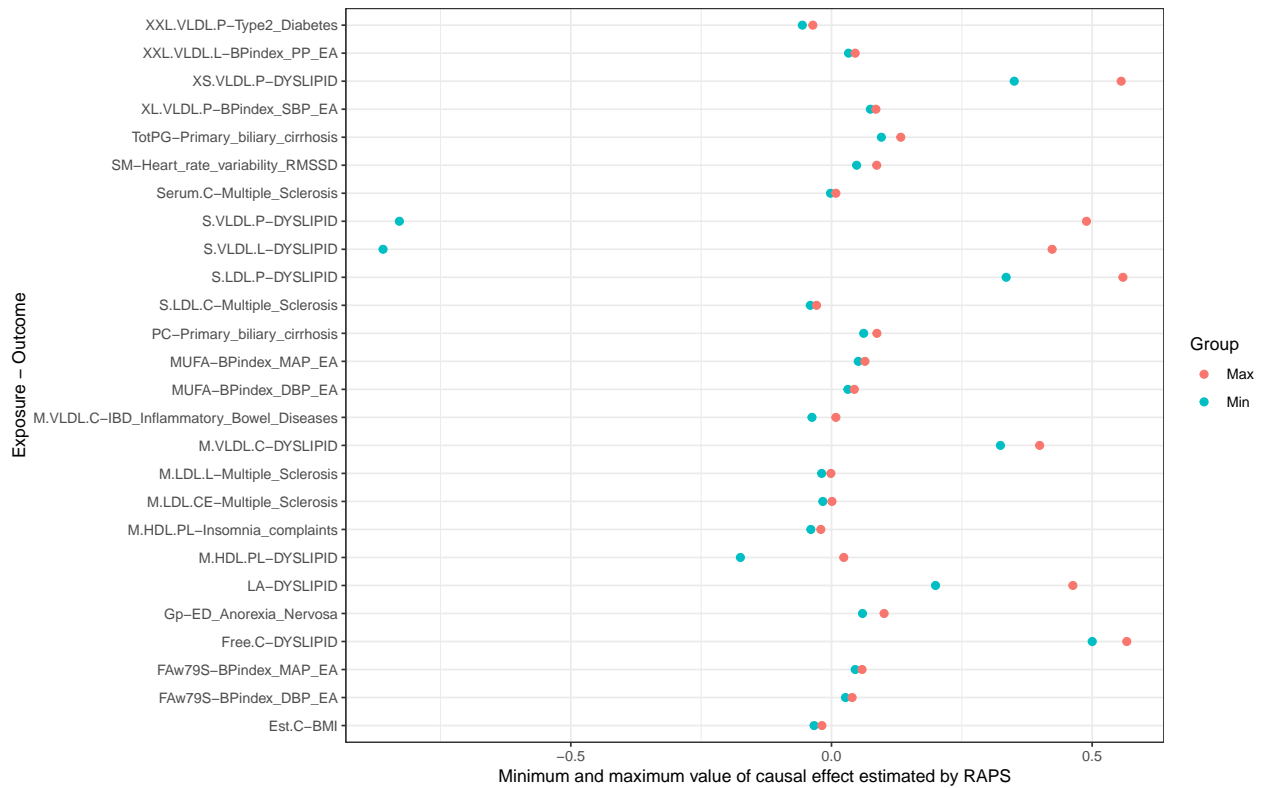


Figure 45: Numerical instability of RAPS. We implemented the method RAPS to estimate the causal effects of metabolites on human traits. To test the stability of the method, we repeated 300 times for each pair of exposure and outcome. The plot shows the cases that estimations from RAPS are not the same ( $0.01 < \text{maximum value} - \text{minimum value} < 2$ ).

- Detailed results from GSMR

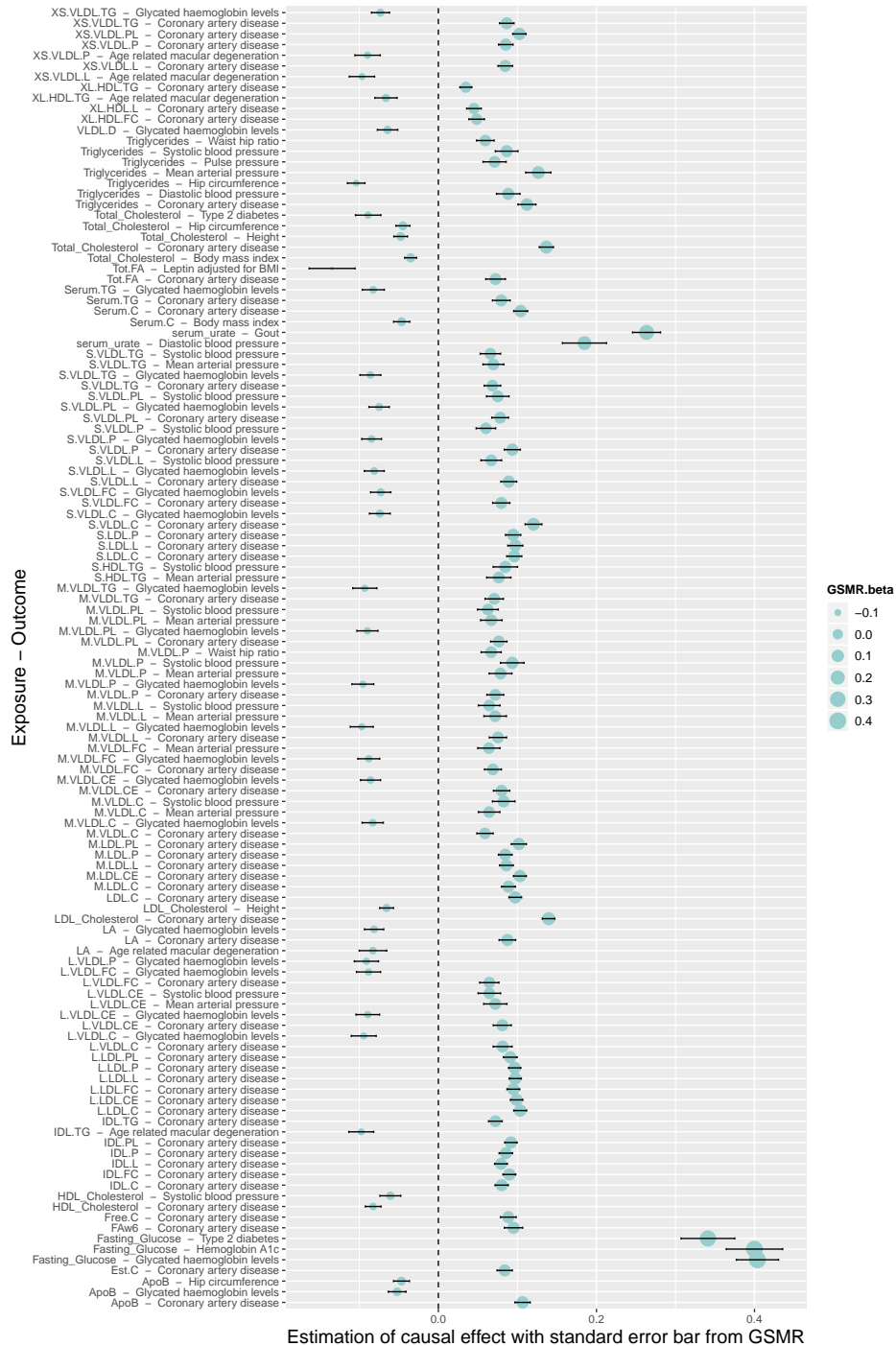


Figure 46: Significant causal effects of metabolites on complex human traits estimated by GSMR. We selected SNPs as IVs by the  $p$ -value threshold  $5 \times 10^{-8}$  and controlled the type I error rate after Bonferroni correction at level 0.05.

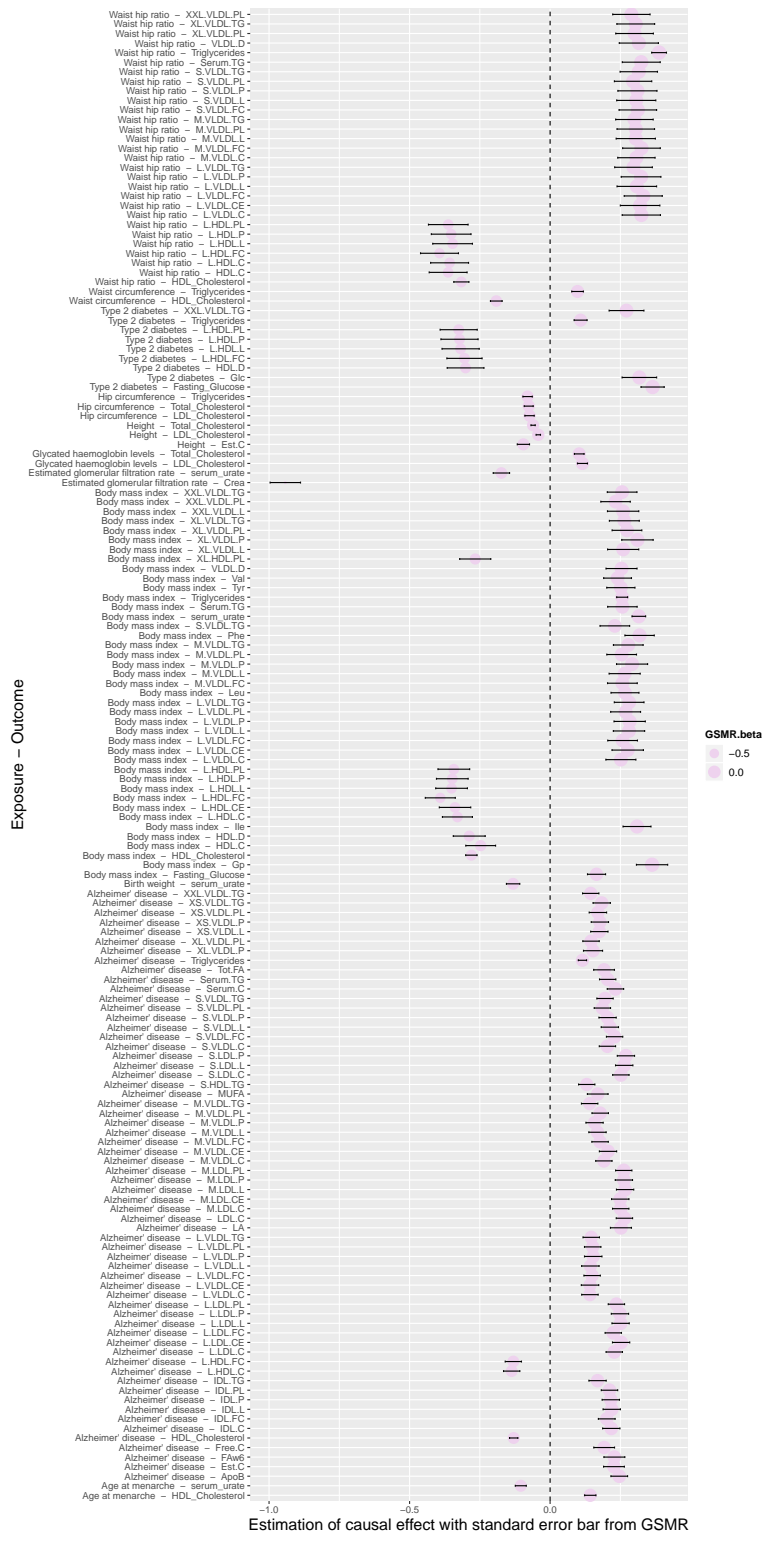


Figure 47: Significant causal effects of complex human traits on metabolites estimated by GSMR. We selected SNPs as IVs by the  $p$ -value threshold  $5 \times 10^{-8}$  and controlled the type I error rate after Bonferroni correction at level 0.05.

- Detailed results from Egger

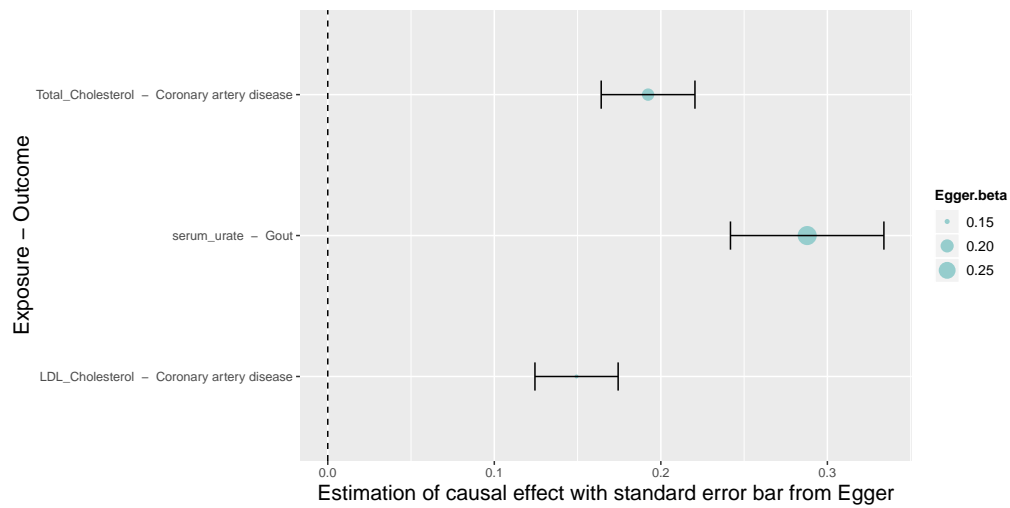


Figure 48: Significant causal effects of metabolites on complex human traits estimated by Egger. We selected SNPs as IVs by the  $p$ -value threshold  $5 \times 10^{-8}$  and controlled the type I error rate after Bonferroni correction at level 0.05.

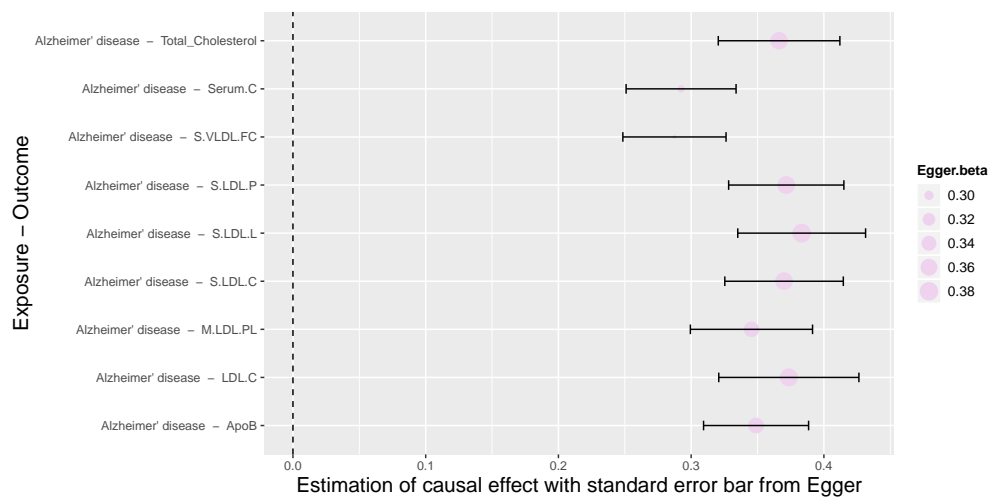


Figure 49: Significant causal effects of complex human traits on metabolites estimated by Egger. We selected SNPs as IVs by the  $p$ -value threshold  $5 \times 10^{-8}$  and controlled the type I error rate after Bonferroni correction at level 0.05.

## References

- Baiocchi, M., J. Cheng, and D. S. Small (2014). Instrumental variable methods for causal inference. *Statistics in medicine* 33(13), 2297–2340.
- Bentham, J., D. L. Morris, D. S. C. Graham, C. L. Pinder, P. Tomblinson, T. W. Behrens, J. Martín, B. P. Fairfax, J. C. Knight, L. Chen, et al. (2015). Genetic association analyses implicate aberrant regulation of innate and adaptive immunity genes in the pathogenesis of systemic lupus erythematosus. *Nature genetics* 47(12), 1457.
- Benyamin, B., J. He, Q. Zhao, J. Gratten, F. Garton, P. J. Leo, Z. Liu, M. Mangelsdorf, A. Al-Chalabi, L. Anderson, et al. (2017). Cross-ethnic meta-analysis identifies association of the gpx3-tnip1 locus with amyotrophic lateral sclerosis. *Nature Communications* 8(1), 611.
- Blei, D. M., A. Kucukelbir, and J. D. McAuliffe (2017). Variational inference: A review for statisticians. *Journal of the American Statistical Association* 112(518), 859–877.
- Bowden, J., G. D. Smith, and S. Burgess (2015). Mendelian Randomization Methodology Mendelian randomization with invalid instruments : effect estimation and bias detection through Egger regression. *International Journal of Epidemiology* (June), 512–525.
- Bradfield, J. P., H. R. Taal, N. J. Timpson, A. Scherag, C. Lecoeur, N. M. Warrington, E. Hypponen, C. Holst, B. Valcarcel, E. Thiering, et al. (2012). A genome-wide association meta-analysis identifies new childhood obesity loci. *Nature genetics* 44(5), 526.
- Burgess, S., A. Butterworth, and S. G. Thompson (2013). Mendelian randomization analysis with multiple genetic variants using summarized data. *Genetic epidemiology* 37(7), 658–665.
- Censin, J., C. Nowak, N. Cooper, P. Bergsten, J. A. Todd, and T. Fall (2017). Childhood adiposity and risk of type 1 diabetes: A mendelian randomization study. *PLoS medicine* 14(8), e1002362.

- Chung, D., C. Yang, C. Li, J. Gelernter, and H. Zhao (2014, 11). GPA: A Statistical Approach to Prioritizing GWAS Results by Integrating Pleiotropy and Annotation. *PLOS Genetics* 10(11), 1–14.
- Cordell, H. J., Y. Han, G. F. Mells, Y. Li, G. M. Hirschfield, C. S. Greene, G. Xie, B. D. Juran, D. Zhu, D. C. Qian, et al. (2015). International genome-wide meta-analysis identifies new primary biliary cirrhosis risk loci and targetable pathogenic pathways. *Nature communications* 6, 8019.
- Cross-Disorder Group of the Psychiatric Genomics Consortium et al. (2013). Identification of risk loci with shared effects on five major psychiatric disorders: a genome-wide analysis. *The Lancet* 381(9875), 1371–1379.
- Dalbeth, N., A. Phipps-Green, C. Frampton, T. Neogi, W. J. Taylor, and T. R. Merriman (2018). Relationship between serum urate concentration and clinically evident incident gout: an individual participant data analysis. *Annals of the rheumatic diseases* 77(7), 1048–1052.
- Day, F. R., K. S. Ruth, D. J. Thompson, K. L. Lunetta, N. Pervjakova, D. I. Chasman, L. Stolk, H. K. Finucane, P. Sulem, B. Bulik-Sullivan, et al. (2015). Large-scale genomic analyses link reproductive aging to hypothalamic signaling, breast cancer susceptibility and brca1-mediated dna repair. *Nature genetics* 47(11), 1294.
- De Moor, M. H., P. T. Costa, A. Terracciano, R. F. Krueger, E. J. De Geus, T. Toshiko, B. W. Penninx, T. Esko, P. A. Madden, J. Derringer, et al. (2012). Meta-analysis of genome-wide association studies for personality. *Molecular psychiatry* 17(3), 337.
- Den Hoed, M., M. Eijgelsheim, T. Esko, B. J. Brundel, D. S. Peal, D. M. Evans, I. M. Nolte, A. V. Segrè, H. Holm, R. E. Handsaker, et al. (2013). Identification of heart rate-associated loci and their effects on cardiac conduction and rhythm disorders. *Nature genetics* 45(6), 621.
- Dubois, P. C., G. Trynka, L. Franke, K. A. Hunt, J. Romanos, A. Curtotti, A. Zhernakova, G. A. Heap, R. Ádány, A. Aromaa, et al. (2010). Multiple common variants for celiac disease influencing immune gene expression. *Nature genetics* 42(4), 295.

- Duncan, L., Z. Yilmaz, H. Gaspar, R. Walters, J. Goldstein, V. Anttila, B. Bulik-Sullivan, S. Ripke, E. D. W. G. of the Psychiatric Genomics Consortium, L. Thornton, et al. (2017). Significant locus and metabolic genetic correlations revealed in genome-wide association study of anorexia nervosa. *American journal of psychiatry* 174(9), 850–858.
- Dupuis, J., C. Langenberg, I. Prokopenko, R. Saxena, N. Soranzo, A. U. Jackson, E. Wheeler, N. L. Glazer, N. Bouatia-Naji, A. L. Gloyn, et al. (2010). New genetic loci implicated in fasting glucose homeostasis and their impact on type 2 diabetes risk. *Nature genetics* 42(2), 105.
- Efron, B. (2011). Tweedies formula and selection bias. *Journal of the American Statistical Association* 106(496), 1602–1614.
- Evans, D. M. and G. Davey Smith (2015). Mendelian randomization: new applications in the coming age of hypothesis-free causality. *Annual review of genomics and human genetics* 16, 327–350.
- Ference, B. A., H. N. Ginsberg, I. Graham, K. K. Ray, C. J. Packard, E. Bruckert, R. A. Hegele, R. M. Krauss, F. J. Raal, H. Schunkert, et al. (2017). Low-density lipoproteins cause atherosclerotic cardiovascular disease. 1. Evidence from genetic, epidemiologic, and clinical studies. A consensus statement from the European Atherosclerosis Society Consensus Panel. *European heart journal* 38(32), 2459–2472.
- Furberg, H., Y. Kim, J. Dackor, E. Boerwinkle, N. Franceschini, D. Ardissino, L. Bernardinelli, P. M. Mannucci, F. Mauri, P. A. Merlini, et al. (2010). Genome-wide meta-analyses identify multiple loci associated with smoking behavior. *Nature genetics* 42(5), 441.
- Gao, J., L. K. Davis, A. B. Hart, S. Sanchez-Roige, L. Han, J. T. Cacioppo, and A. A. Palmer (2017). Genome-wide association study of loneliness demonstrates a role for common variation. *Neuropsychopharmacology* 42(4), 811.
- Giordano, R., T. Broderick, and M. I. Jordan (2018). Covariances, Robustness and Variational Bayes. *The Journal of Machine Learning Research* 19(1), 1981–2029.

- Giordano, R. J., T. Broderick, and M. I. Jordan (2015). Linear response methods for accurate covariance estimates from mean field variational bayes. In *Advances in Neural Information Processing Systems*, pp. 1441–1449.
- Hammerschlag, A. R., S. Stringer, C. A. de Leeuw, S. Sniekers, E. Taskesen, K. Watanabe, T. F. Blanken, K. Dekker, B. H. Te Lindert, R. Wassing, et al. (2017). Genome-wide association analysis of insomnia complaints identifies risk genes and genetic overlap with psychiatric and metabolic traits. *Nature genetics* 49(11), 1584.
- Hemani, G., J. Zheng, B. Elsworth, K. H. Wade, V. Haberland, D. Baird, C. Laurin, S. Burgess, J. Bowden, R. Langdon, et al. (2018). The MR-Base platform supports systematic causal inference across the human phenome. *Elife* 7, e34408.
- Horikoshi, M., R. N. Beaumont, F. R. Day, N. M. Warrington, M. N. Kooijman, J. Fernandez-Tajés, B. Feenstra, N. R. Van Zuydam, K. J. Gaulton, N. Grarup, et al. (2016). Genome-wide associations for birth weight and correlations with adult disease. *Nature* 538(7624), 248.
- Hunter, D. J., P. Kraft, K. B. Jacobs, D. G. Cox, M. Yeager, S. E. Hankinson, S. Wacholder, Z. Wang, R. Welch, A. Hutchinson, et al. (2007). A genome-wide association study identifies alleles in *fgfr2* associated with risk of sporadic postmenopausal breast cancer. *Nature genetics* 39(7), 870.
- Jones, S. E., J. Tyrrell, A. R. Wood, R. N. Beaumont, K. S. Ruth, M. A. Tuke, H. Yaghootkar, Y. Hu, M. Teder-Laving, C. Hayward, et al. (2016). Genome-wide association analyses in 128,266 individuals identifies new morningness and sleep duration loci. *PLoS genetics* 12(8), e1006125.
- Katan, M. (1986). Apoprotein E isoforms, serum cholesterol, and cancer. *The Lancet* 327(8479), 507–508.
- Kettunen, J., A. Demirkan, P. Würtz, H. H. Draisma, T. Haller, R. Rawal, A. Vaarhorst, A. J. Kangas, L.-P. Lyytikäinen, M. Pirinen, et al. (2016). Genome-wide study for circulating metabolites identifies 62 loci and reveals novel systemic effects of LPA. *Nature communications* 7, 11122.

- Kilpeläinen, T. O., J. F. M. Carli, A. A. Skowronski, Q. Sun, J. Kriebel, M. F. Feitosa, Å. K. Hedman, A. W. Drong, J. E. Hayes, J. Zhao, et al. (2016). Genome-wide meta-analysis uncovers novel loci influencing circulating leptin levels. *Nature communications* 7, 10494.
- Klarin, D., S. M. Damrauer, K. Cho, Y. V. Sun, T. M. Teslovich, J. Honerlaw, D. R. Gagnon, S. L. DuVall, J. Li, G. M. Peloso, et al. (2018). Genetics of blood lipids among ~ 300,000 multi-ethnic participants of the Million Veteran Program. *Nature genetics* 50(11), 1514.
- Köttgen, A., E. Albrecht, A. Teumer, V. Vitart, J. Krumsiek, C. Hundertmark, G. Pitsis, D. Ruggiero, C. M. O’Seaghdha, T. Haller, et al. (2013). Genome-wide association analyses identify 18 new loci associated with serum urate concentrations. *Nature genetics* 45(2), 145.
- Lambert, J.-C., C. A. Ibrahim-Verbaas, D. Harold, A. C. Naj, R. Sims, C. Bellenguez, G. Jun, A. L. DeStefano, J. C. Bis, G. W. Beecham, et al. (2013). Meta-analysis of 74,046 individuals identifies 11 new susceptibility loci for alzheimer’s disease. *Nature genetics* 45(12), 1452.
- Lawlor, D. A., R. M. Harbord, J. A. Sterne, N. Timpson, and G. Davey Smith (2008). Mendelian randomization: using genes as instruments for making causal inferences in epidemiology. *Statistics in medicine* 27(8), 1133–1163.
- Li, M., Y. Li, O. Weeks, V. Mijatovic, A. Teumer, J. E. Huffman, G. Tromp, C. Fuchsberger, M. Gorski, L.-P. Lyytikäinen, et al. (2017). Sos2 and acp1 loci identified through large-scale exome chip analysis regulate kidney development and function. *Journal of the American Society of Nephrology* 28(3), 981–994.
- Liu, C., A. T. Kraja, J. A. Smith, J. A. Brody, N. Franceschini, J. C. Bis, K. Rice, A. C. Morrison, Y. Lu, S. Weiss, et al. (2016). Meta-analysis identifies common and rare variants influencing blood pressure and overlapping with metabolic trait loci. *Nature genetics* 48(10), 1162.
- Liu, J. Z., S. van Sommeren, H. Huang, S. C. Ng, R. Alberts, A. Takahashi, S. Ripke, J. C. Lee, L. Jostins, T. Shah, et al. (2015). Association analyses identify 38 susceptibility

- loci for inflammatory bowel disease and highlight shared genetic risk across populations. *Nature genetics* 47(9), 979.
- Locke, A. E., B. Kahali, S. I. Berndt, A. E. Justice, T. H. Pers, F. R. Day, C. Powell, S. Vedantam, M. L. Buchkovich, J. Yang, et al. (2015). Genetic studies of body mass index yield new insights for obesity biology. *Nature* 518(7538), 197.
- Lu, Y., F. R. Day, S. Gustafsson, M. L. Buchkovich, J. Na, V. Bataille, D. L. Cousminer, Z. Dastani, A. W. Drong, T. Esko, et al. (2016). New loci for body fat percentage reveal link between adiposity and cardiometabolic disease risk. *Nature communications* 7, 10495.
- Manning, A. K., M.-F. Hivert, R. A. Scott, J. L. Grimsby, N. Bouatia-Naji, H. Chen, D. Rybin, C.-T. Liu, L. F. Bielak, I. Prokopenko, et al. (2012). A genome-wide approach accounting for body mass index identifies genetic variants influencing fasting glycemic traits and insulin resistance. *Nature genetics* 44(6), 659.
- Manousaki, D., T. Dudding, S. Haworth, Y.-H. Hsu, C.-T. Liu, C. Medina-Gómez, T. Voortman, N. Van Der Velde, H. Melhus, C. Robinson-Cohen, et al. (2017). Low-frequency synonymous coding variation in *cyp2r1* has large effects on vitamin d levels and risk of multiple sclerosis. *The American Journal of Human Genetics* 101(2), 227–238.
- McCullagh, P. and R. Tibshirani (1990). A simple method for the adjustment of profile likelihoods. *Journal of the Royal Statistical Society: Series B (Methodological)* 52(2), 325–344.
- Moffatt, M. F., I. G. Gut, F. Demenais, D. P. Strachan, E. Bouzigon, S. Heath, E. Von Mutius, M. Farrall, M. Lathrop, and W. O. Cookson (2010). A large-scale, consortium-based genomewide association study of asthma. *New England Journal of Medicine* 363(13), 1211–1221.
- Morris, A. P., B. F. Voight, T. M. Teslovich, T. Ferreira, A. V. Segre, V. Steinthorsdottir, R. J. Strawbridge, H. Khan, H. Grallert, A. Mahajan, et al. (2012). Large-scale association analysis provides insights into the genetic architecture and pathophysiology of type 2 diabetes. *Nature genetics* 44(9), 981.

- Nikpay, M., A. Goel, H.-H. Won, L. M. Hall, C. Willenborg, S. Kanoni, D. Saleheen, T. Kyriakou, C. P. Nelson, J. C. Hopewell, et al. (2015). A comprehensive 1000 genomes–based genome-wide association meta-analysis of coronary artery disease. *Nature genetics* 47(10), 1121.
- Nolte, I. M., M. L. Munoz, V. Tragante, A. T. Amare, R. Jansen, A. Vaez, B. Von Der Heyde, C. L. Avery, J. C. Bis, B. Dierckx, et al. (2017). Genetic loci associated with heart rate variability and their effects on cardiac disease risk. *Nature communications* 8, 15805.
- Okbay, A., B. M. Baselmans, J.-E. De Neve, P. Turley, M. G. Nivard, M. A. Fontana, S. F. W. Meddens, R. K. Linnér, C. A. Rietveld, J. Derringer, et al. (2016). Genetic variants associated with subjective well-being, depressive symptoms, and neuroticism identified through genome-wide analyses. *Nature genetics* 48(6), 624.
- Otowa, T., K. Hek, M. Lee, E. M. Byrne, S. S. Mirza, M. G. Nivard, T. Bigdeli, S. H. Aggen, D. Adkins, A. Wolen, et al. (2016). Meta-analysis of genome-wide association studies of anxiety disorders. *Molecular psychiatry* 21(10), 1391.
- Pankratz, N., G. W. Beecham, A. L. DeStefano, T. M. Dawson, K. F. Doheny, S. A. Factor, T. H. Hamza, A. Y. Hung, B. T. Hyman, A. J. Iverson, et al. (2012). Meta-analysis of parkinson’s disease: identification of a novel locus, rit2. *Annals of neurology* 71(3), 370–384.
- Pappa, I., B. St Pourcain, K. Benke, A. Cavadino, C. Hakulinen, M. G. Nivard, I. M. Nolte, C. M. Tiesler, M. J. Bakermans-Kranenburg, G. E. Davies, et al. (2016). A genome-wide approach to children’s aggressive behavior: The eagle consortium. *American Journal of Medical Genetics Part B: Neuropsychiatric Genetics* 171(5), 562–572.
- Paternoster, L., M. Standl, J. Waage, H. Baurecht, M. Hotze, D. P. Strachan, J. A. Curtin, K. Bønnelykke, C. Tian, A. Takahashi, et al. (2015). Multi-ancestry genome-wide association study of 21,000 cases and 95,000 controls identifies new risk loci for atopic dermatitis. *Nature genetics* 47(12), 1449.

- Perry, J. R., F. Day, C. E. Elks, P. Sulem, D. J. Thompson, T. Ferreira, C. He, D. I. Chasman, T. Esko, G. Thorleifsson, et al. (2014). Parent-of-origin-specific allelic associations among 106 genomic loci for age at menarche. *Nature* 514(7520), 92.
- Purcell, S., B. Neale, K. Todd-Brown, L. Thomas, M. A. Ferreira, D. Bender, J. Maller, P. Sklar, P. I. De Bakker, M. J. Daly, et al. (2007). PLINK: a tool set for whole-genome association and population-based linkage analyses. *The American journal of human genetics* 81(3), 559–575.
- Rietveld, C. A., T. Esko, G. Davies, T. H. Pers, P. Turley, B. Benyamin, C. F. Chabris, V. Emilsson, A. D. Johnson, J. J. Lee, et al. (2014). Common genetic variants associated with cognitive performance identified using the proxy-phenotype method. *Proceedings of the National Academy of Sciences* 111(38), 13790–13794.
- Rietveld, C. A., S. E. Medland, J. Derringer, J. Yang, T. Esko, N. W. Martin, H.-J. Westra, K. Shakhbazov, A. Abdellaoui, A. Agrawal, et al. (2013). Gwas of 126,559 individuals identifies genetic variants associated with educational attainment. *science* 340(6139), 1467–1471.
- Sawcer, S., G. Hellenthal, M. Pirinen, C. C. Spencer, N. A. Patsopoulos, L. Moutsianas, A. Dilthey, Z. Su, C. Freeman, S. E. Hunt, et al. (2011). Genetic risk and a primary role for cell-mediated immune mechanisms in multiple sclerosis. *Nature* 476(7359), 214.
- Schumann, G., C. Liu, P. O'Reilly, H. Gao, P. Song, B. Xu, B. Ruggeri, N. Amin, T. Jia, S. Preis, et al. (2016). Klb is associated with alcohol drinking, and its gene product  $\beta$ -klotho is necessary for fgf21 regulation of alcohol preference. *Proceedings of the National Academy of Sciences* 113(50), 14372–14377.
- Shungin, D., T. W. Winkler, D. C. Croteau-Chonka, T. Ferreira, A. E. Locke, R. Mägi, R. J. Strawbridge, T. H. Pers, K. Fischer, A. E. Justice, et al. (2015). New genetic loci link adipose and insulin biology to body fat distribution. *Nature* 518(7538), 187.
- Sklar, P., S. Ripke, L. J. Scott, O. A. Andreassen, S. Cichon, N. Craddock, H. J. Edenberg, J. I. Nurnberger Jr, M. Rietschel, D. Blackwood, et al. (2011). Large-scale genome-wide

- association analysis of bipolar disorder identifies a new susceptibility locus near *od4*. *Nature genetics* 43(10), 977.
- Sniekers, S., S. Stringer, K. Watanabe, P. R. Jansen, J. R. Coleman, E. Krapohl, E. Taskesen, A. R. Hammerschlag, A. Okbay, D. Zabaneh, et al. (2017). Genome-wide association meta-analysis of 78,308 individuals identifies new loci and genes influencing human intelligence. *Nature genetics* 49(7), 1107.
- Solovieff, N., C. Cotsapas, P. H. Lee, S. M. Purcell, and J. W. Smoller (2013). Pleiotropy in complex traits: challenges and strategies. *Nature Reviews Genetics* 14(7), 483.
- Stewart, S. E., D. Yu, J. M. Scharf, B. M. Neale, J. A. Fagerness, C. A. Mathews, P. D. Arnold, P. D. Evans, E. R. Gamazon, L. Osiecki, et al. (2013). Genome-wide association study of obsessive-compulsive disorder. *Molecular psychiatry* 18(7), 788.
- Strawbridge, R. J., J. Dupuis, I. Prokopenko, A. Barker, E. Ahlqvist, D. Rybin, J. R. Petrie, M. E. Travers, N. Bouatia-Naji, A. S. Dimas, et al. (2011). Genome-wide association identifies nine common variants associated with fasting proinsulin levels and provides new insights into the pathophysiology of type 2 diabetes. *Diabetes* 60(10), 2624–2634.
- Taal, H. R., B. St Pourcain, E. Thiering, S. Das, D. O. Mook-Kanamori, N. M. Warrington, M. Kaakinen, E. Kreiner-Møller, J. P. Bradfield, R. M. Freathy, et al. (2012). Common variants at 12q15 and 12q24 are associated with infant head circumference. *Nature genetics* 44(5), 532.
- Teramoto, T., J. Sasaki, H. Ueshima, G. Egusa, M. Kinoshita, K. Shimamoto, H. Daida, S. Biro, K. Hirobe, T. Funahashi, et al. (2007). Diagnostic criteria for Dyslipidemia. *Journal of atherosclerosis and thrombosis* 14(4), 155–158.
- Teumer, A., A. Tin, R. Sorice, M. Gorski, N. C. Yeo, A. Y. Chu, M. Li, Y. Li, V. Mijatovic, Y.-A. Ko, et al. (2016). Genome-wide association studies identify genetic loci associated with albuminuria in diabetes. *Diabetes* 65(3), 803–817.
- The 1000 Genomes Project Consortium et al. (2012). An integrated map of genetic variation from 1,092 human genomes. *Nature* 491(7422), 56.

- van der Valk, R. J., E. Kreiner-Møller, M. N. Kooijman, M. Guxens, E. Stergiakouli, A. Sääf, J. P. Bradfield, F. Geller, M. G. Hayes, D. L. Cousminer, et al. (2015). A novel common variant in *dcst2* is associated with length in early life and height in adulthood. *Human Molecular Genetics* 24(4), 1155–1168.
- Verbanck, M., C.-Y. Chen, B. Neale, and R. Do (2018). Detection of widespread horizontal pleiotropy in causal relationships inferred from Mendelian randomization between complex traits and diseases. *Nature genetics* 50(5), 693.
- Visscher, P. M., N. R. Wray, Q. Zhang, P. Sklar, M. I. McCarthy, M. A. Brown, and J. Yang (2017). 10 years of GWAS discovery: biology, function, and translation. *The American Journal of Human Genetics* 101(1), 5–22.
- Wang, Y., A. Kucukelbir, and D. M. Blei (2016). Robust Probabilistic Modeling with Bayesian Data Reweighting. *arXiv preprint arXiv:1606.03860*.
- Wheeler, E., A. Leong, C.-T. Liu, M.-F. Hivert, R. J. Strawbridge, C. Podmore, M. Li, J. Yao, X. Sim, J. Hong, et al. (2017). Impact of common genetic determinants of hemoglobin a1c on type 2 diabetes risk and diagnosis in ancestrally diverse populations: A transethnic genome-wide meta-analysis. *PLoS medicine* 14(9), e1002383.
- Willer, C. J., E. M. Schmidt, S. Sengupta, G. M. Peloso, S. Gustafsson, S. Kanoni, A. Ganna, J. Chen, M. L. Buchkovich, S. Mora, et al. (2013). Discovery and refinement of loci associated with lipid levels. *Nature genetics* 45(11), 1274.
- Wood, A. R., T. Esko, J. Yang, S. Vedantam, T. H. Pers, S. Gustafsson, A. Y. Chu, K. Estrada, J. Luan, Z. Kutalik, et al. (2014). Defining the role of common variation in the genomic and biological architecture of adult human height. *Nature genetics* 46(11), 1173.
- Yang, C., C. Li, Q. Wang, D. Chung, and H. Zhao (2015). Implications of pleiotropy: challenges and opportunities for mining Big Data in biomedicine. *Frontiers in genetics* 6, 229.

Zhao, Q., J. Wang, J. Bowden, and D. S. Small (2018). Statistical inference in two-sample summary-data Mendelian randomization using robust adjusted profile score. *arXiv preprint arXiv:1801.09652*.

Zhong, H. and R. L. Prentice (2008, 02). Bias-reduced estimators and confidence intervals for odds ratios in genome-wide association studies. *Biostatistics* 9(4), 621–634.

Zhu, Z., Z. Zheng, F. Zhang, Y. Wu, M. Trzaskowski, R. Maier, M. R. Robinson, J. J. McGrath, P. M. Visscher, N. R. Wray, et al. (2018). Causal associations between risk factors and common diseases inferred from GWAS summary data. *Nature communications* 9(1), 224.